SUPPLEMENTARY INFORMATION

Donor Acceptor Fluorophores: Synthesis, Optical Properties, TD-DFT and Cytotoxicity Studies

Zahraa M Essam [‡, a, b], Guliz Ersoy Ozmen [‡, a], Dani Setiawan[a], Riri Rizkianty Hamid[c], Reda M Abd El-Aal[b], Ritu Aneja[c], Donald Hamelberg[a, d], Maged Henary*[, a, d]

[a] Department of Chemistry, Petit Science Center, Georgia State University, 100 Piedmont Avenue SE, Atlanta, Georgia, 30303, United States

[b] Department of Chemistry, Suez University, Suez, Egypt

[c] Department of Biology, Petit Science Center, Georgia State University, 100 Piedmont Avenue SE, Atlanta, Georgia, 30303, United States

[d] Center of Diagnostics and Therapeutics, Petit Science Center, Georgia State University, 100 Piedmont Avenue SE, Atlanta, Georgia, 30303, United States

‡ Equal contribution

*Corresponding Author: mhenary1@gsu.edu; Tel: +1 404-413-5566 (MH)

Table of Contents

General

All chemicals were American Chemical Society grade or HPLC purity, bought from Sigma Aldrich (Saint Louis, MO) and TCI America (Waltham, MA) and used without further purification. The ^{1}H-NMR (400 MHz) and ^{13}C-NMR (100 MHz) spectra were recorded on a Bruker Avance spectrometer using DMSO-d_6 (Cambridge Isotope Laboratories, Andover, MA) and $CDCl_3$ containing tetramethylsilane (TMS) as an internal calibration standard. The melting points (mp) were recorded on Thomas Hoover apparatus using open Pyrex capillary tubes. UV-vis absorption spectra were recorded on a Varian Cary 50 spectrophotometer (Santa Clara, CA) and fluorescence emission spectra were recorded on Shimadzu RF-5301PC spectrofluorometer. The fluorophores were dissolved in ethanol using VWR disposable two-sided polystyrene cuvettes with path length 1 cm. The quantum yields of dyes were measured according to the reported method with reference to indocyanine green (ICG)[1].

Synthetic Procedure for Acceptor and Linker Group

DCM (9 mL) and *N, N* -dimethylformamide (9 mL) placed in a 25 ml round bottom flask and then the flask was immersed in an ice bath followed by the dropwise addition of $POCl_3$ (7.5 mL, 29 mmol) to the reaction mixture and stirred for 30 min. Cyclohexanone (2.25 mL, 24 mmol) was added to the reaction mixture while the ice bath removed and the mixture refluxed above 70 ˚C. The completion of the reaction was checked by thin layer chromatography (TLC) and when the starting material consumed, the reaction mixture poured onto ice and stirred for 2 h. The yellow precipitate washed by filtration to yield bis-aldehyde **2**. In the second step, compound **2** (1.16 mmol) was added to chloroacetic acid (1.16 mmol) and acetic anhydride (2 mL) in a round bottom flask (25 mL) and stirred until dissolved. Then, sodium acetate (2.32 mmol) was added to the reaction mixture and stirred at 70 ˚C for 4 h. After cooling, the crude product poured onto ice and washed with water to give pale yellow precipitate of compound **3** (Scheme 1).

General Synthetic Procedure for Fluorophores 4-20

As outlined in Scheme 1, (*E*)-2-chloro-3-(hydroxymethylene) cyclohex-1-ene-1-carbaldehyde (**2**) was synthesized starting from cyclohexanone (**1**) via Vilsmeier Haack formylation. Then, the carbaldehyde was allowed to react with chloroacetic acid to synthesize (Z)-2-chloro-3-((E)-2-chloro-3-(hydroxymethylene) cyclohex-1-en-1-yl) acrylic acid (**3**), which is the acceptor unit together with the linker. The individual heterocyclic salt (1.2 mol) was dissolved in

ethanol (8 mL) in a 50 mL round bottom flask, then 1 mol of acceptor **3** and one drop of triethyl amine to the reaction mixture, followed by stirring at 70 ˚C for the required time which was ranging between 1-15 h for individual heterocyclic salt. The reaction mixture was monitored using UV-vis spectroscopy and TLC and stopped when the dye signal appeared in UV-vis spectroscopy and the peak of starting salt was disappeared. After the reaction was completed, it dried under vacuum and purified by recrystallization with MeOH: EOAc (1:2). In case of fluorophores **12-15** and **16-20**, the starting material peak didn't disappear therefore additional purification was needed by column chromatography using methanol and different ratios of dichloromethane.

(Z)-2-chloro-3-((E)-2-chloro-3-(hydroxymethylene)cyclohex-1-en-1-yl) acrylic acid ***(3)*****:** mp 52-54 ◦C, 62% yield ;^{1}H NMR (400 MHz, DMSO-d_6): ***δ*** 1.58 (s, 2H), 2.28 (s, 2H), 2.46 (s, 2H), 5.64 (s, 1H), 7.90 (s, 1H), 10.2 (s, 1H), ^{13}C NMR (100 MHz, DMSO-d_6): ***δ*** 20.12, 20.95, 24.44, 24.58, 120.41, 133.95, 137.93, 142.62, 167.71, 190.64.

(Z)-2-chloro-3-((E)-2-chloro-3-(2-((E)-1,3,3-trimethylindolin-2-ylidene) ethylidene) cyclohex-1-en-1-yl) acrylic acid ***(4)***: mp 152-154 ◦C; 73% yield; ^{1}H NMR (400 MHz, DMSO-d_6): ***δ*** 1.24 (s, 2H), 1.67 (s, 6H), 1.87 (s, 2H), 2.71 (s, 2H), 3.69 (s, 3H), 6.32 (d, J = 13.2 Hz, 1H), 7.45 (s, 2H), 7.62 (s, 1H), 7.76 (s, 1H), 7.80 (s, 1H), 8.26 (d, J = 11.2 Hz, 1H), 10.17 (s, 1H), ^{13}C NMR (100 MHz, DMSO-d_6): ***δ*** 20.90, 24.17, 26.34, 27.79, 31.98, 49.34, 102.33, 111.72, 111.89, 121.32, 122.86, 125.61, 126.52, 129.03, 141.47, 143.17, 143.32, 173.13.

(Z)-3-((E)-3-(2-((E)-1-butyl-3,3-dimethylindolin-2-ylidene)ethylidene)-2- chlorocyclohex-1-en-1-yl)-2-chloroacrylic acid ***(5)****:* mp >200◦C , 75% yield; ^{1}H NMR (400 MHz, DMSO-d_6): ***δ*** 0.96 (t, J = 7.20 Hz, 3H), 1.24 (s, 1H), 1.43 (dd, J =15.2 Hz, 2H), 1.57 (s, 1H), 1.67 (s, 6H), 2.73 (t, J = 5.60 Hz, 2H),4.24 (t, J = 6.80 Hz, 2H), 6.35 (d, J = 14.4 Hz, 1H), 7.29 (q, J = 6.40 Hz, 1H), 7.46 (q, J = 6.8 Hz, 3H), 7.65 (d, J = 7.20 Hz, 1H), 8.28 (d, J = 14.4 Hz, 1H), 10.18 (s, 1H); ^{13}C NMR (100 MHz, DMSO-d_6): ***δ*** 14.24, 20.00, 20.86, 26.30, 27.96, 29.66, 44.11, 49.49, 102.08, 112.05, 123.02, 125.66, 126.59, 129.12, 141.55, 142.56, 143.44,148.45, 172.70.

(Z)-3-((E)-3-(2-((E)-5-bromo-1,3,3-trimethylindolin-2-ylidene)ethylidene)-2-chlorocyclohex-1-en-1-yl)-2-chloroacrylic acid ***(6)***: mp >200◦ C; ^{1}H NMR (400 MHz, $CDCl_3$): ***δ*** 1.25 (s, 1H), 1.71 (s, 6H), 1.96 (t, J = 5.60 Hz, 2H), 2.76 (t, J = 5.40 Hz, 4H), 3.76 (s, 3H), 6.26 (d, J = 14.0 Hz, 1H), 7.07 (d, J = 8.40 Hz, 1H), 7.46 (s, 2H), 7.51 (d, J = 8.40 Hz, 1H), 8.31 (d, J = 14.0 Hz, 1H); ^{13}C

NMR (100 MHz, $CDCl_3$): ***δ*** 20.62, 26.87, 28.06, 33.00, 49.22, 102.34, 112.24, 118.39, 125.55, 128.75, 131.82, 141.96, 142.81, 144.28, 150.92, 172.19.

(Z)-3-((E)-3-(2-((E)-5-bromo-1-ethyl-3,3-dimethylindolin-2ylidene)ethylidene)-2-chlorocyclohex-1-en-1-yl)-2-chloroacrylic acid ***(7)***: mp >200◦ C, 74% yield; ^{1}H NMR (400 MHz, DMSO-d_6): ***δ*** 1.27 (t, *J* = 7.00 Hz, 3H), 1.67 (s, 6H), 1.84 (t, *J* = 5.60 Hz, 1H), 2.50 (s, 1H), 2.7 (t, *J* = 5.60 Hz, 2H), 3.36 (s, 3H), 4.22 (q, *J* = 6.80 Hz, 2H), 6.32 (d, *J* = 14.0 Hz, 1H), 7.42 (d, *J* = 8.40 Hz, 1H), 7.62 (d, *J* = 6.80 Hz, 1H), 7.92 (s, 1H), 8.24 (d, *J* = 14.0 Hz, 1H); ^{13}C NMR (100 MHz, DMSO-d_6): ***δ*** 20.84, 26.32, 27.58, 32.17, 49.51, 102.71, 113.74, 117.90, 126.12, 127.25, 131.76, 142.72, 143.29, 143.75, 148.55, 172.79.

(Z)-2-chloro-3-((E)-2-chloro-3-(2-((E)-5-chloro-1-ethyl-3,3-dimethylindolin-2-ylidene)ethylidene) cyclohex-1-en-1-yl) acrylic acid ***(8)***: mp >200◦ C, ^{1}H NMR (400 MHz, DMSO-d_6): ***δ*** 1.28 (t, *J* = 7.00 Hz, 3H), 1.67 (s, 6H), 1.84 (s, 1H), 2.50 (s, 1H), 2.72 (t, *J* = 5.00 Hz, 2H), 2.88 (s, 1H), 3.16 (s, 1H), 4.24 (m, 2H), 6.32 (d, *J* = 14.0 Hz, 1H), 7.47 (d, *J* = 8.40 Hz, 1H), 7.50 (d, *J* = 8.40, 1H), 7.80 (s, 1H), 8.25 (d, *J* = 14.0 Hz, 1H); ^{13}C NMR (100 MHz, DMSO-d_6): ***δ*** 20.79, 26.33, 47.48, 49.62, 58.70, 103.05, 114.25, 117.77, 126.01, 127.17, 131.62, 142.51, 143.37, 143.79, 148.46, 173.22.

(Z)-3-((E)-3-(2-((E)-5-bromo-1-(2-hydroxyethyl)-3,3-dimethylindolin-2-ylidene) ethylidene)-2-chlorocyclohex-1-en-1-yl)-2-chloroacrylic acid ***(9)***: mp >200◦ C; 70% yield; ^{1}H NMR (400 MHz, DMSO-d_6): ***δ*** 1.68 (s, 6H), 1.82 (t, *J* = 5.20, 1H), 2.68 (m, 2H), 2.72 (s, 2H), 2.88 (s, 2H), 3.77 (t, *J* = 5.00 Hz, 2H), 4.27 (t, *J* = 5.00 Hz, 2H), 6.40 (d, *J* = 14.0 Hz, 1H), 7.40 (d, *J* = 8.40 Hz, 1H), 7.60 (m, 1H), 7.90 (s, 1H), 7.93 (s, 1H), 8.23 (d, *J* = 14.0 Hz, 1H); ^{13}C NMR (100 MHz, $CDCl_3$): ***δ*** 12.45, 20.66, 26.96, 28.04, 30.95, 40.46, 49.33, 101.74, 111.66, 122.89, 128.52, 128.98, 130.91, 140.48, 142.79, 144.37, 150.80, 171.33.

(Z)-2-chloro-3-((E)-2-chloro-3-(2-((E)-5-methoxy-1,3,3-trimethylindolin-2-ylidene)ethylidene)cyclohex-1-en-1-yl)acrylic acid ***(10)***: mp 108-110◦ C; 70% yield; ^{1}H-NMR (400 MHz, DMSO-d_6): ***δ*** 1.60 (s, 6H), 1.80 (s, 1H), 2.09 (s, 1H), 2.35 (s, 2H), 2.68 (s, 2H), 3.65 (s, 3H), 6.22 (d, *J* = 11.6 Hz, 1H), 7.00 (d, *J* = 7.60 Hz, 1H), 7.30 (s, 1H), 7.37 (d, *J* = 8.00 Hz, 1H), 7.97 (s, 1H), 8.19 (d, *J* = 10.8 Hz, 1H), 10.19 (s, 1H); ^{13}C NMR (100 MHz, DMSO-d_6): ***δ*** 9.10, 20.97, 26.33, 27.76, 32.08, 46.20, 49.48, 56.36, 101.87, 108.44, 109.56, 112.56, 114.04, 125.63, 132.17, 136.86, 141.98, 143.23, 147.07, 158.37, 172.08, 189.34.

(Z)-3-((E)-3-(2-((E)-1-butyl-5-methoxy-3,3-dimethylindolin-2-ylidene)ethylidene)-2-chlorocyclohex-1-en-1-yl)-2-chloroacrylic acid ***(11)***: mp 118-120° C; 74% yield; ^{1}H NMR (400 MHz, DMSO-d_6): ***δ*** 0.93 (t, *J* = 7.20 Hz, 4H), 1.24 (s, 1H), 1.40 (d, *J* = 8.00 Hz, 2H), 1.66 (s, 9H), 1.87 (t, *J* = 5.60 Hz, 1H), 2.68 (s, 2H), 3.82 (s, 3H), 4.20 (t, *J* = 7.20 Hz, 2H), 6.26 (d, *J* = 14.4 Hz, 1H), 7.00 (dd, *J* = 8.80 Hz, 1H), 7.32 (d, *J* = 2.40 Hz, 1H), 7.39 (d, *J* = 8.80 Hz, 1H) 8.21 (d, *J* = 14.0 Hz, 1H), 10.18 (s, 1H); ^{13}C NMR (100 MHz, DMSO-d_6): ***δ*** 14.23, 19.98, 20.92, 26.28, 27.92, 29.68, 44.16, 49.61, 56.36, 101.61, 109.65, 112.74, 114.20, 125.66, 136.06, 142.21, 143.35, 147.32, 158.37, 171.67.

(Z)-2-chloro-3-((E)-2-chloro-3-((Z)-2-(3-ethylbenzo[d]thiazol-2(3H)-ylidene)ethylidene)cyclohex-1-en-1-yl)acrylic acid ***(12)***: mp 118-120 °C ; 70% yield; ^{1}H NMR (400 MHz, DMSO-d_6): ***δ*** 1.23 (s,2H), 1.34 (t, *J* = 7.20 Hz, 3H), 1.85 (t, *J* = 4.80 Hz, 2H), 2.68 (s, 2H), 4.49 (d, *J* = 7.20 Hz, 2H),6.52 (d, *J* = 13.6 Hz, 1H), 7.40 (t, *J* = 7.60 Hz, 1H) , 7.58 (t, *J* = 7.20 Hz, 2H), 7.82 (q, *J* = 13.6 Hz, 2H), 7.98 (d, *J* = 7.60 Hz, 1H); ^{13}C NMR (100 MHz, DMSO-d_6): ***δ*** 13.24, 15.64, 21.24, 27.00, 65.39, 89.97, 100.25, 110.68, 113.84, 123.64, 124.85, 126.04, 128.68, 137.97, 141.08, 141.74, 144.70, 146.35, 163.58, 189.26.

(Z)-2-chloro-3-((E)-2-chloro-3-((E)-2-(3-hexyl-1,1-dimethyl-1,3-dihydro-2H-benzo[e]indol-2-ylidene)ethylidene)cyclohex-1-en-1-yl)acrylic acid ***(13)***: mp 114-116° C; 75% yield; ^{1}H NMR (400 MHz, DMSO-d_6): ***δ*** 0.84 (s, 2H), 1.20 (s, 4H), 1.64 (s, 9H), 1.83 (s, 2H), 1.94 (s, 2H), 2.66 (s, 2H), 4.10 (s, 2H), 6.20 (d, *J* = 14.0 Hz, 2H), 6.98 (s, 1H), 7.34 (t, *J* = 7.20 Hz, 3H), 7.50 (s, 1H), 7.60 (s, 1H), 8.18 (d, *J* = 14.0 Hz, 1H). ^{13}C NMR (100 MHz, DMSO-d_6): *δ* 14.26, 20.93, 22.41, 26.30, 27.74, 31.99, 49.46, 56.32, 101.79, 109.48, 112.53, 114.04, 125.68, 136.81, 141.99, 143.23, 147.07, 158.33, 172.10.

(Z)-3-((E)-3-((Z)-2-(6-bromo-3-methylbenzo[d]thiazol-2(3H)-ylidene)ethylidene)-2-chlorocyclohex-1-en-1-yl)-2-chloroacrylic acid ***(14)***: mp >200 °C, 50% yield; ^{1}H NMR (400 MHz, DMSO-d_6): ***δ*** 2.63 (m, 4H), 3.17 (s, 2H), 3.81 (s, 3H), 6.42 (d, *J* = 13.2 Hz, 1H), 7.12 (d, *J* = 6.40 Hz, 1H), 7.28 (t, *J* = 7.20 Hz, 1H), 7.48 (m, 2H), 8.18 (s, 1H). ^{13}C NMR (100 MHz, DMSO-d_6): 21.25, 49.57, 84.30, 101.08, 117.61, 118.49, 125.54, 125.96, 128.51, 138.04, 140.80, 146.26.

(Z)-3-((E)-3-((Z)-2-(3-butylbenzo[d]thiazol-2(3H)-ylidene)ethylidene)-2-chlorocyclohex-1-en-1-yl)-2-chloroacrylic acid ***(15)***: mp >200 °C; 50% yield; ^{1}H NMR (400 MHz, DMSO-d_6): ***δ*** 0.94 (t, *J* = 7.40 Hz, 3H), 1.41 (q, *J* = 7.40 Hz, 2H), 1.72 (m, 2H), 1.85 (s, 2H), 2.67 (s, 4H), 4.45 (s, 2H), 6.50 (d, *J* = 14.0 Hz, 1H), 6.98 (s, 1H), 7.42 (m, 1H), 7.58 (m,1H), 7.76 (d, *J* = 8.00 Hz, 1H), 7.82

(d, *J* = 14.0 Hz, 1H), 7.98 (d, *J* = 4.00 Hz, 1H). ^{13}C NMR (100 MHz, DMSO-d_6): 14.05, 14.15, 19.79, 21.00, 26.95, 46.47, 59.74, 100.48, 114.08, 123.58, 124.87, 125.72, 125.86, 128.69, 129.89, 140.94, 142.10, 144.68, 163.86.

(Z)-2-chloro-3-((E)-2-chloro-3-((E)-2-(1,1,3-trimethyl-1,3-dihydro-2H-benzo[e]indol-2-ylidene)ethylidene)cyclohex-1-en-1-yl)acrylic acid ***(16)***: mp 148-150° C; 76% yield; ^{1}H NMR (400 MHz, DMSO-d_6): ***δ*** 1.09 (s, 6H), 1.96 (t, *J* = 18.0 Hz, 4H), 2.6 (s, 2H), 3.8 (s, 3H), 6.37 (d, *J* = 14.0 Hz, 1H), 7.53 (d, *J* = 6.80 Hz, 1H), 7.67 (d, *J* = 6.40 Hz, 1H), 7.8 (d, *J* = 8.40 Hz, 1H), 7.90 (d, *J* = 6.00 Hz, 1H), 8.12 (t, *J* = 8.00 Hz, 2H), 8.31 (d, *J* = 18.0 Hz, 1H), 8.39 (d, *J* = 14.0 Hz, 1H), 10.13 (s, 1H); ^{13}C NMR (100 MHz, DMSO-d_6): ***δ*** 20.96, 24.67, 26.42, 27.35, 32.44, 101.07, 102.03, 112.23, 116.94, 121.40, 122.77, 125.43, 127.87, 128.26, 131.95, 133.91, 139.02, 140.95, 142.18, 142.84, 147.55, 150.71, 164.44, 174.28.

(Z)-2-chloro-3-((E)-2-chloro-3-((E)-2-(3-hexyl-1,1-dimethyl-1,3-dihydro-2H-benzo[e]indol-2-ylidene)ethylidene)cyclohex-1-en-1-yl)acrylic acid ***(17)***: mp 114-116° C; 75% yield; ^{1}H NMR (400 MHz, DMSO-d_6): ***δ*** 0.84 (s, 2H), 1.2 (s, 4H), 1.64 (s, 9H), 1.83 (s, 2H), 1.94 (s, 2H), 2.66 (s, 2H), 4.10 (s, 2H), 6.20 (d, *J* = 14.0 Hz, 2H), 6.98 (s, 1H), 7.34 (t, *J* = 7.20 Hz, 3H), 7.50 (s, 1H), 7.60 (s, 1H), 8.18 (d, *J* = 14.0 Hz, 1H). ^{13}C NMR (100 MHz, DMSO-d_6): ***δ*** 14.26, 20.93, 22.41, 26.30, 27.74, 31.99, 49.46, 56.32, 101.79, 109.48, 112.53, 114.04, 125.68, 136.81, 141.99, 143.23, 147.07, 158.33, 172.10.

(Z)-3-((E)-3-(2-((E)-1-benzylquinolin-4(1H)-ylidene)ethylidene)-2-chlorocyclohex-1-en-1-yl)-2-chloroacrylic acid ***(18)***: mp 163-165° C ; 66% yield; ^{1}H NMR (400 MHz, DMSO-d_6): ***δ*** 1.69 (s, 2H), 2.39 (s, 2H) 2.71 (s, 2H), 5.20 (s, 2H), 6.50 (d, *J* = 6.80 Hz, 1H), 6.64 (d, *J* = 12.4 Hz, 2H), 7.19 (d, *J* = 7.60 Hz, 1H), 7.25 (t, *J* = 7.20 Hz, 4H), 7.43 (d, *J* = 6.80 Hz, 4H), 7.74 (d, *J* = 6.80 Hz, 2H), 8.1 (d, *J* = 7.20 Hz, 1H), 10.1 (s, 1H).

(E)-2-((E)-2-(3-((Z)-2-carboxy-2-chlorovinyl)-2-chlorocyclohex-2-en-1-ylidene)ethylidene)-1-methyl-1,2-dihydroquinoline-6-carboxylic acid ***(19)***: mp >200° C; 65% yield; ^{1}H NMR (400 MHz, DMSO-d_6): ***δ*** 1.20 (t, *J* = 11.2 Hz, 2H), 1.67 (s, 2H), 1.90 (s, 2H), 2.35 (s, 3H), 5.60 (s, 2H), 7.30 (d, *J* = 16.8 Hz, 2H), 7.60 (s, 2H), 7.94 (d, *J* = 18.0 Hz, 2H), 10.06 (s, 2H); ^{13}C NMR (100 MHz, DMSO-d_6): 22.11, 24.55, 27, 44, 50.66, 96.12, 114,34, 117.44, 120.11, 122.23, 123.21, 124.22, 127.44, 129.33, 130.11, 131.22, 136.33, 140.22, 146.11, 147.33, 180.11.s

(Z)-3-((E)-3-(2-((E)-1-benzylquinolin-2(1H)-ylidene)ethylidene)-2-chlorocyclohex-1-en-1-yl)-2-chloroacrylic acid ***(20)***: mp: 158-160° C; 72% yield; ^{1}H NMR (400 MHz, DMSO-d_6): ***δ*** 1 (d, *J* =

13.60 Hz, 1H), 1.20 (s, 1H), 1.50 (s, 2H), 2.20 (s, 2H), 5.30 (s, 2H), 5.40 (d, J = 12.8 Hz, 1H), 5.70 (s, 1H), 6.10 (d, J = 13.6 Hz, 1H), 7.10 (d, J = 7.20 Hz, 1H), 7.2 (s, 2H), 7.3 (d, J = 5.60 Hz, 2H), 7.40 (d, J = 11.20 Hz, 2H), 7.70 (t, J = 15.2 Hz, 1H), 7.90 (d, J = 7.60 Hz, 1H), 8.11 (d, J = 10.0 Hz, 1H); ^{13}C NMR (100 MHz, DMSO-d_6): $\boldsymbol{\delta}$ 20.95, 24.65, 27.08, 50.62, 97.31, 114.64, 118.16, 120.31, 122.17, 122.64, 123.49, 126.74, 127.69, 128.61, 129.38, 131.46, 131.50, 131.84, 132.08, 136.05, 141.42, 143.25, 146.51, 148.62, 189.13.

Computational Methods

Geometry optimization and vibrational frequency calculations for fluorophores **4**-**20** were carried out with BLYP[2, 3] density functional with Pople's 6-311G(d,p) basis set[4] in implicit equilibrium, Linear Response Polarizable Continuum Model (PCM)[5-8] with ethanol as the solvent. Each was carried out using an ultrafine integration grid[9] with tight convergence criteria in the geometry optimization (i.e. for changes in the density matrix during SCF calculations 10^{-8} a.u.; for forces and displacements 10^{-6} a.u. during the geometry optimizations) to guarantee a reliable calculation of vibrational frequencies. Each optimized geometry is found to be in energy minimum and contains no imaginary frequencies. For compound **20**, due to the existence of a rotatable bond connecting the phenyl group with the methylamine of the quinoline group (Supporting Information, Figure S55), two unique different conformations are possible. However, these conformations are found to be degenerate in total energy.

The adiabatic time-dependent Density Functional Theory (TD-DFT)[10] calculations were performed at BLYP/6-311+G(d,p) level of theory in ethanol with implicit PCM to calculate the ten lowest singlet excited states for each compound. The Natural Transition Orbitals (NTO)[11] for the two highest occupied molecular orbitals (HOMO) and two lowest unoccupied molecular orbitals (LUMO) for each compound, corresponds to the $S_0 \rightarrow S_1$ transitions were also calculated and analyzed (Supporting Information Table S2). Due to well-known deficiency of TD-DFT in the calculation of charge-transfer states, the analysis is also assisted with the frontier natural orbitals obtained at HF/6-311+G(d,p) level of theory (Supporting Information, Figure S37 – S53). All calculations were done using Gaussian16 program Revision A.03.[12] The depiction of the natural orbitals were done using Jmol at 0.02 electron isodensity surface[13].

Cell Culture

Triple negative breast cancer (TNBC) cell lines HCC1806, HCC70 and BT-20 were cultured in their respective media; RPMI-1640, 1X (Corning, USA) for HCC1806 and HCC70 and Eagle's Minimum Essential Medium (Corning, USA) for BT-20 supplemented with 10% of fetal bovine serum (Gibco, USA) and 1% of penicillin-streptomycin-gentamycin (Thermo Scientific, USA) at 37 ^{o}C and 5% CO_2 incubator. Stock solutions from the synthesis of D – π – A, fluorophores **4**, **7**, **10**, **12** and docetaxel were prepared to a final concentration of 10 mM in 100% sterile dimethyl sulfoxide (DMSO). TNBC cell lines were counted and suspended into 96-well plate to a final volume of 100 µL/well. Cells were seeded in different quantities depending on their doubling time (4000 cells/mL of HCC1806, 4500 cells/mL of HCC70, and 5500 cells/mL of BT-20). Seeded plates were incubated for 24 h at 37 ^{o}C and 5% CO_2.

Cytotoxic Assay

Measurement of cytotoxic activity of fluorophore analogs *in vitro* was done by MTT 3-(4,5-dimethylthiazol-2-yl)-2,5-diphenyltetrazolium bromide assay. A 96-well plate seeded with cells was treated with increasing concentration of the analogs diluted in respective medium with an initial concentration of 10 mM dissolved in DMSO. Post-48 h incubation, medium in each well was replaced with fresh 100 µL of respective media containing 0.5 mg/mL of MTT (3-(4,5-dimethylthiazol-2-yl)-2,5-diphenyltetrazolium bromide) dye. Prior to 4 h incubation at 37 ^{o}C and 5% CO_2, 100 µL of 100% DMSO was added to each well. Measurement of cell viability by its absorbance on SpectraMax microplate reader was done at optical density of 570 nm. Data obtained were analyzed with Prism 8 GraphPad statistical software to generate inhibitory concentration at 50% (IC_{50}) values.

^{1}H and ^{13}C NMR Spectra of the Fluorophores

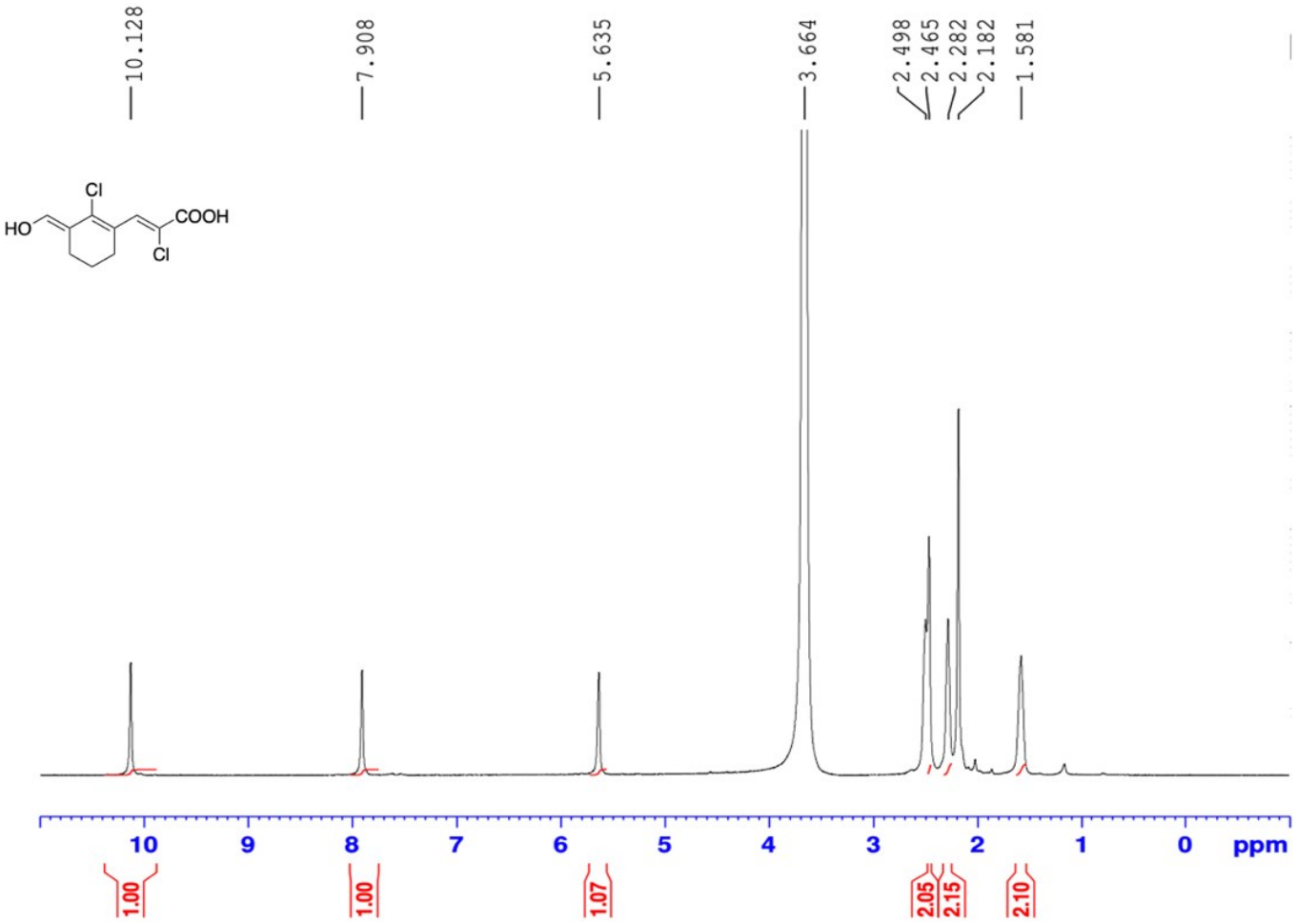

Figure S1. ^{1}H NMR of acceptor and linker unit **(3)** in DMSO-*d6*.

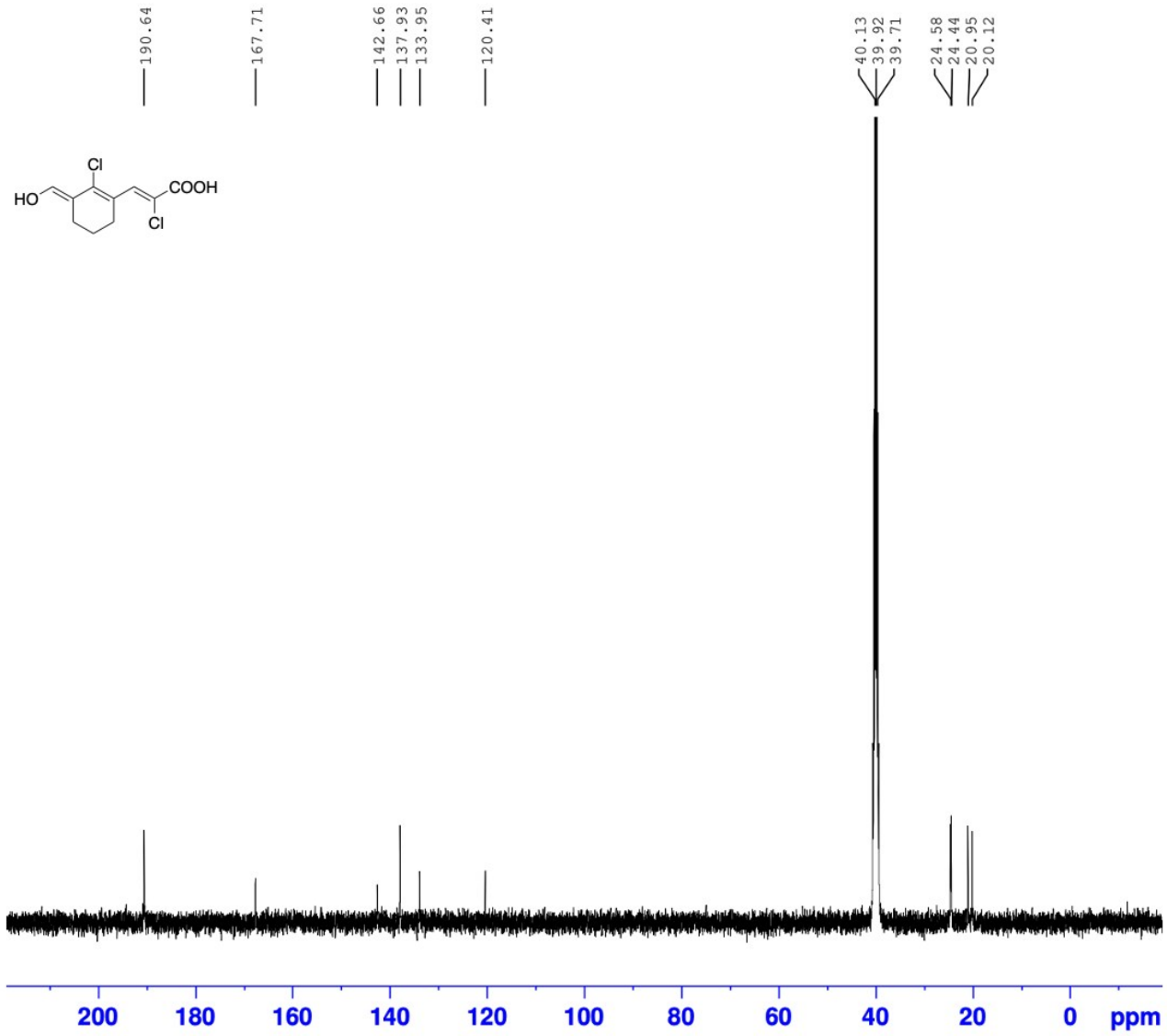

Figure S2. ^{13}C NMR of acceptor and linker unit **(3)** in DMSO-*d6*.

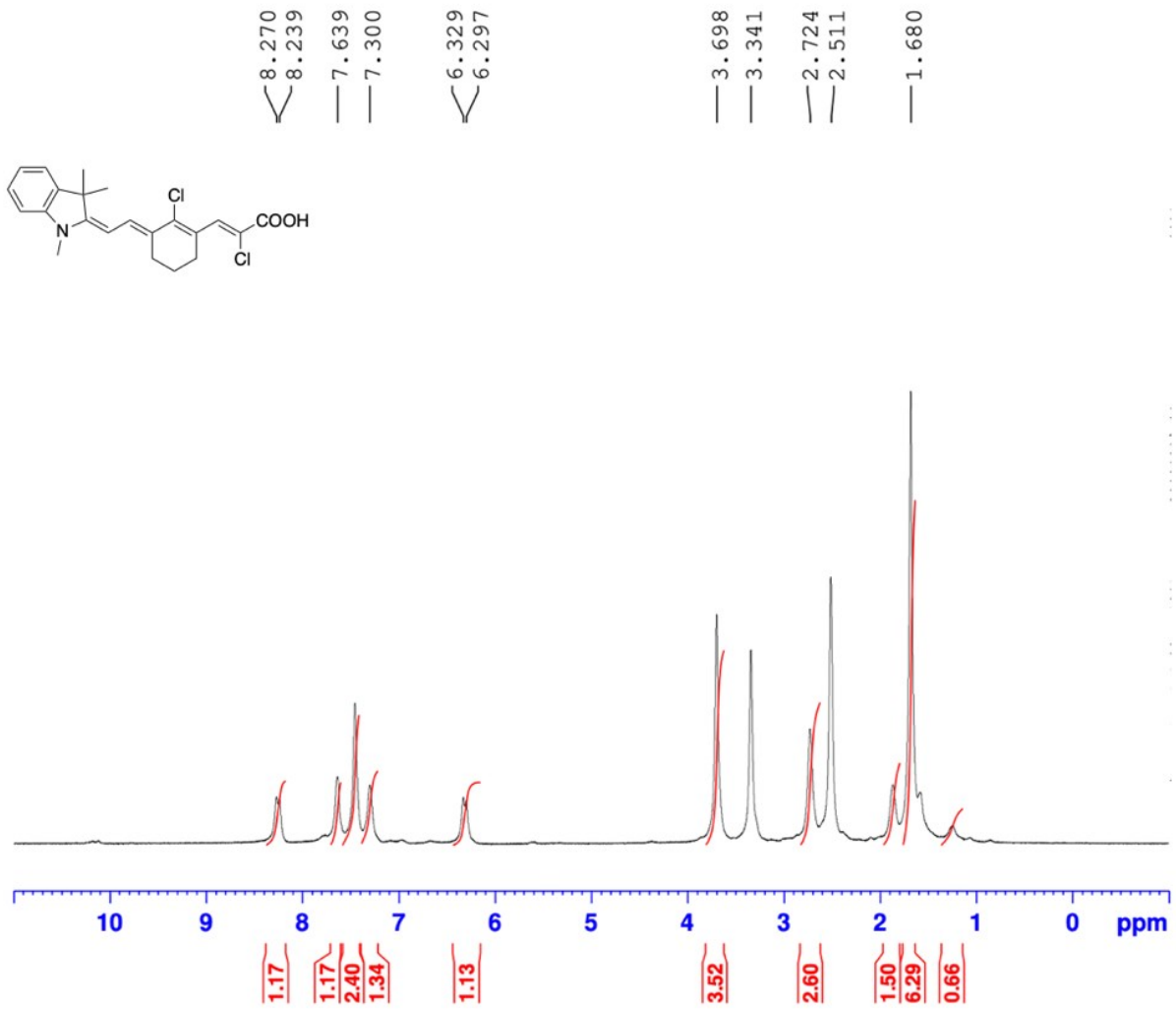

Figure S3. ^{1}H NMR of fluorophore **4** in DMSO-*d6*.

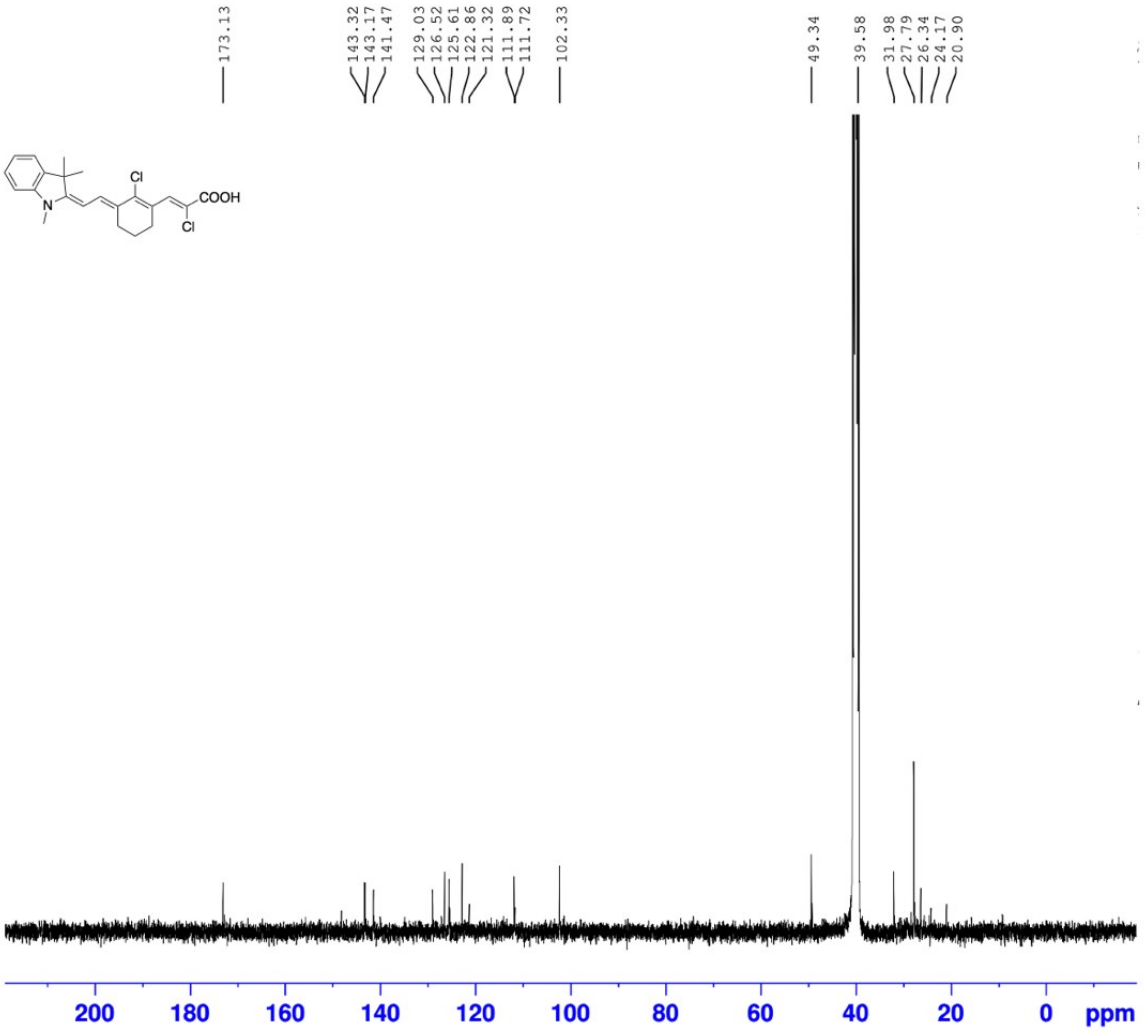

Figure S4. ^{13}C NMR of fluorophore **4** in DMSO-*d6*.

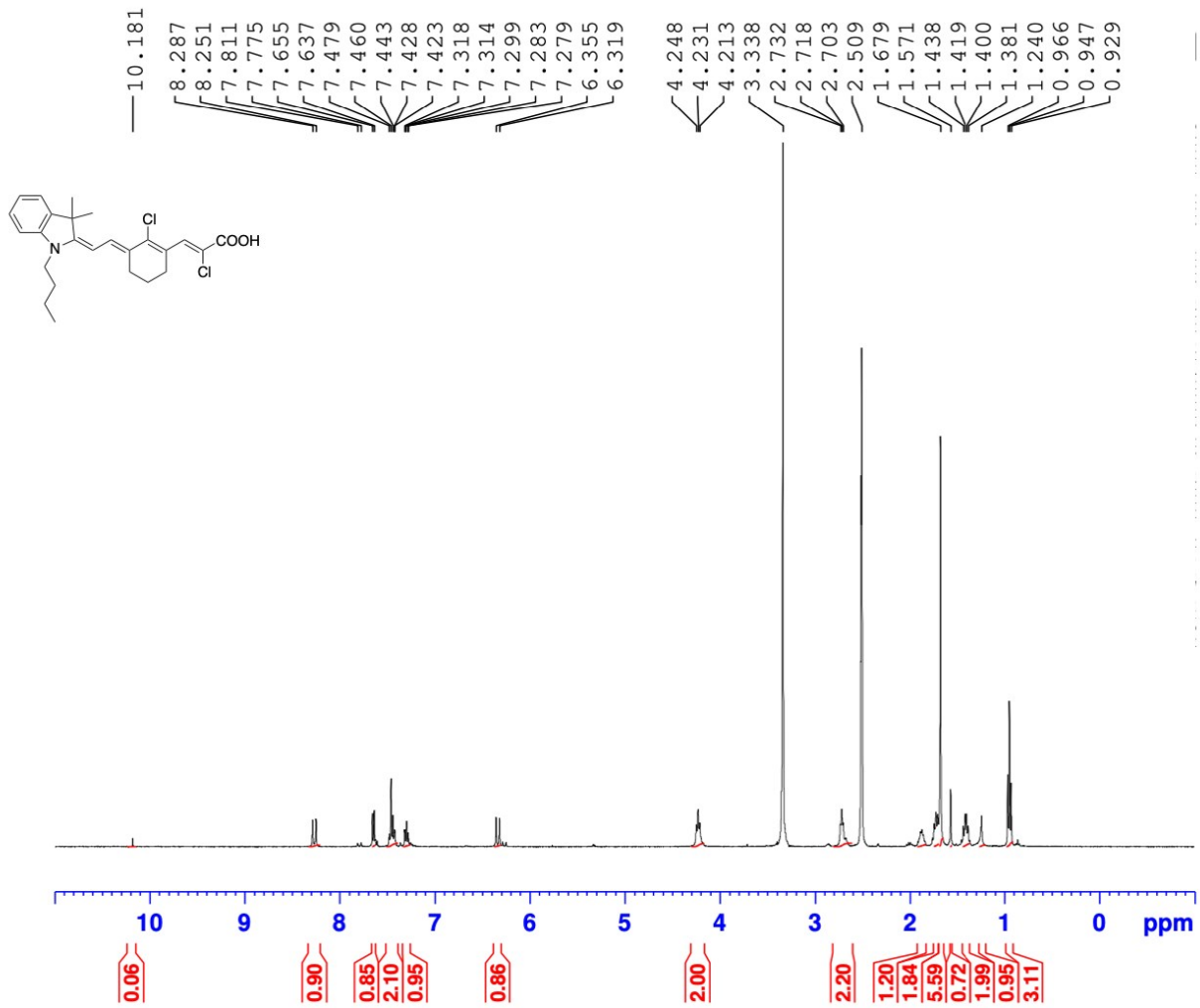

Figure S5. [1]H NMR of fluorophore **5** in DMSO-*d6*.

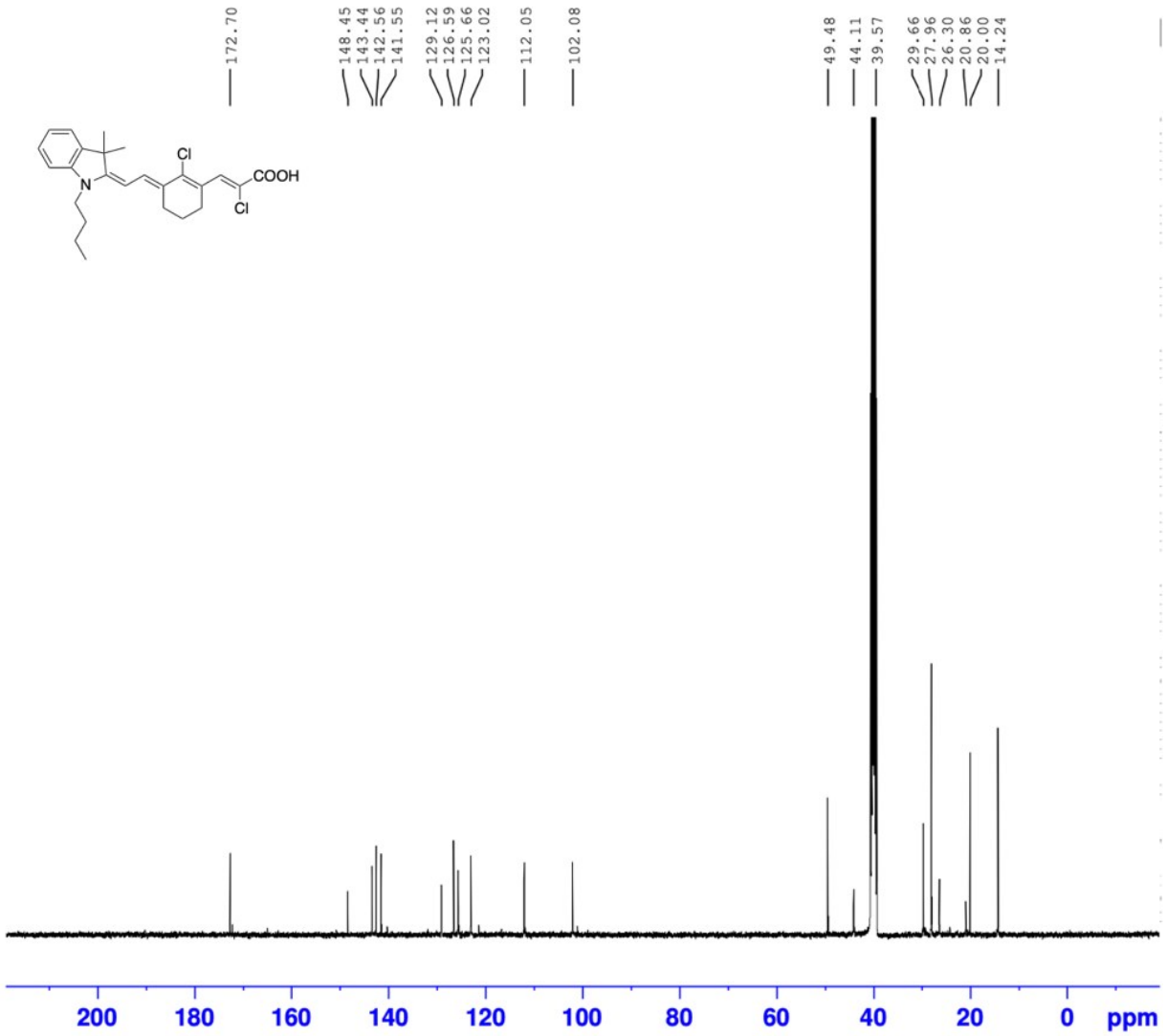

Figure S6. ^{13}C NMR of fluorophore **5** in DMSO-*d6*.

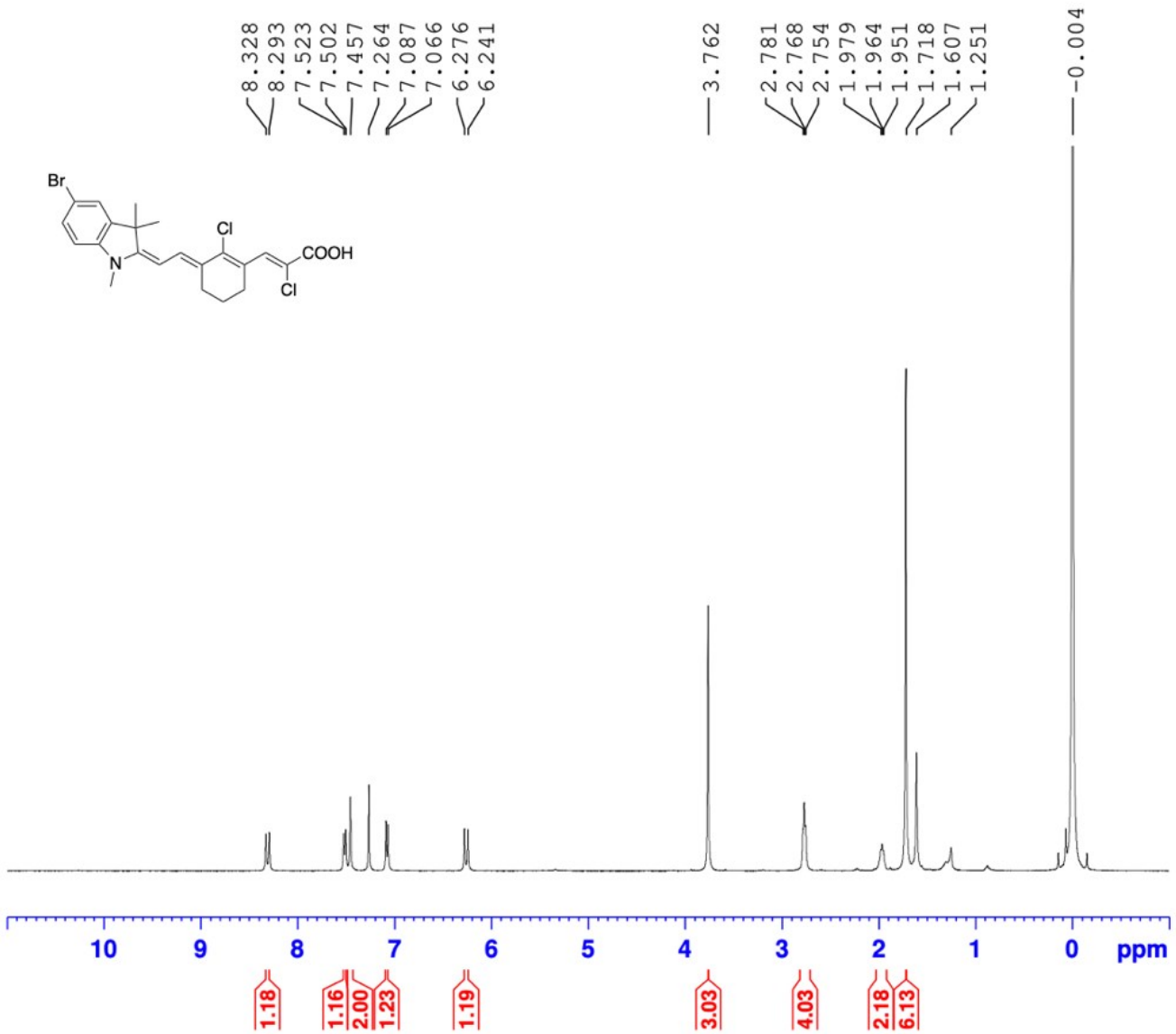

Figure S7. ^{1}H NMR spectra of fluorophore **6** in $CDCl_3$.

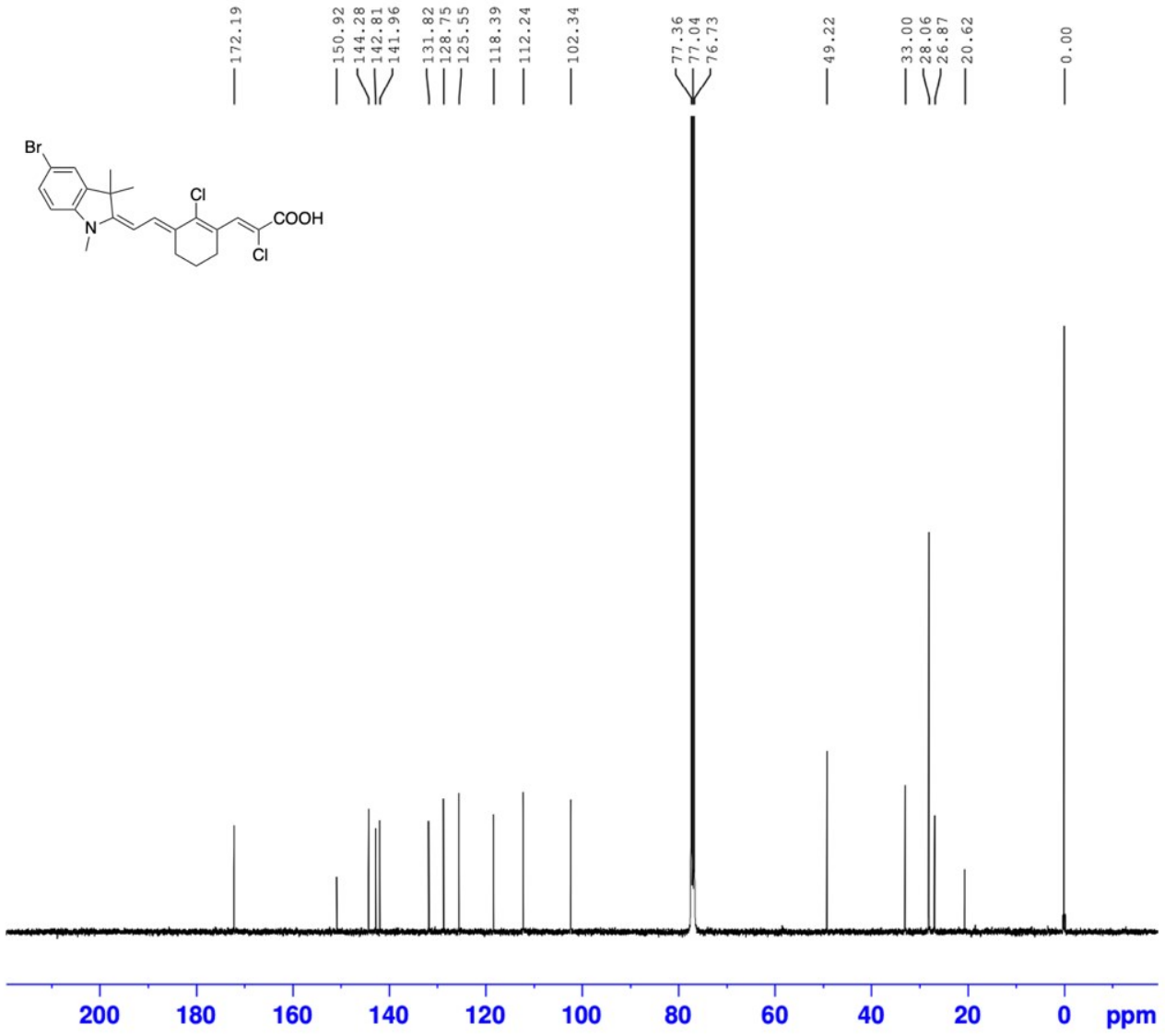

Figure S8. [1]H NMR spectra of fluorophore **6** in DMSO-*d6*.

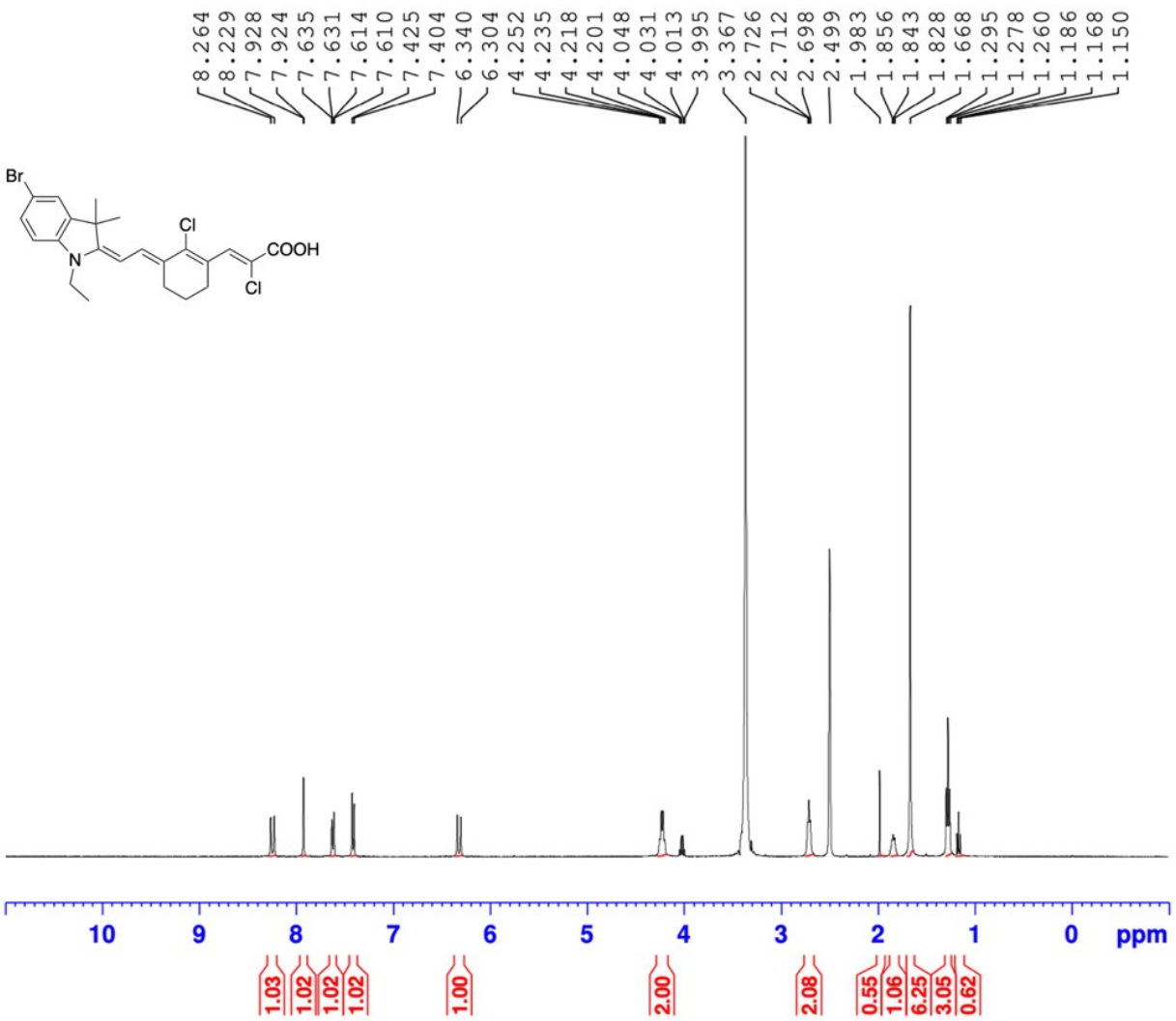

Figure S9. ^{13}C NMR spectra of fluorophore **7** in DMSO-*d6*.

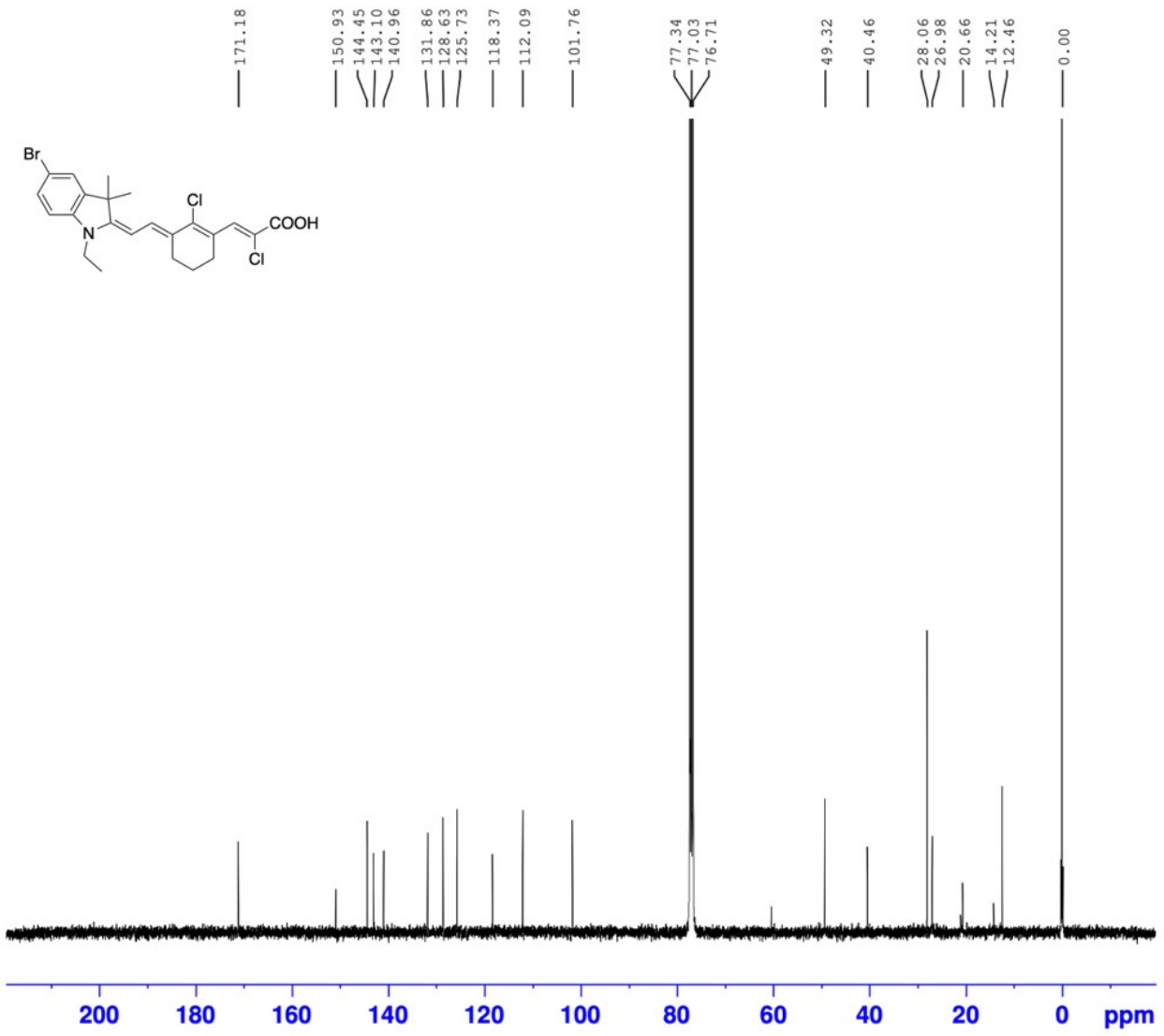

Figure S10. ^{13}C NMR spectra of fluorophore **7** in DMSO-*d6*.

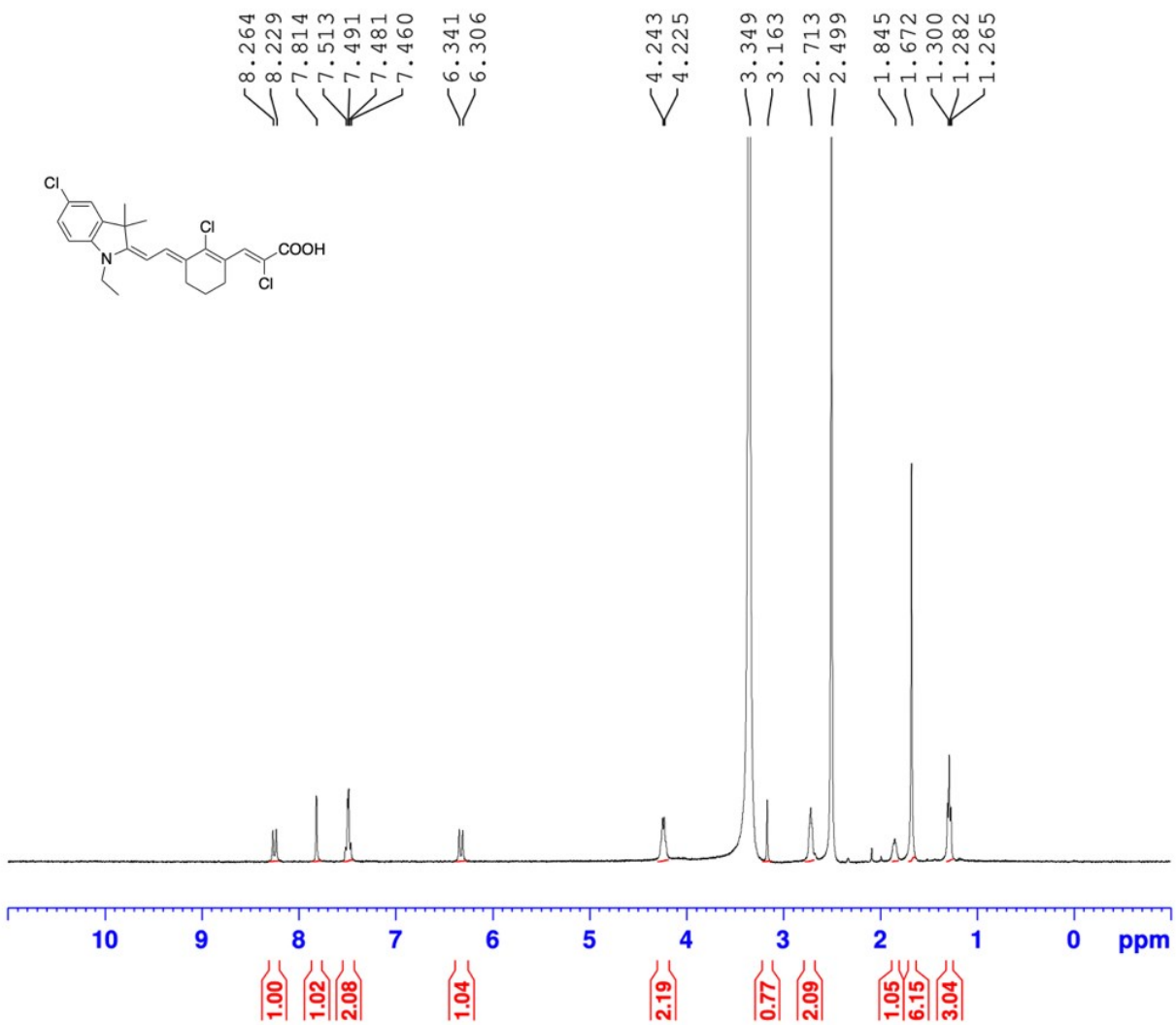

Figure S11. [1]H NMR of fluorophore **8** in DMSO-*d6*.

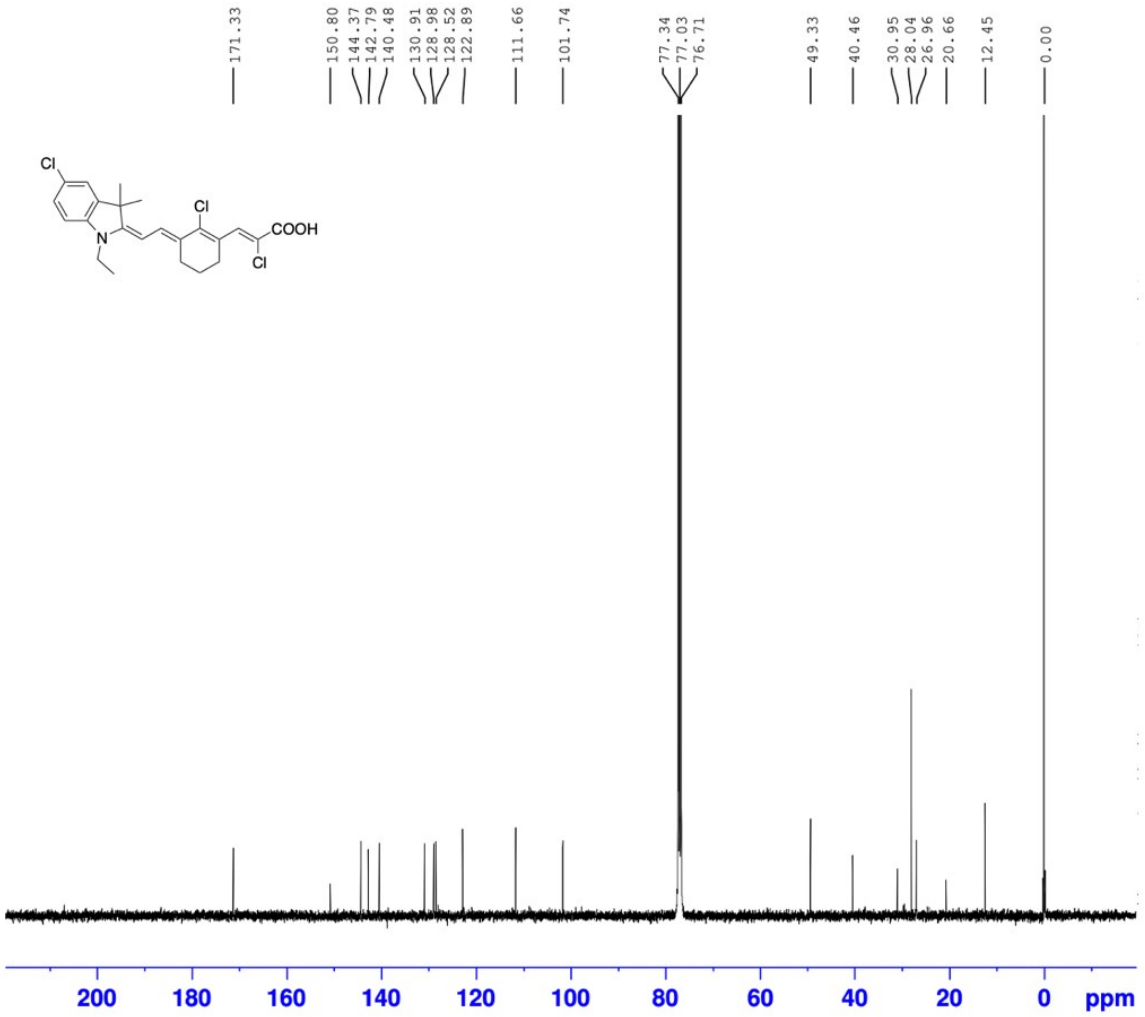

Figure S12. ^{13}C NMR of fluorophore **8** in DMSO-*d6*.

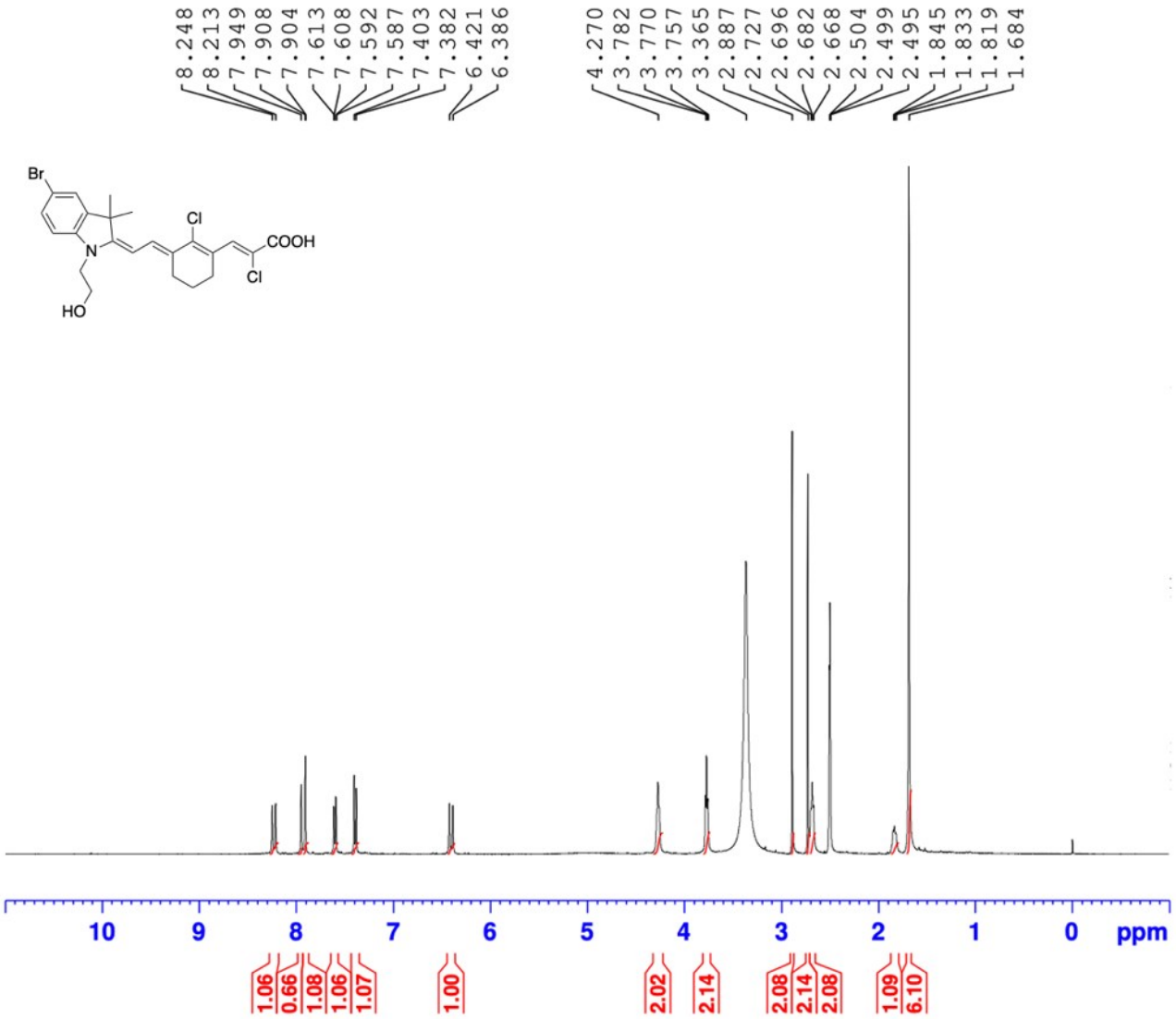

Figure S13. ^{1}H NMR of fluorophore **9** in DMSO-*d6*.

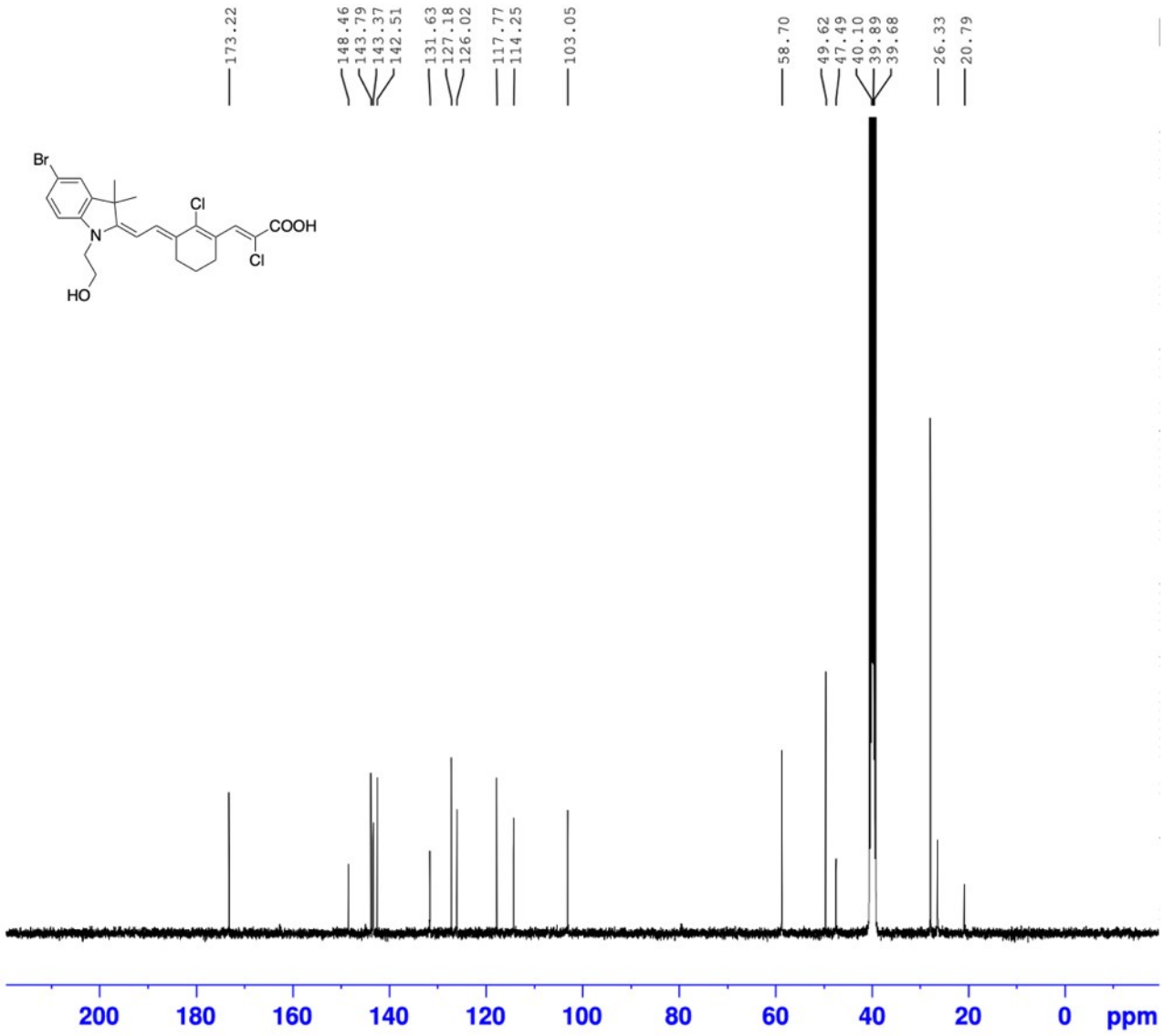

Figure S14. ^{13}C NMR of fluorophore **9** in DMSO-*d6*.

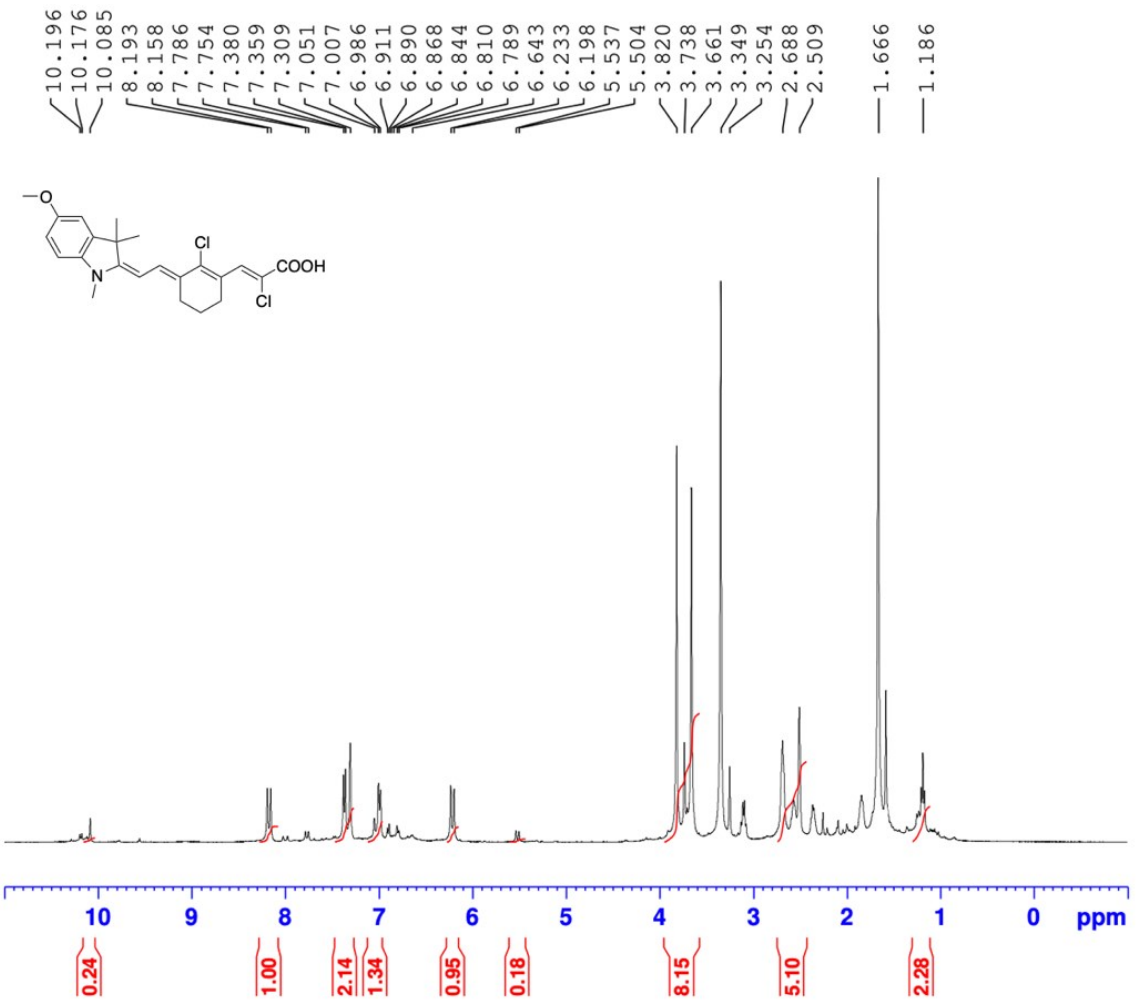

Figure S15. ^{1}H NMR spectra of fluorophore **10** in DMSO-*d6*.

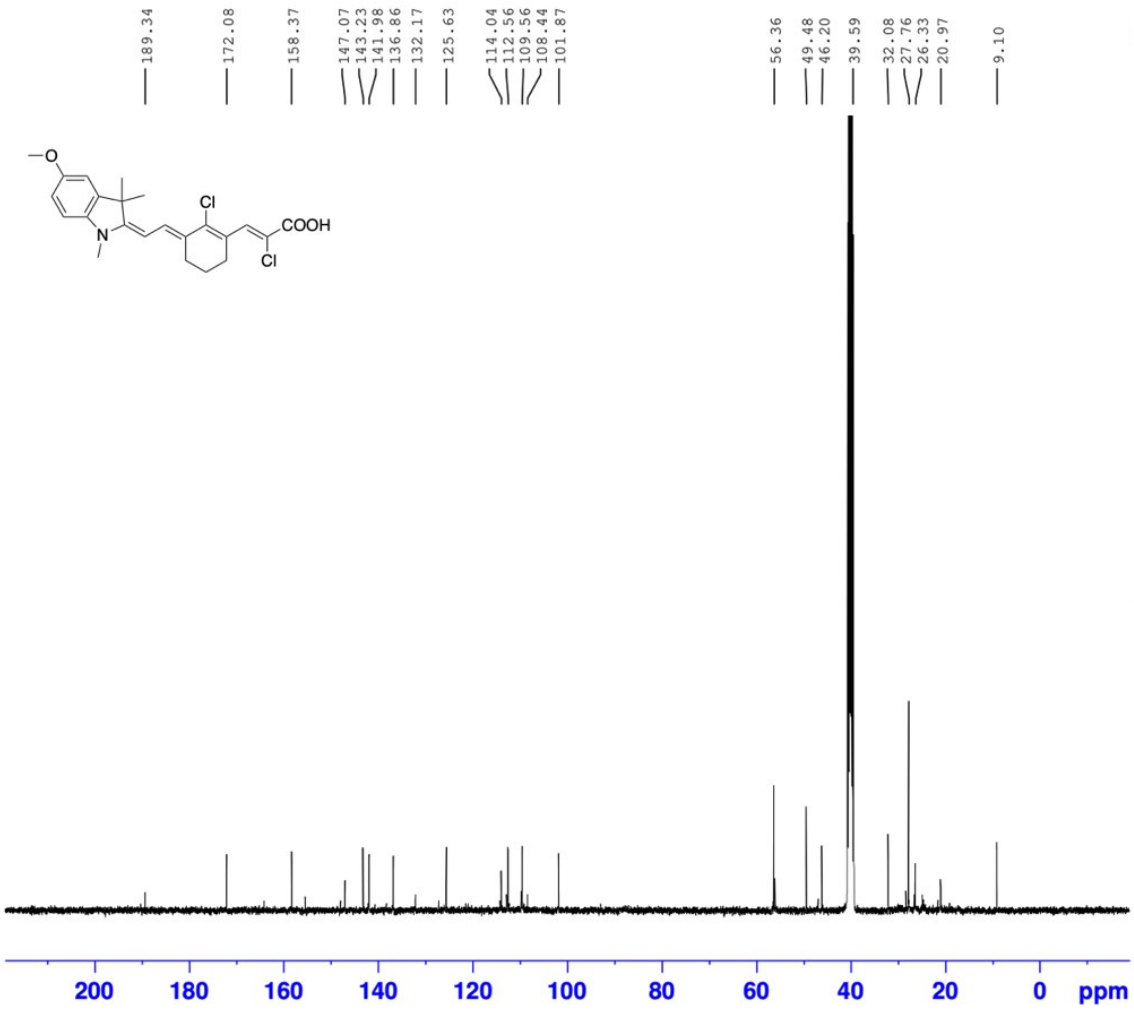

Figure S16. ^{13}C NMR spectra of fluorophore **10** in DMSO-*d6*.

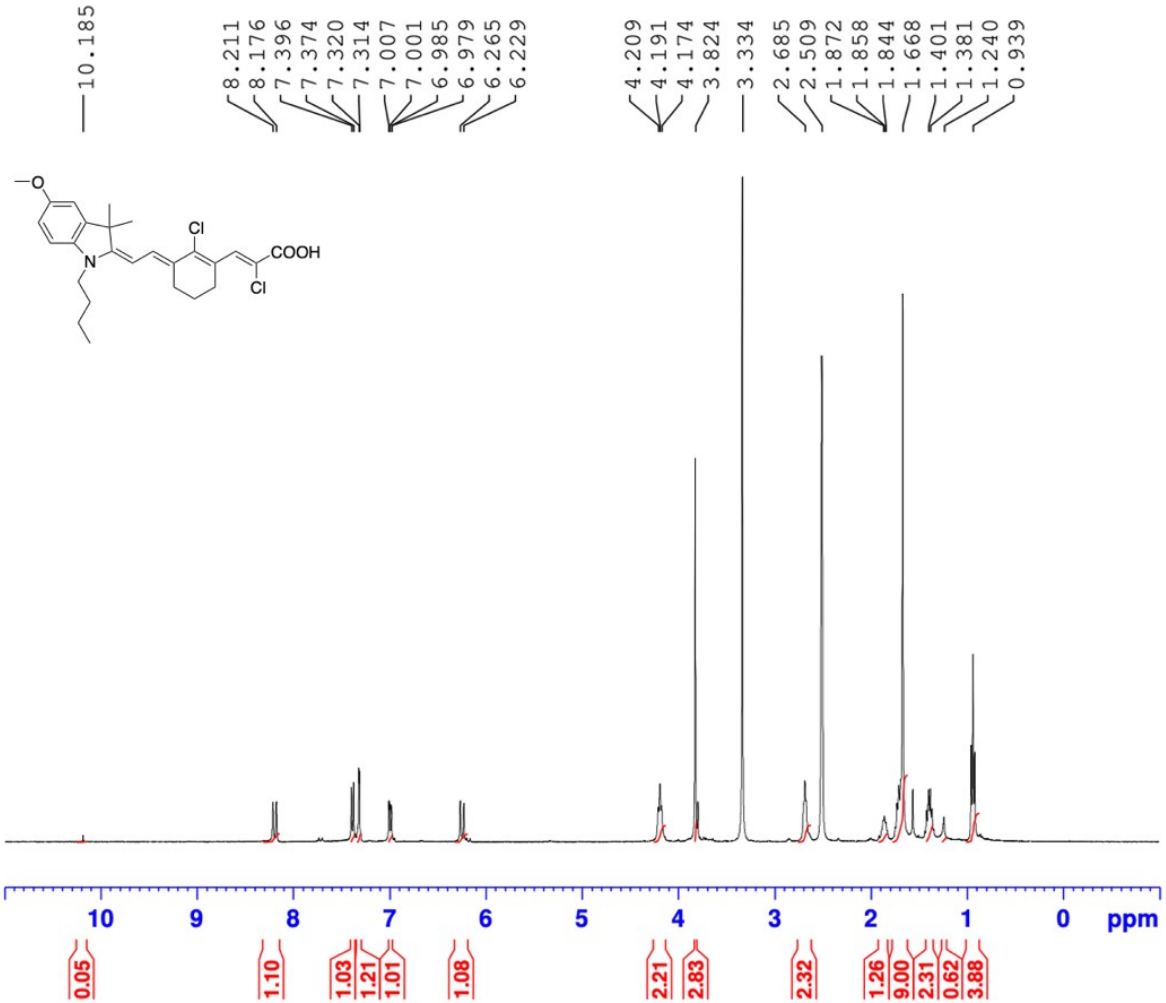

Figure S17. ^{1}H NMR spectra of fluorophore **11** in DMSO-*d6*.

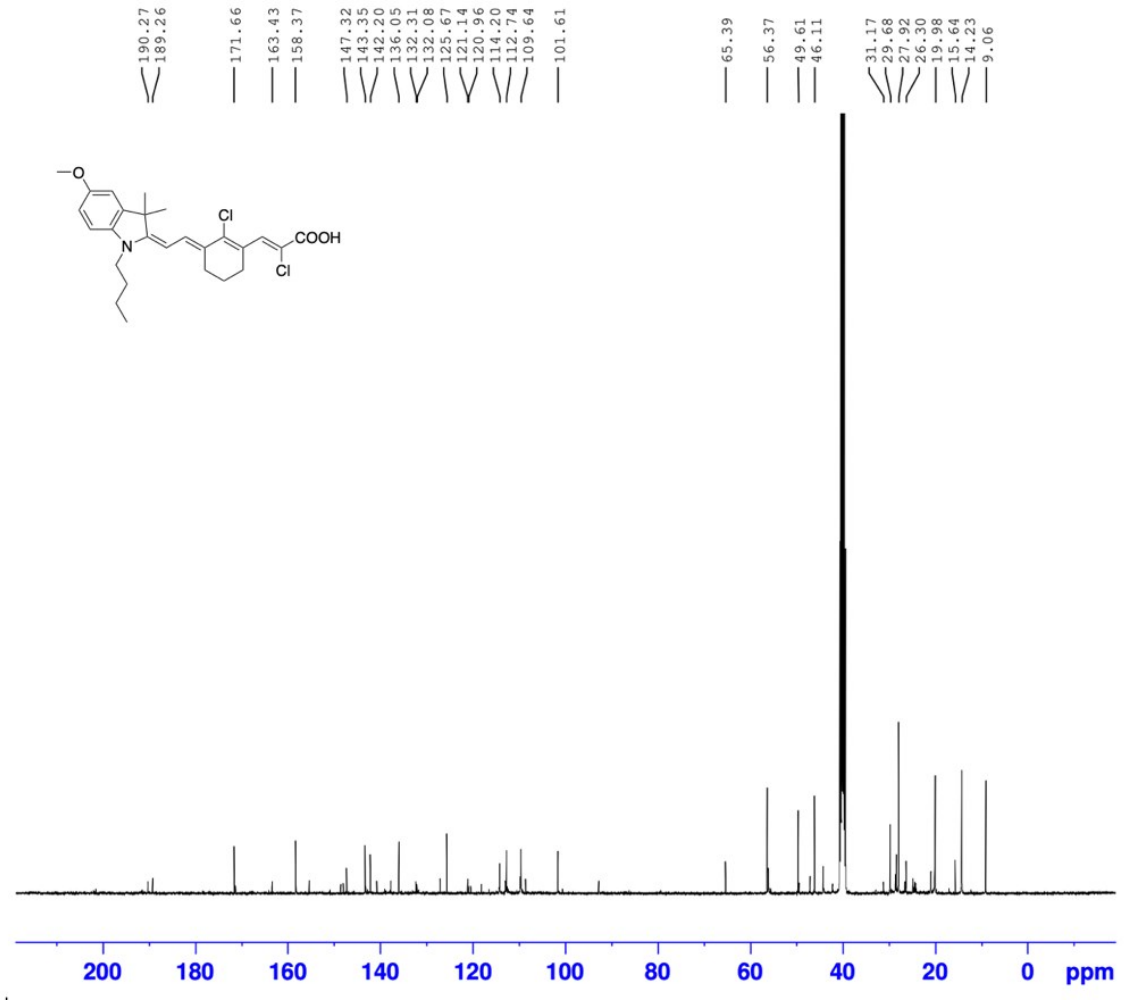

Figure S18. ^{13}C NMR spectra of fluorophore **11** in DMSO-*d6*.

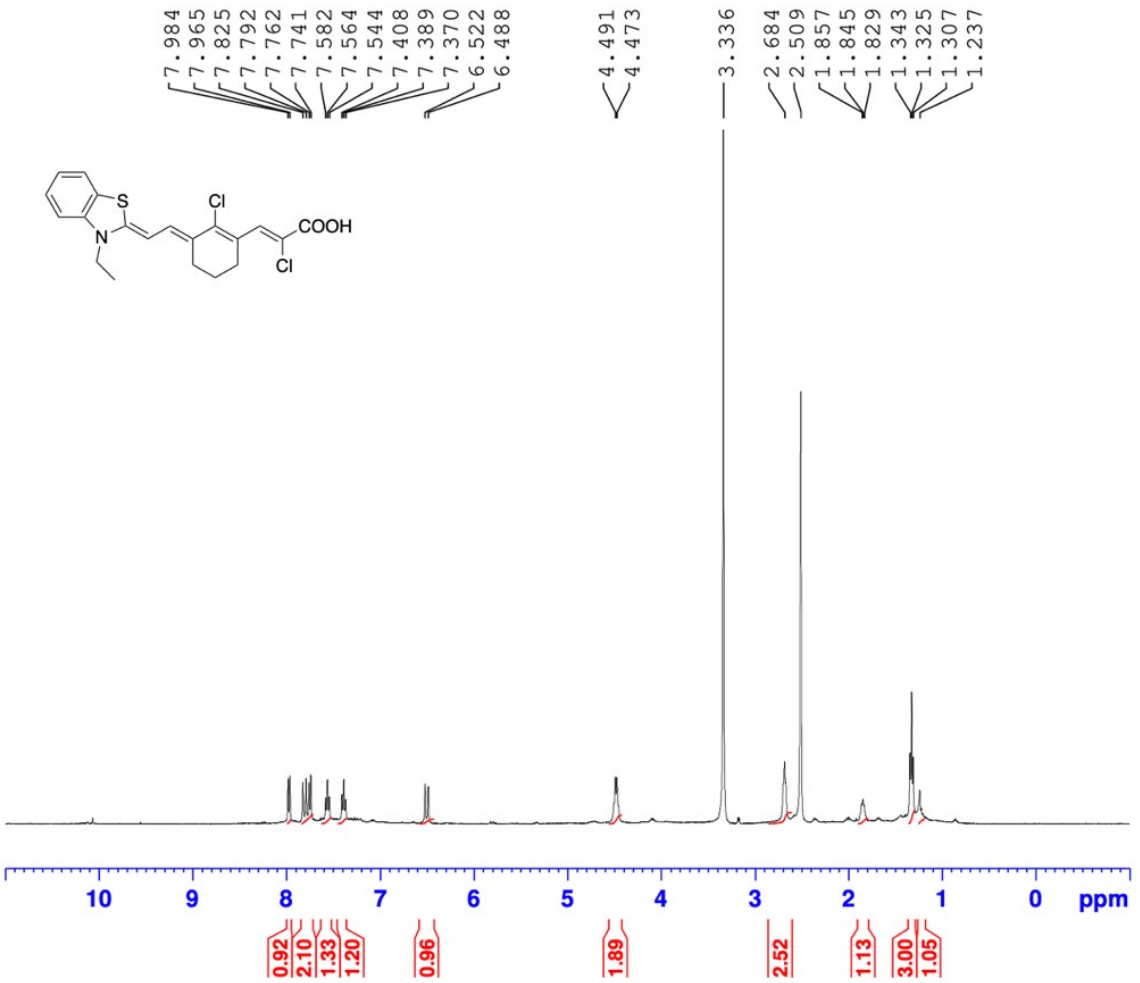

Figure S19. [1]H NMR spectra of fluorophore **12** in DMSO-*d6*.

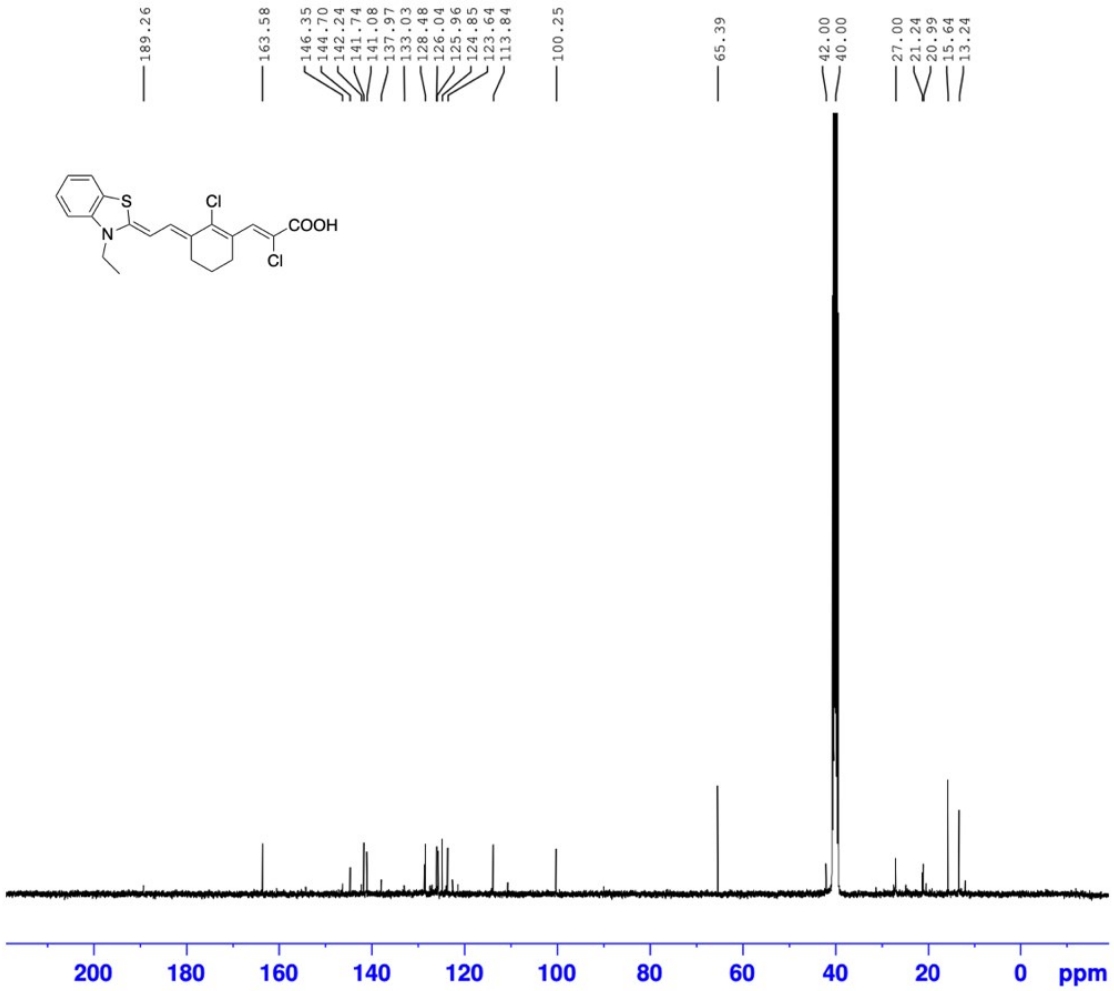

Figure S20. ^{13}C NMR spectra of fluorophore **12** in DMSO-*d6*.

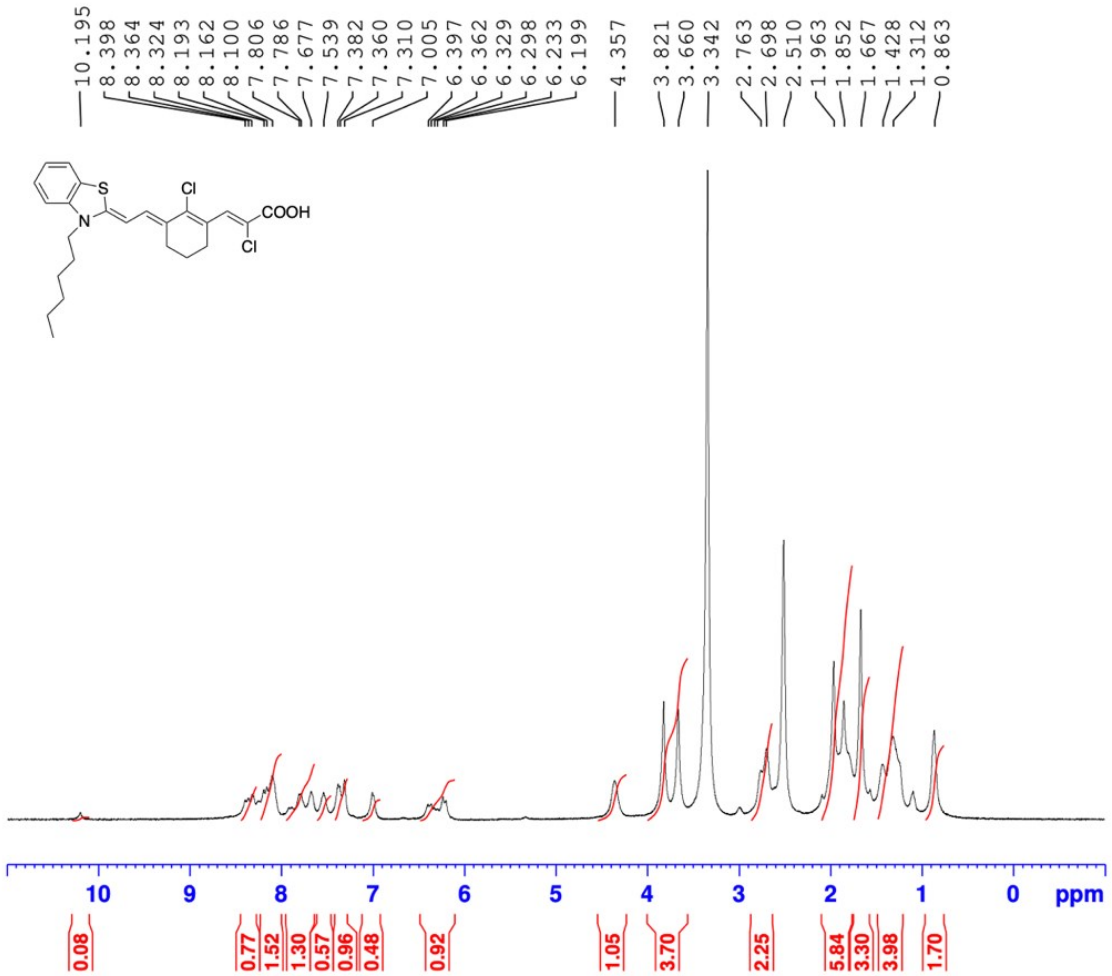
10.195
8.398
8.364
8.324
8.193
8.162
8.100
7.806
7.786
7.677
7.539
7.382
7.360
7.310
7.005
6.397
6.362
6.329
6.298
6.233
6.199
4.357
3.821
3.660
3.342
2.763
2.698
2.510
1.963
1.852
1.667
1.428
1.312
0.863
S
N
Cl
COOH
Cl
10
9
8
7
6
5
4
3
2
1
0
ppm
0.08
0.77
1.52
1.30
0.57
0.96
0.48
0.92
1.05
3.70
2.25
5.84
3.30
3.98
1.70

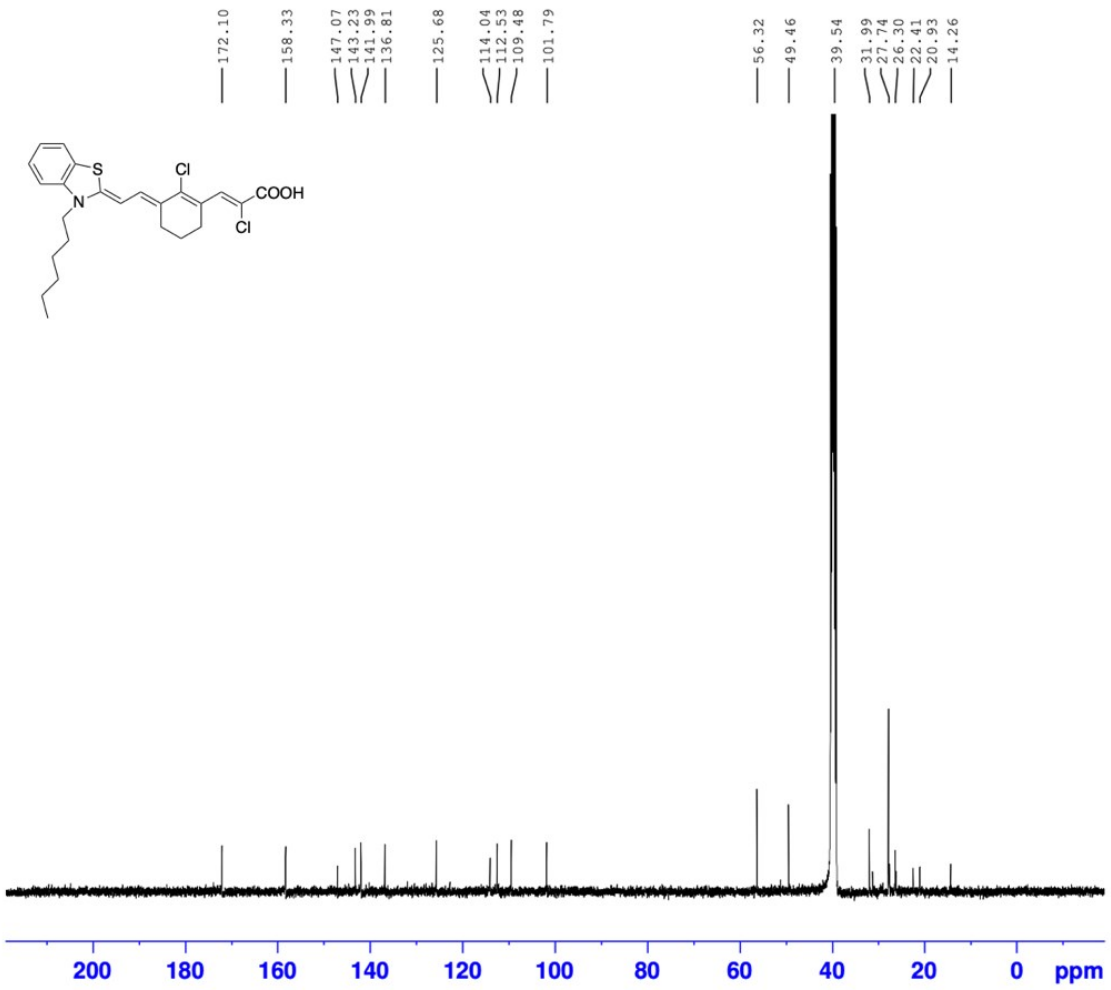

Figure S22. ^{13}C NMR of fluorophore **13** in DMSO-*d6*.

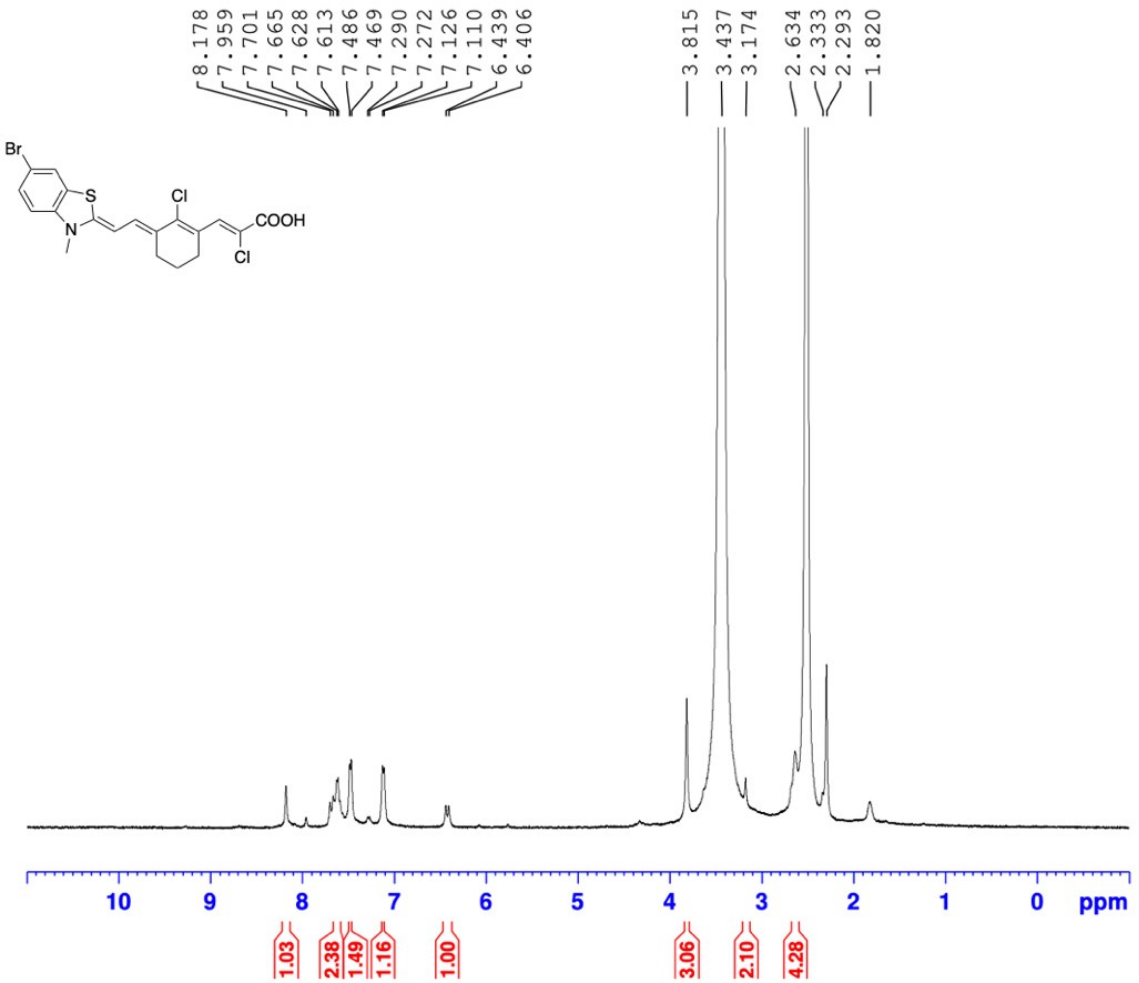

Figure S23. ^{1}H NMR of fluorophore **14** in DMSO-*d6*.

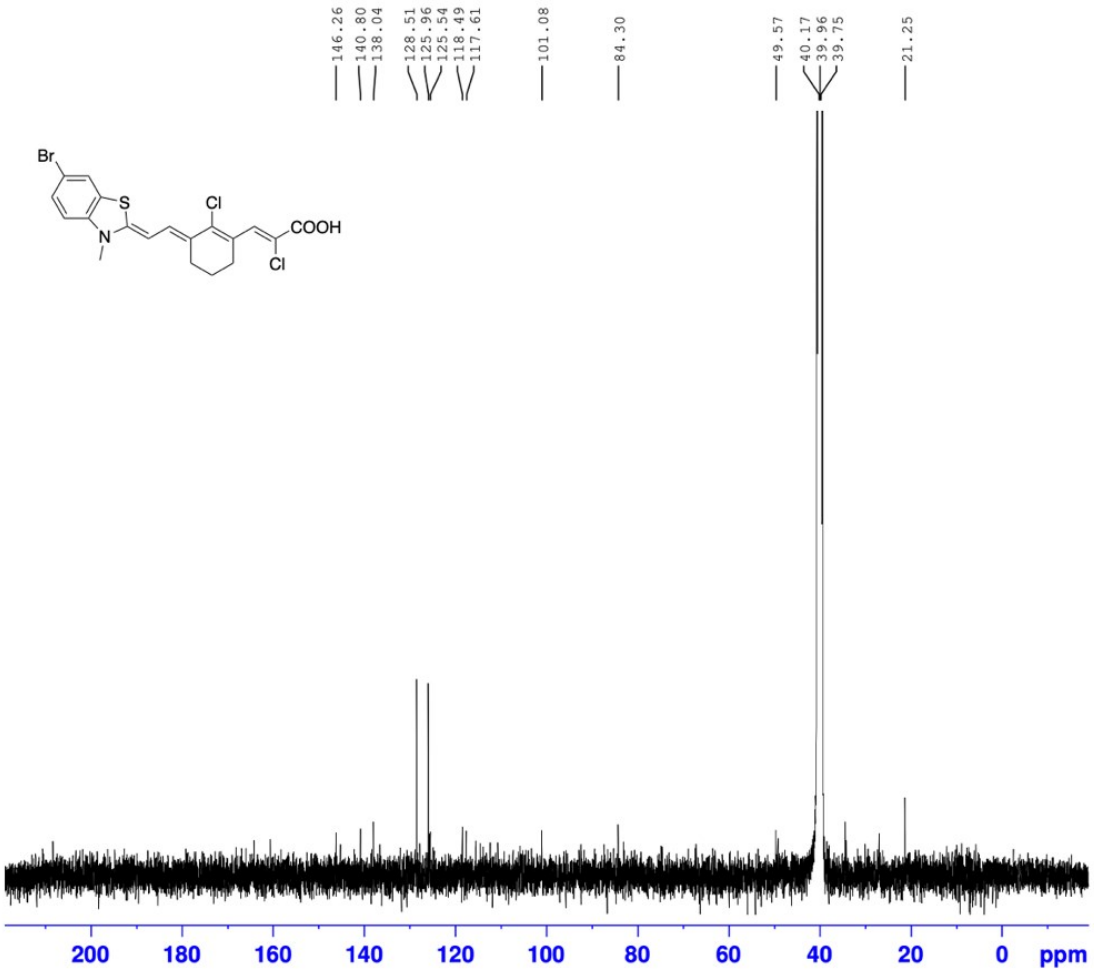

Figure S 24. ^{13}C NMR of fluorophore **14** in DMSO-*d6*.

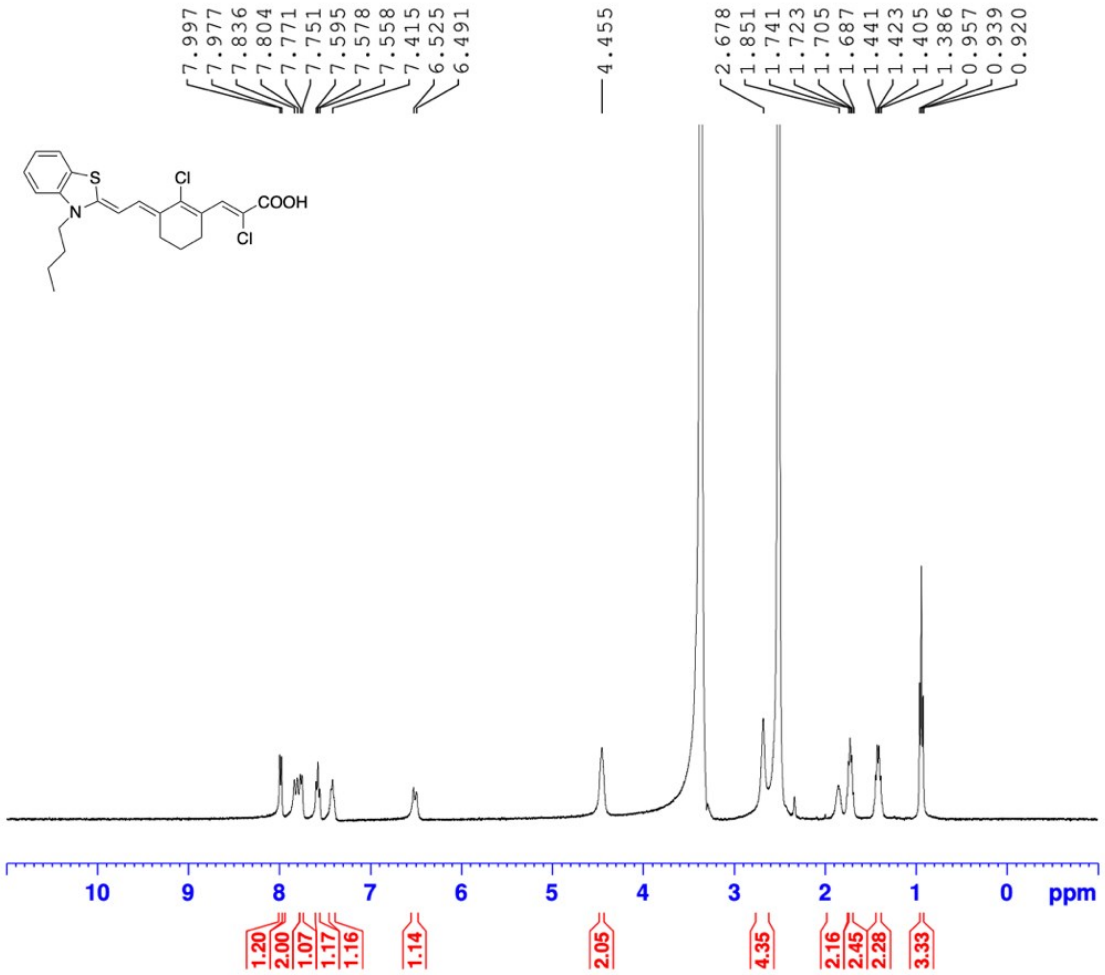

Figure S25. [1]H NMR of fluorophore **15** in DMSO-*d6*.

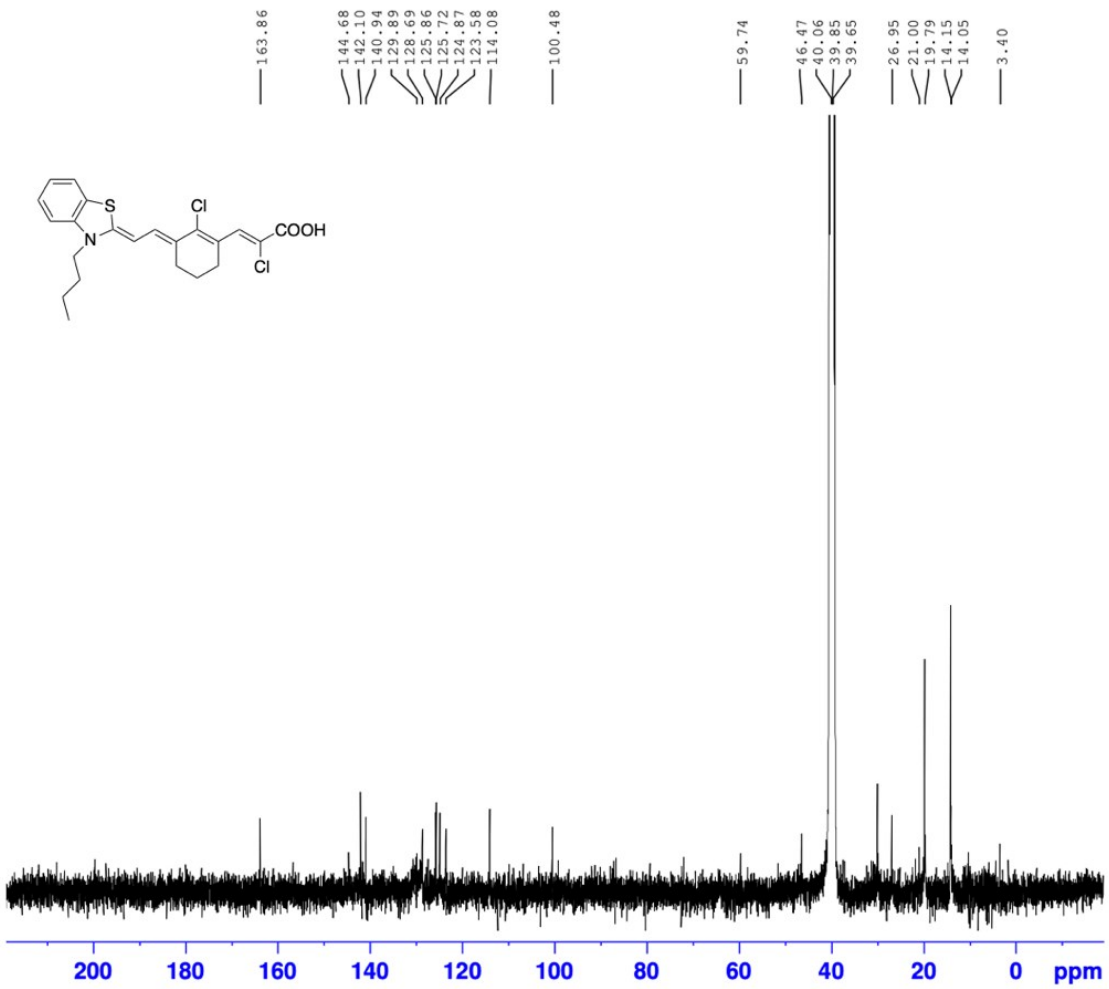

Figure S 26. ^{13}C NMR of fluorophore **15** in DMSO-*d6*.

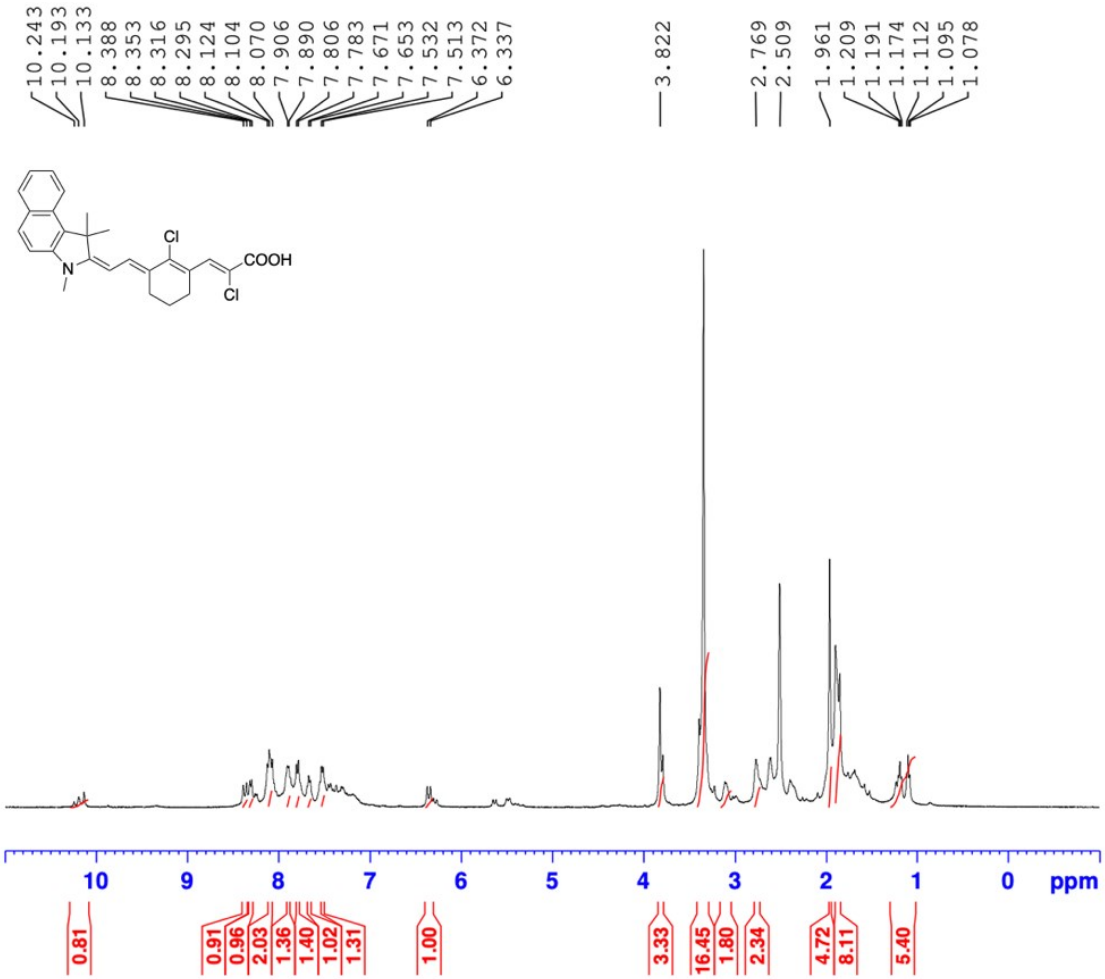

Figure S27. ^{1}H NMR of fluorophore **16** in DMSO-*d6*.

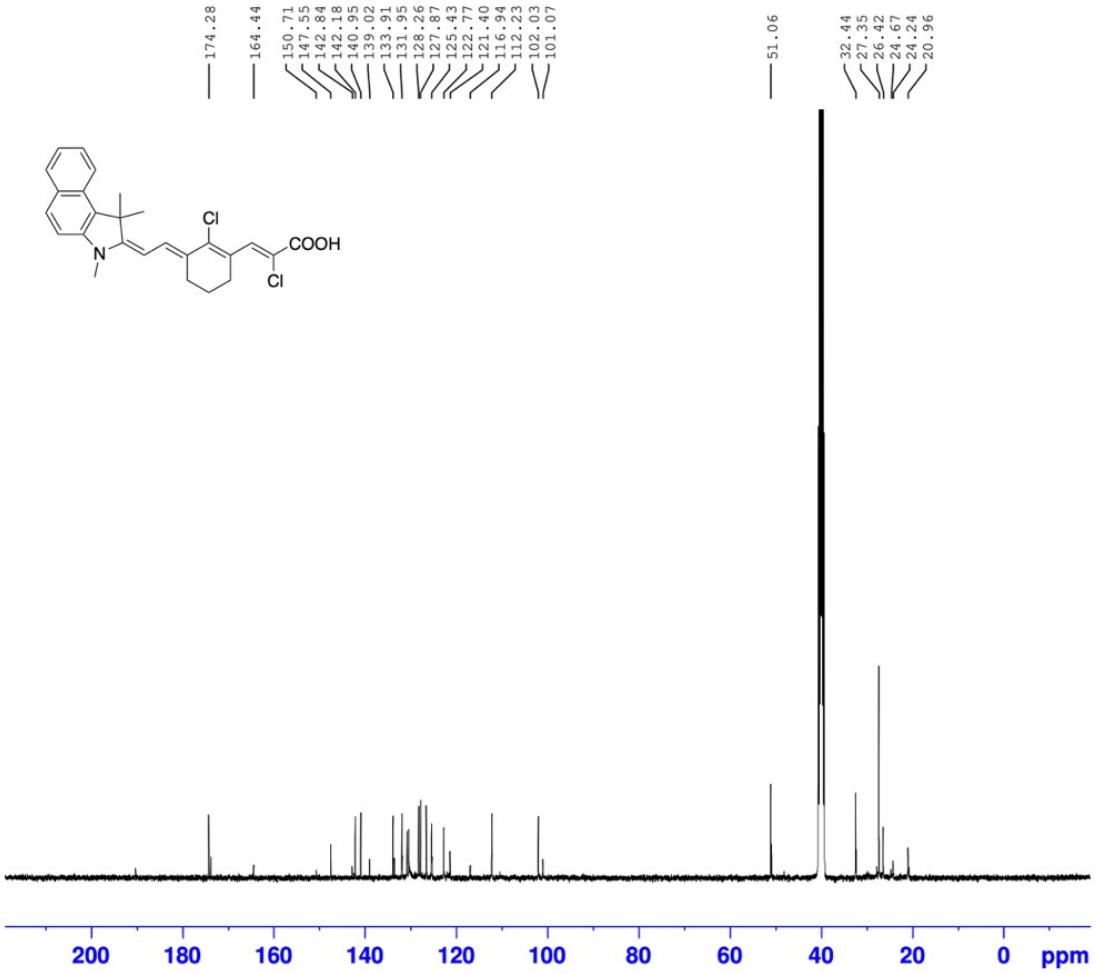

Figure S28. ^{13}C NMR of fluorophore **16** in DMSO-*d6*.

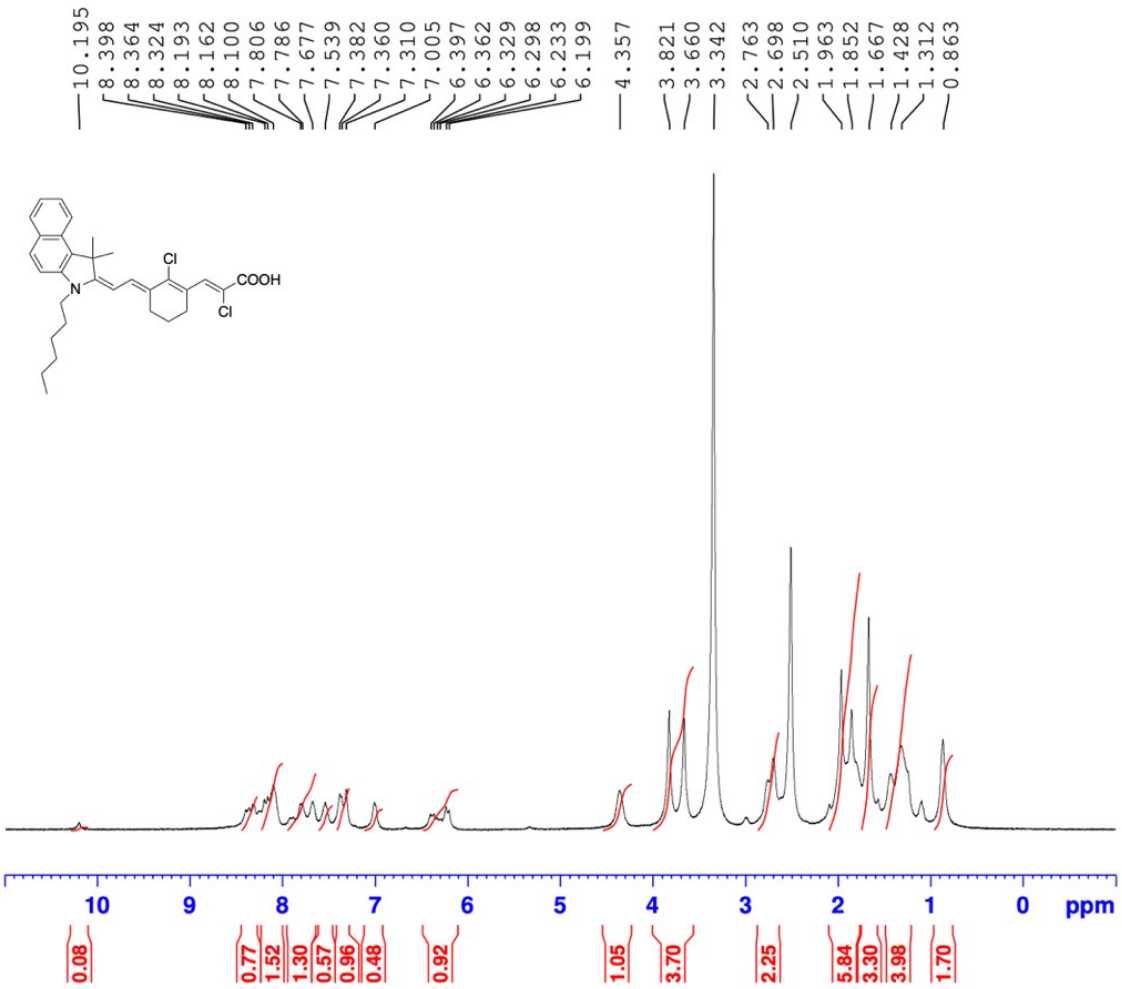

Figure S29. ^{1}H NMR of fluorophore **17** in DMSO-*d6*.

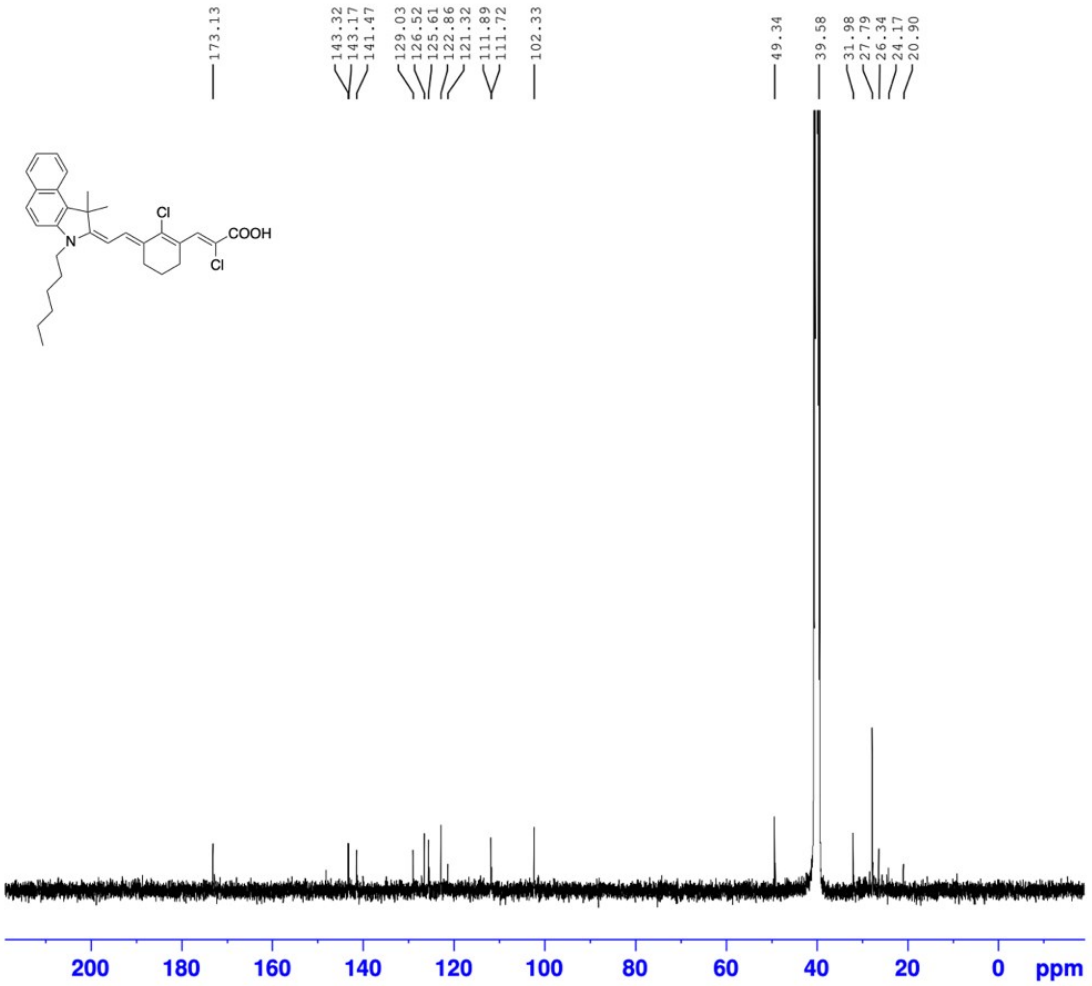

Figure S30. ^{13}C NMR spectra of fluorophore **17** in DMSO-*d6*.

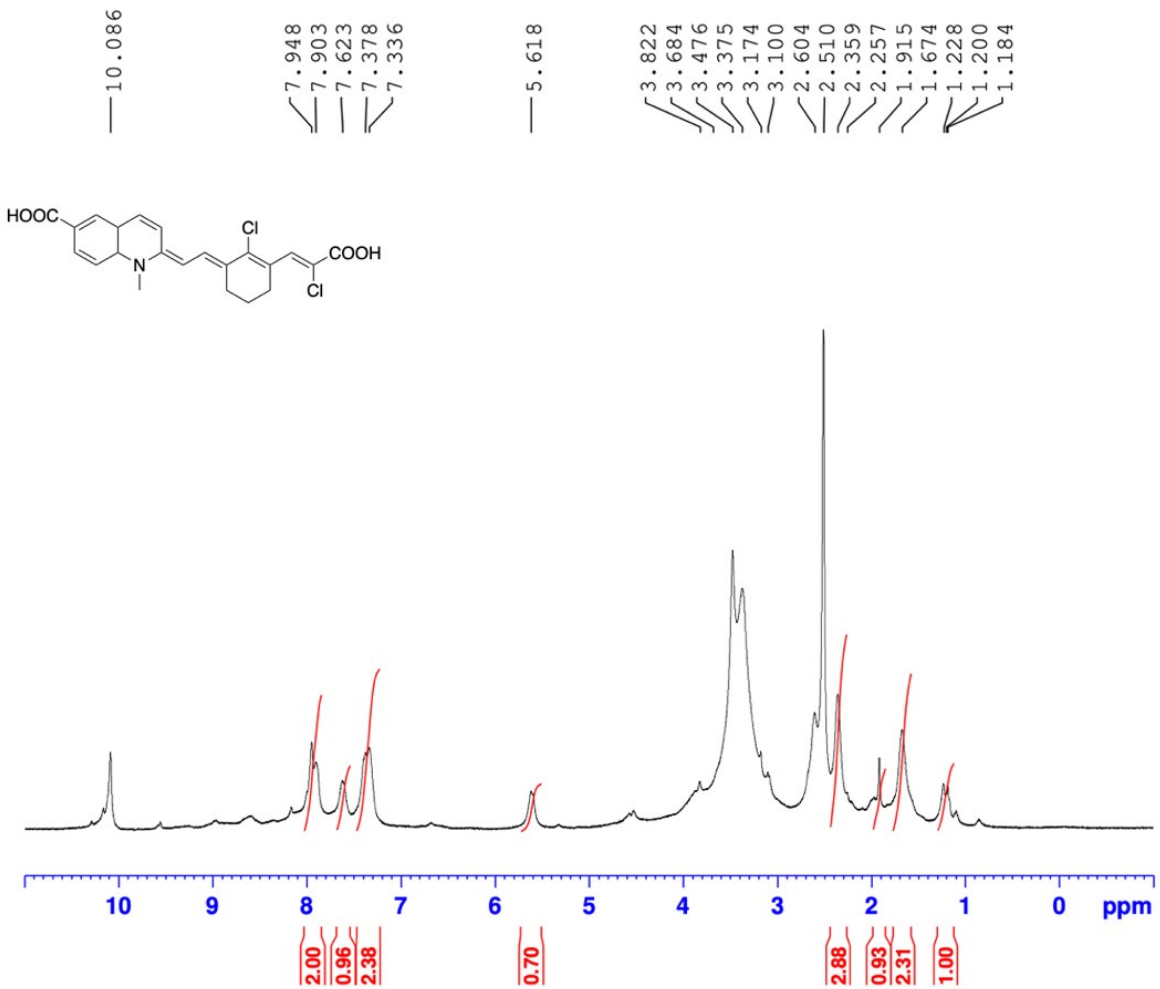

Figure S31. ^{13}C NMR spectra of fluorophore **18** in DMSO-*d6*.

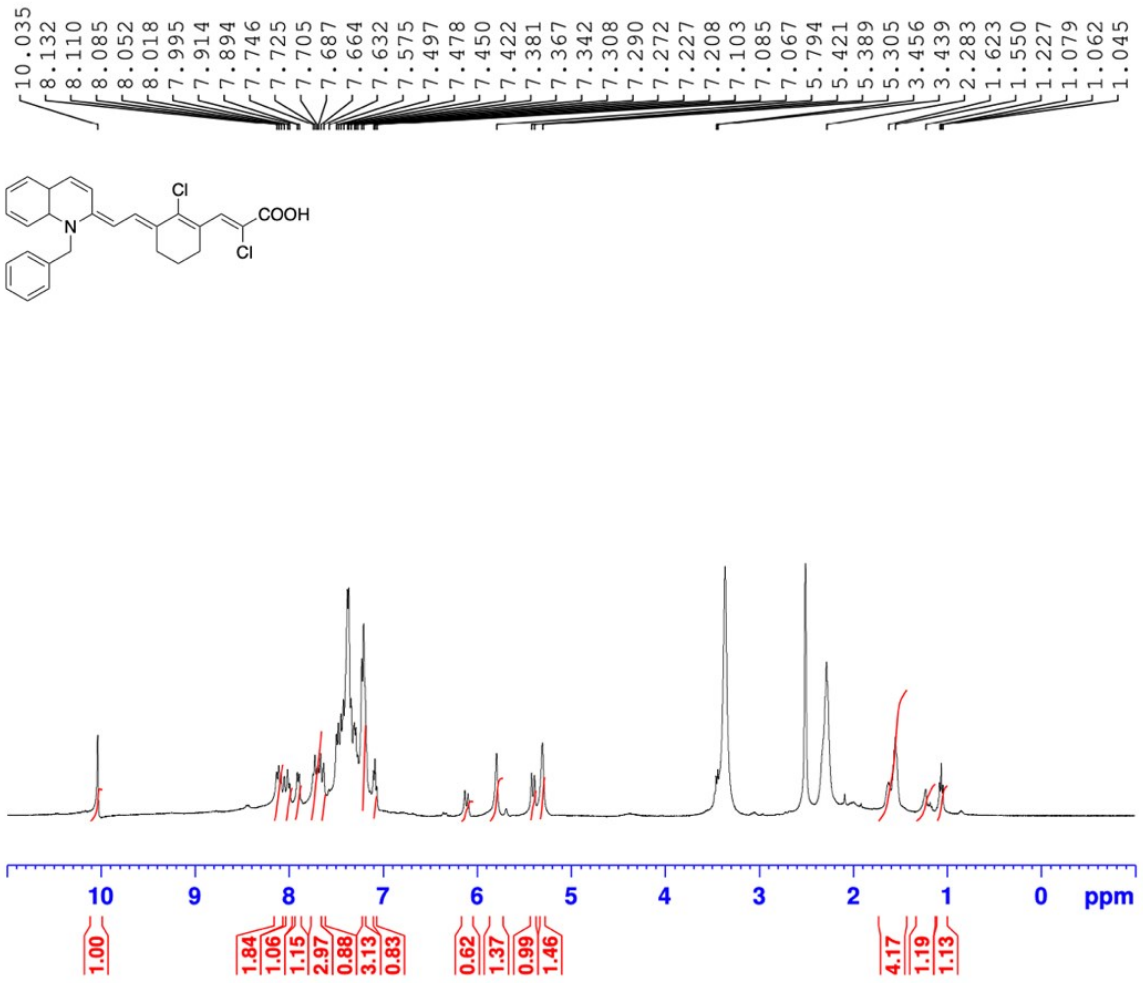

Figure S32. [1]H NMR of fluorophore **19** in DMSO-*d6*.

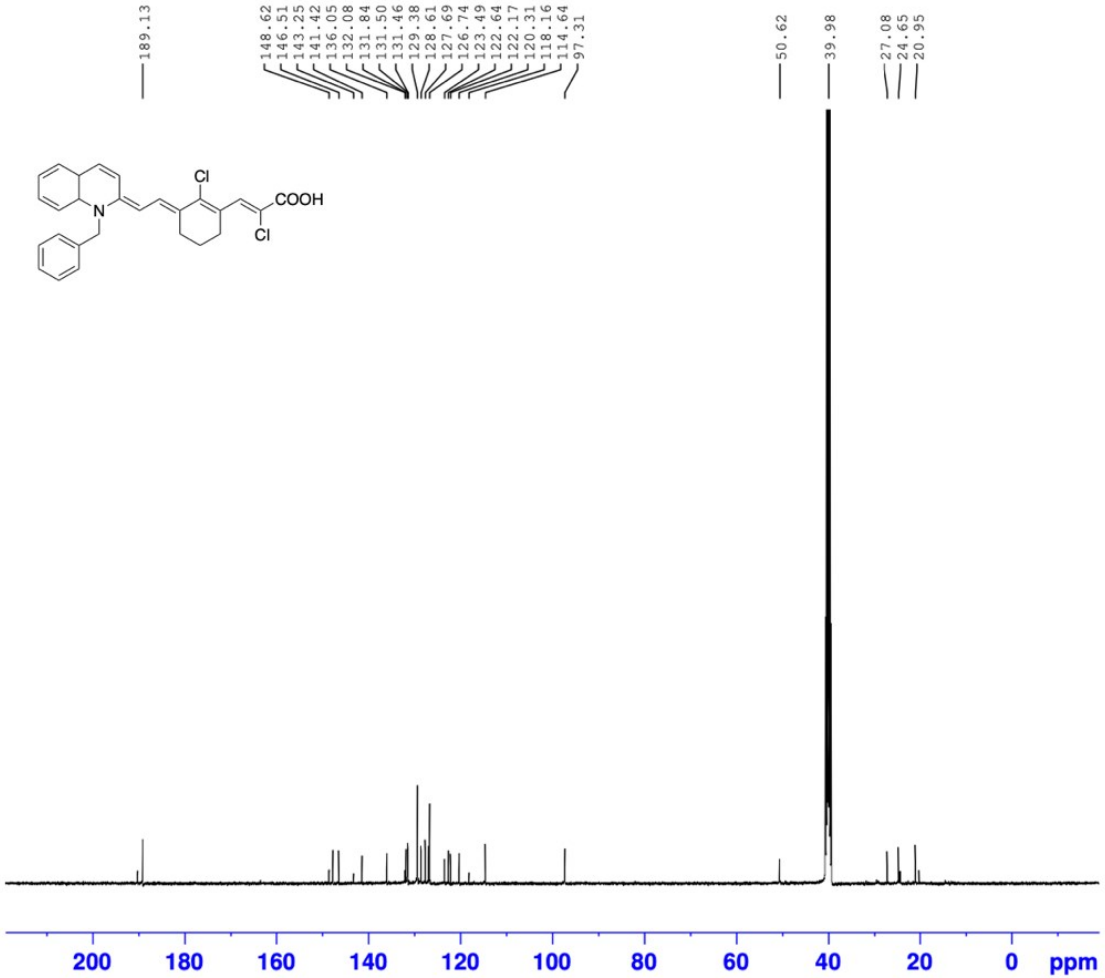

Figure S33. ^{13}C NMR of fluorophore **19** in DMSO-*d6*.

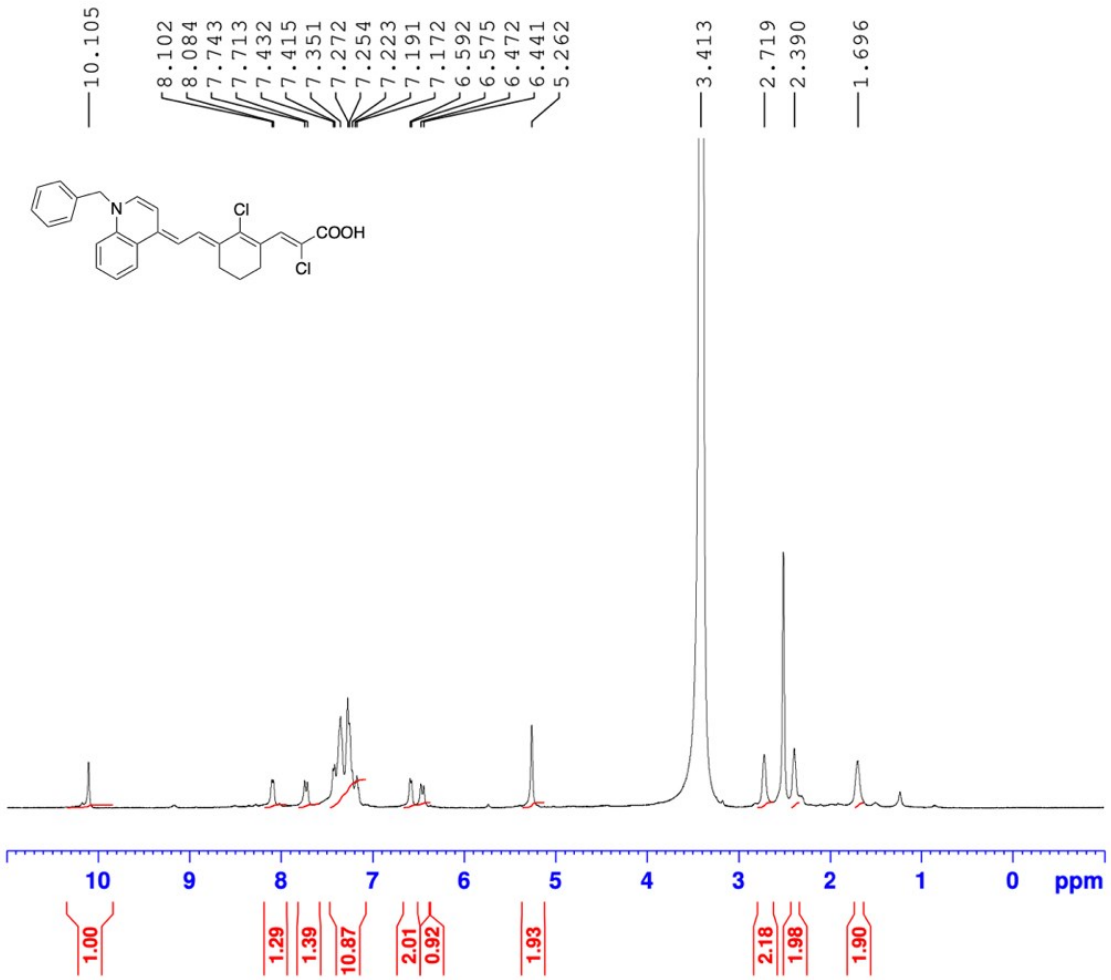

Figure S34. ^{13}C NMR of fluorophore **20** in DMSO-*d6*.

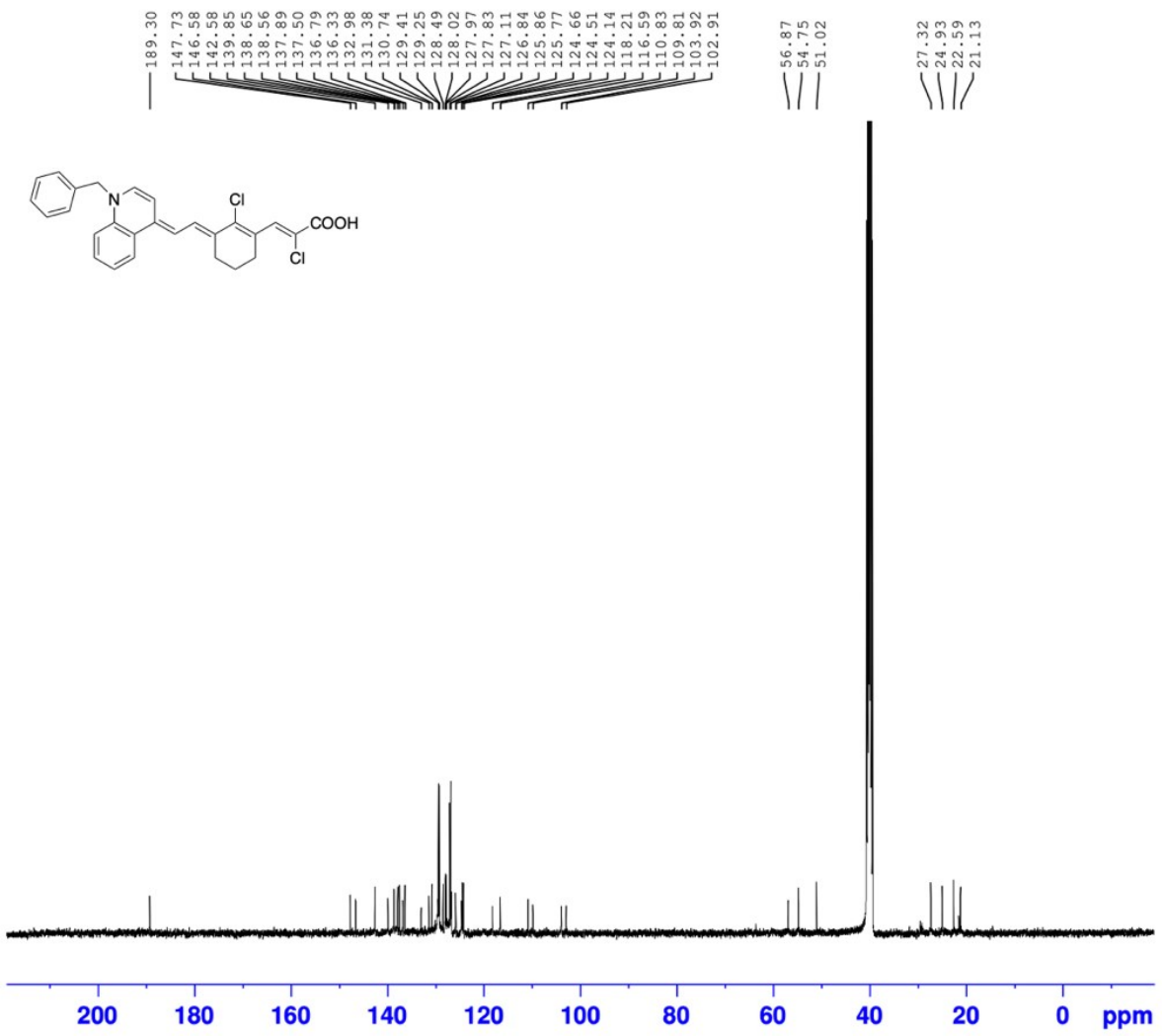

Figure S35. ^{1}H NMR spectra of fluorophore **20** in DMSO-*d6*.

Preparation of Stock Solutions

The stock solutions of fluorophores were prepared by weighing the dye on a 5-digit analytical balance and then dissolving in ethanol via sonication in an amber vial. All the solutions were prepared using a volumetric pipette and solutions were sonicated for 30 min for complete dissolution of the dye to yield 1mM stock solutions. Solutions were kept in dark at 4 ˚C.

Calculation of Extinction Coefficient (ε)

The measurement of extinction coefficients of fluorophores was done by preparing 1mM stock solutions of dyes by dissolving them in ethanol. 5 solutions of dyes were prepared by taking 1μM, 2 μM, 3 μM, 4 μM and 5 μM from the stock solution to prepare 1 x 10^{-6}, 2 x 10^{-6}, 3 x 10^{-6}, 4 x 10^{-6} and 5 x 10^{-6} M solutions respectively. The calculation of extinction coefficients was done using Beer's Law:

$$A = \varepsilon\, b\, c \qquad (1)$$

As an example, the calculation for fluorophore 5 is given here. The Table S1 shows the concentrations and the corresponding absorbances. The path length (b) is 1 cm.

Table S1. Concentration and absorbance data of fluorophore **5**.

Concentration (M)	Absorbance (nm)
1 x 10^{-6}	0.105
2 x 10^{-6}	0.190
3 x 10^{-6}	0.320
4 x 10^{-6}	0.440
5 x 10^{-6}	0.538

After plotting the absorbance vs concentration graph, the extinction coefficient (ε) was found as 111600 M^{-1} cm^{-1} from the slope of the graph. The absorbance vs concentration graph of fluorophore 5 is given in Figure 36. The R^2 found as 0.996 from the graph.

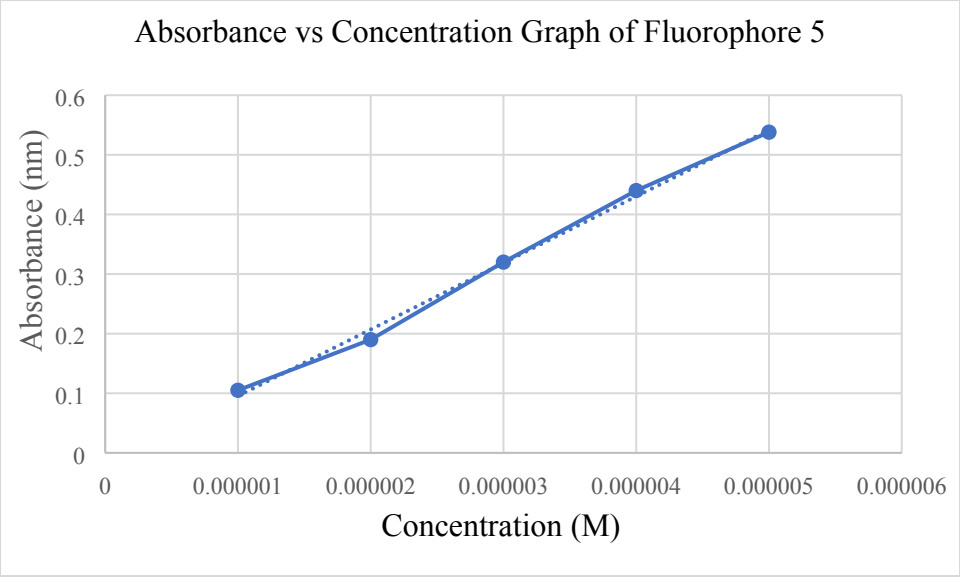

Figure S36. Absorbance vs concentration graph of fluorophore **5**.

Optical Studies of Fluorophores

The fluorescence emission studies of fluorophores were done in ethanol using micropipette to prepare the solutions and dissolving them via sonication. The fluorophores **4-17** were excited at 790 nm and fluorophores **18-20** were excited at 800 nm. The absorption spectra of fluorophores **4-20** with same concentration as 2.8 μM is given in Figure S37.

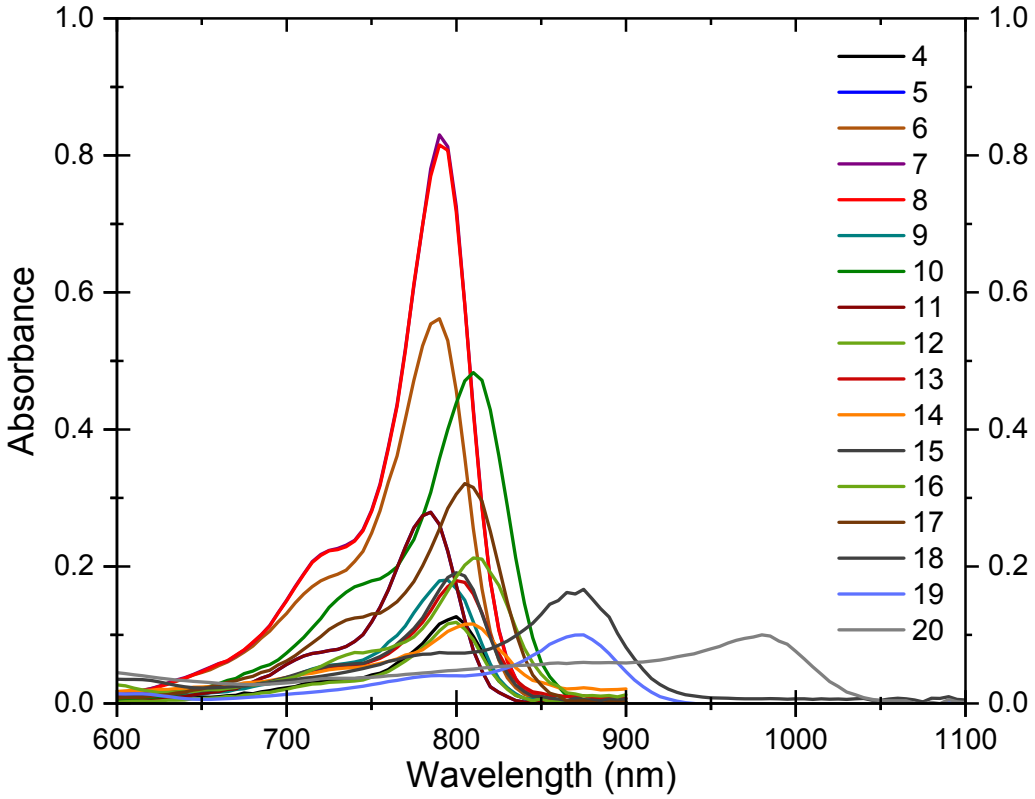

Figure S37. Absorbance graph of fluorophores **4-20** with 2.8 M solution in ethanol.

Solvatochromic Study

We selected four representative compounds with different donor units such as **7** and **8** with indole, **15** with benzothiazole and **17** with benzo[*e*]indole. We studied their absorbance and emission in five different solvents such as ethanol, methanol, dimethylsulfoxide, acetonitrile and dichloromethane. In methanol and acetonitrile, the absorption peak wavelength maxima tend to blue-shift for about 5 nm, while in DMSO and DCM, they are generally red-shifted (~ 2-21 nm). The emission peak maxima also showed blue shift in methanol and acetonitrile and red shift in DMSO and DCM, with exception of compound **8** and compound **17** in DCM which are slightly blue shifted.

Table S2. Solvatochromic properties of selected fluorophores.

Fluorophore	Solvent	λ_{abs}	λ_{em}	Stokes Shift (cm^{-1})
7	Ethanol	790	810	313
	Methanol	785	807	347
	Acetonitrile	785	807	347
	DMSO	805	819	212
	DCM	795	815	309
8	Ethanol	790	820	463
	Methanol	785	807	268
	Acetonitrile	785	807	347
	DMSO	800	820	305
	DCM	795	813	279
15	Ethanol	800	833	495
	Methanol	795	812	263
	Acetonitrile	800	816	245
	DMSO	810	824	210
	DCM	810	820	151
17	Ethanol	810	822	180
	Methanol	805	820	227
	Acetonitrile	805	817	183
	DMSO	820	827	103
	DCM	815	820	75

We used

Lippert-Mataga equation which relates its slope to the dipole moment change. The Lippert-Mataga equation is given below:

$$\Delta\nu = \frac{2\,(\mu_E - \mu_G)^2}{hca^3}\,\Delta f + \text{constant} \quad (1)$$

In this equation $\Delta\nu$ is Stokes shift (cm^{-1}), h is Planck's constant, c is speed of light, a is the Onsager cavity radius, μ_E and μ_G are excited and ground state dipole moments, respectively. Based on the similar approaches in the literature, we assume that Onsager cavity radius is the same for the studied fluorophores. Δf is the orientation polarizability of the solvent molecules and calculated from Equation 2.

$$\Delta f = \frac{(\varepsilon - 1)}{(2\varepsilon + 1)} - \frac{(n^2 - 1)}{(2n^2 + 1)} \quad (2)$$

In Equation 2, ε is the dielectric constant and n is the refractive index of the solvent. The solvent polarizability (Δf) of the different solvents used for the solvatochromic studies are calculated and given in Table 2[14].

Table S3. Polarizability values of different solvents

Solvent	Polarizability (Δf)
Ethanol	0.289
Methanol	0.309
Acetonitrile	0.305
DMSO	0.263
DCM	0.217

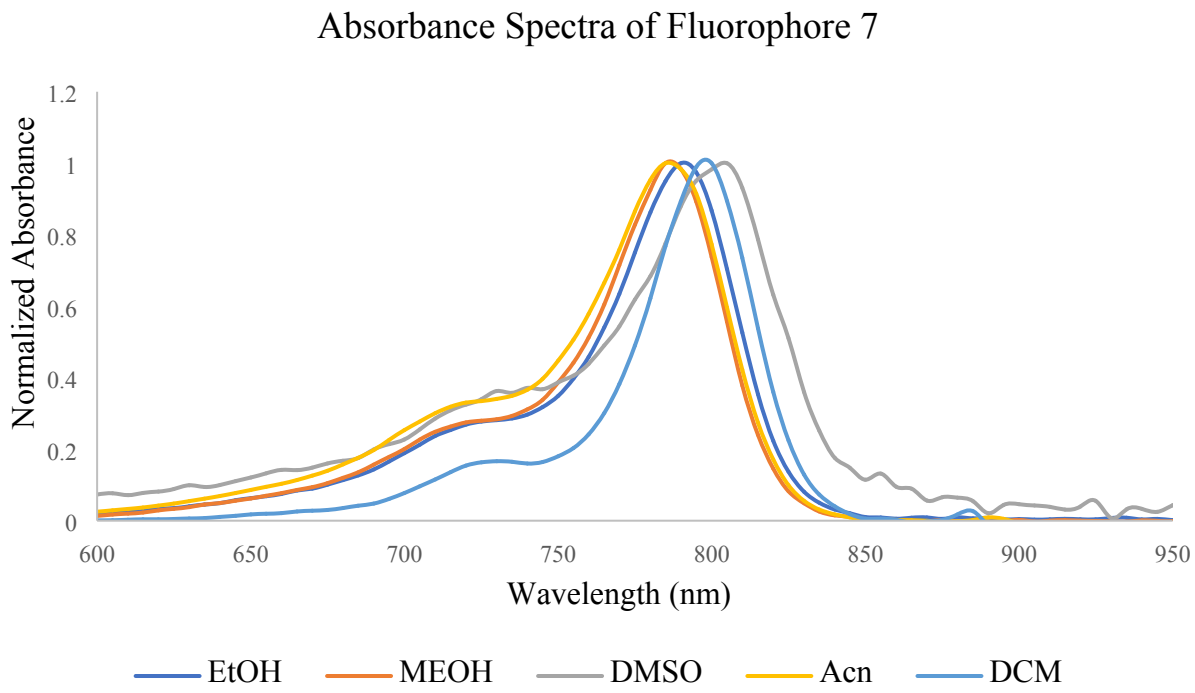

Figure S38. Absorbance spectrum of fluorophore **7** in different solvents

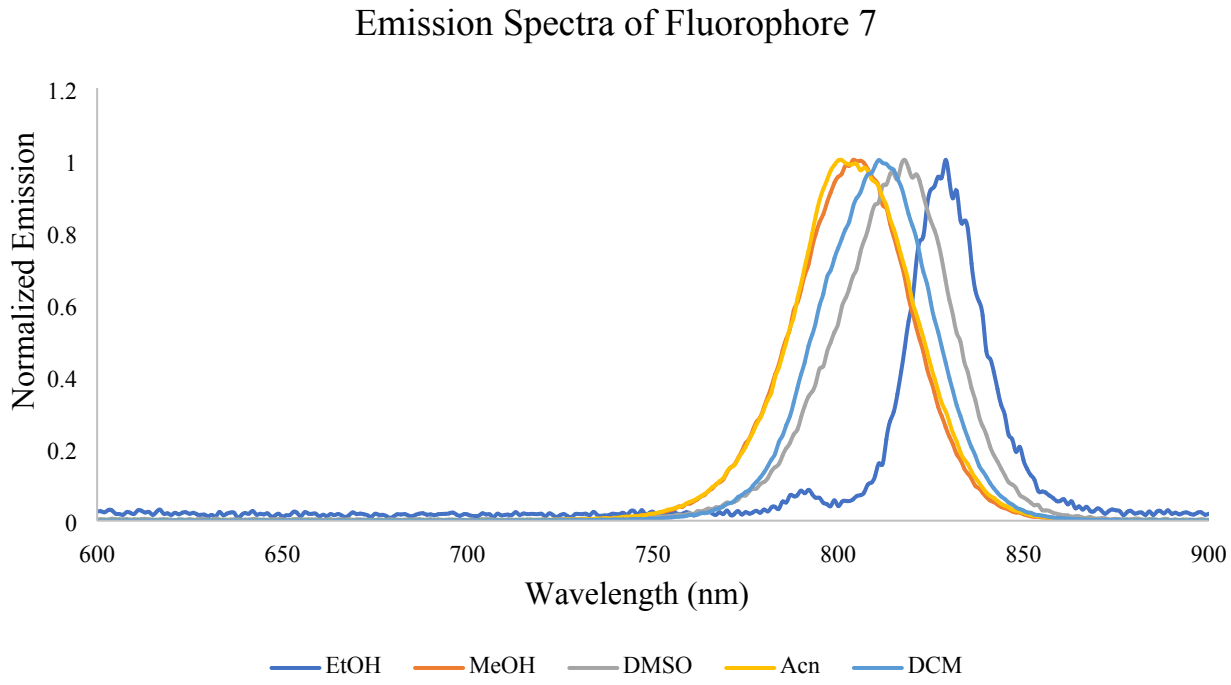

Figure S39. Emission spectrum of fluorophore **7** in different solvents.

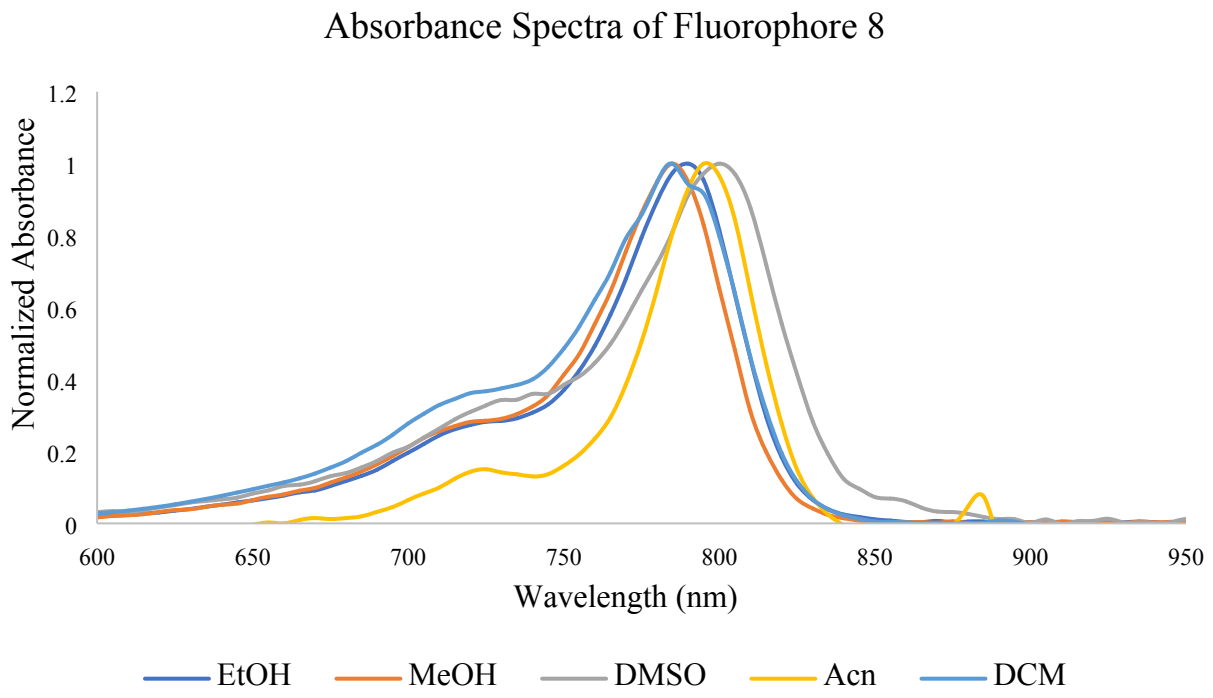

Figure S40. Absorbance spectra of fluorophore **8** in different solvents.

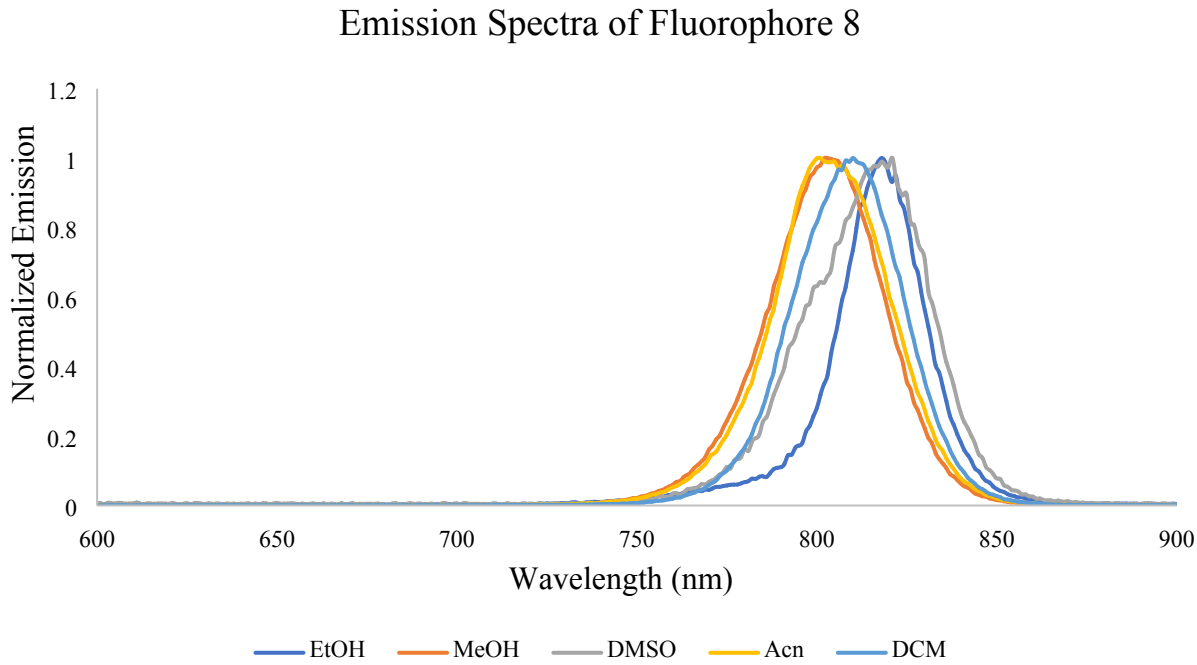

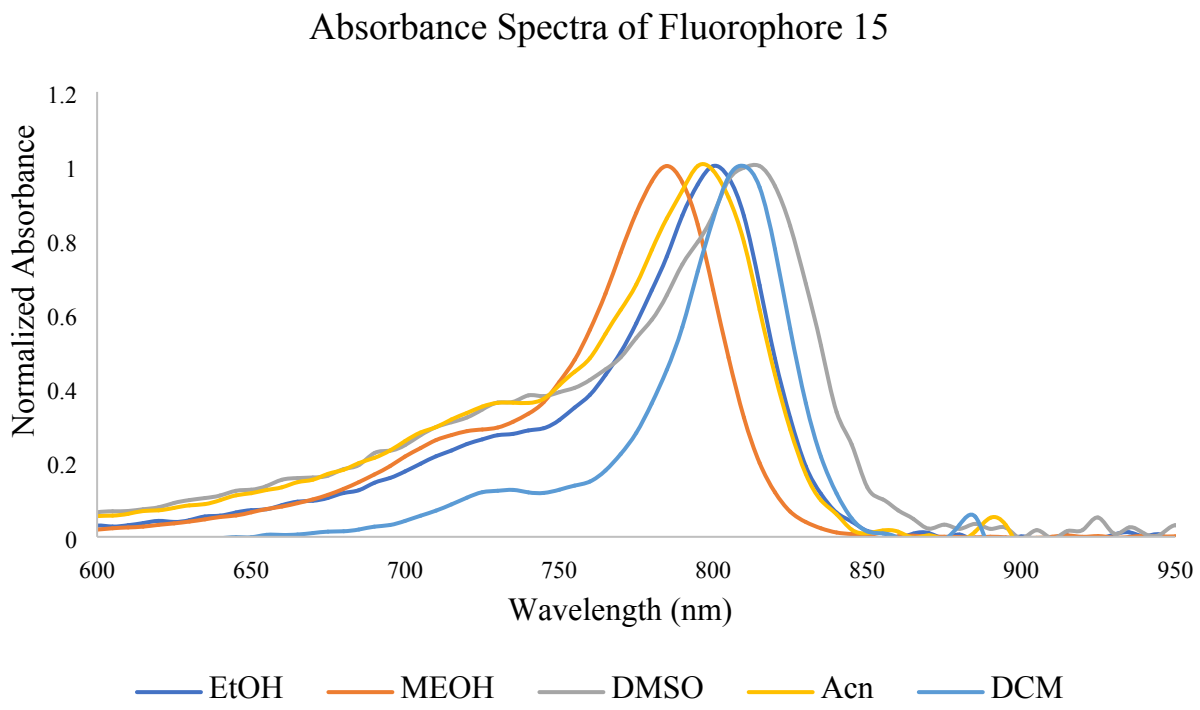

Figure S42. Absorbance spectrum of fluorophore **15** in different solvents.

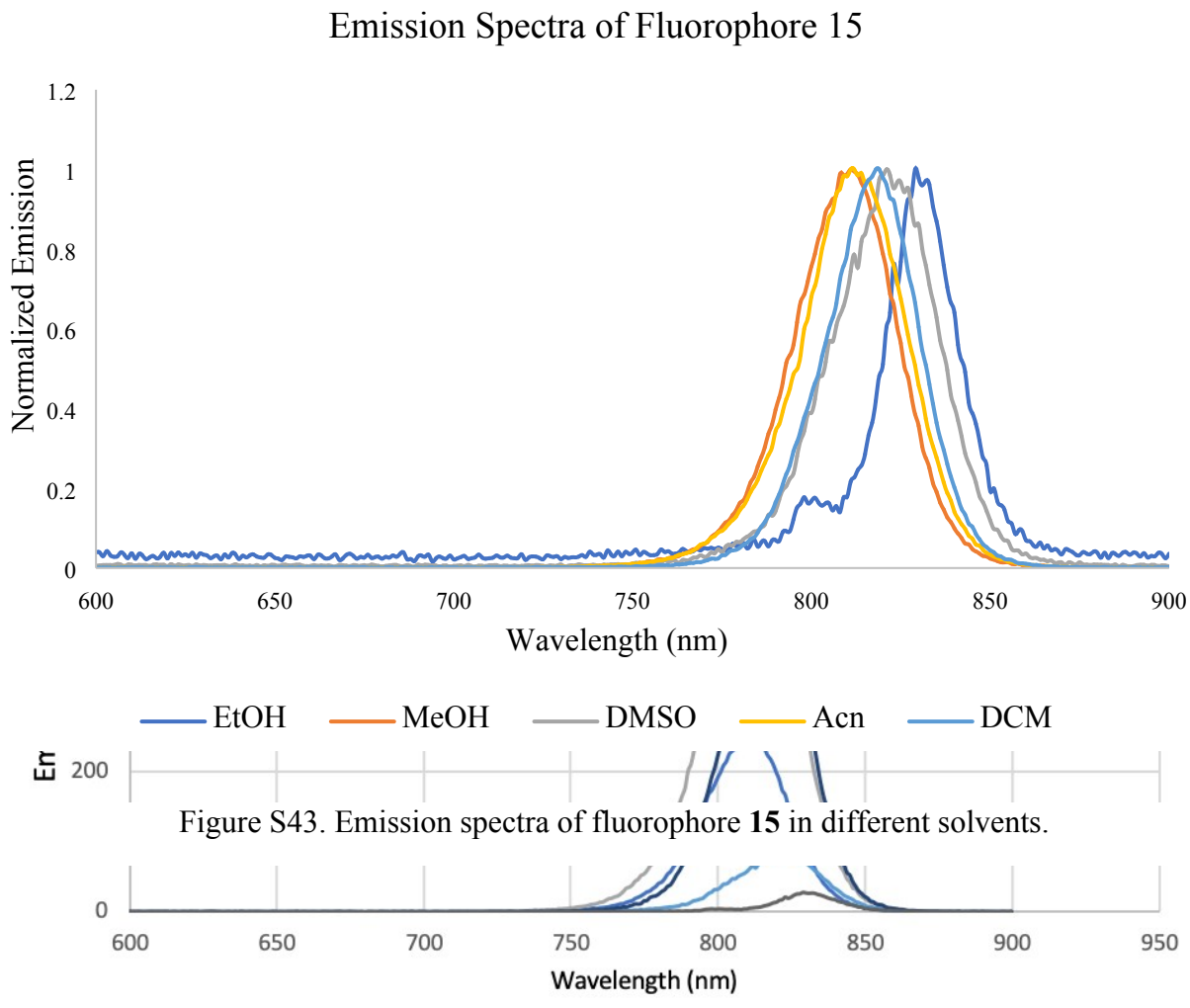

Figure S43. Emission spectra of fluorophore **15** in different solvents.

Figure S 42. Emission spectra of fluorophore **8** in different solvents.

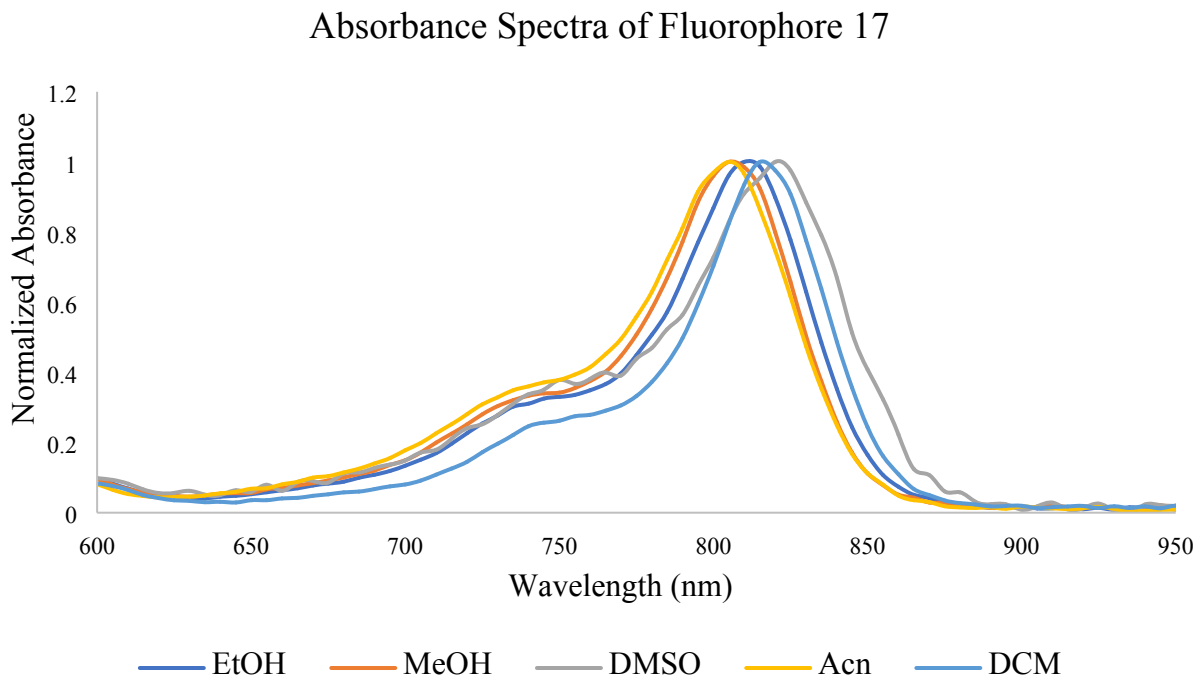

Figure S44. Absorbance spectra of fluorophore **17** in different solvents.

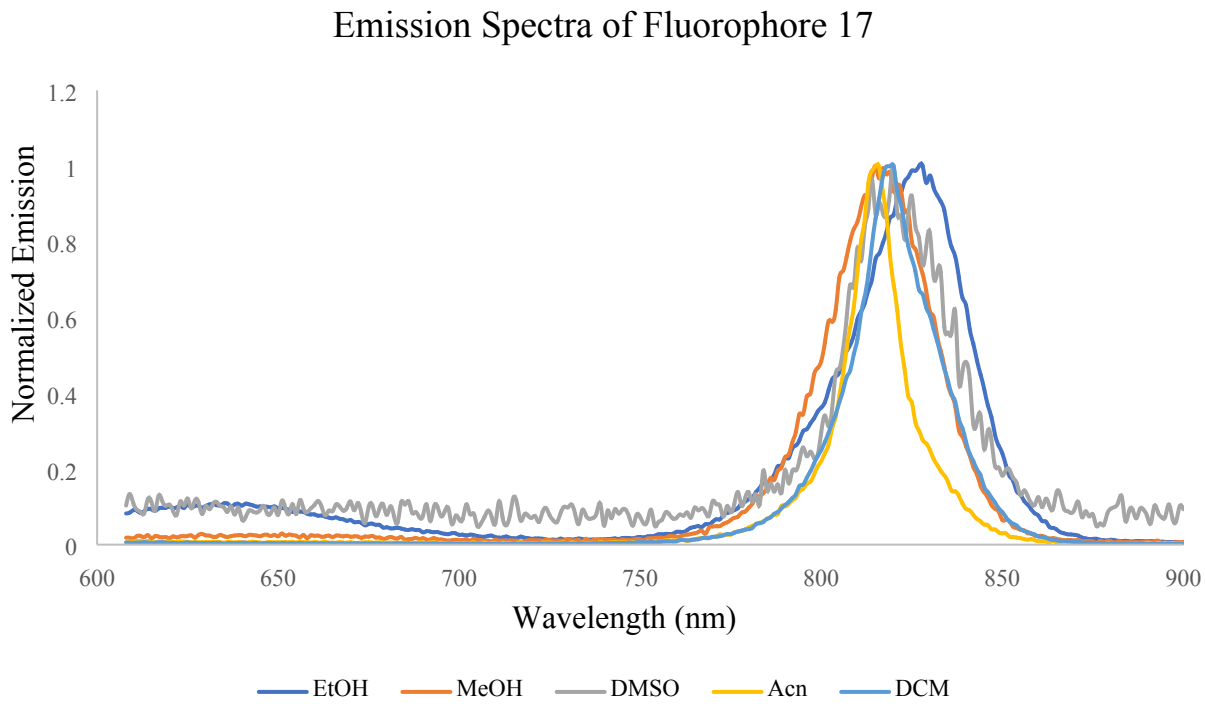

In addition to the experimental studies, we used TD-DFT method to study solvatochromic effect. In these studies, in addition to the experimentally used solvents, we investigated toluene and water. We also included fluorophore 19 with 2-quinoline to these. The results are given in Table S4.

Table S4. Absorbance maxima of fluorophores **7, 8, 15, 17** and **19** in different solvents using TD-DFT.

	Toluene	**DCM**	**DMSO**	**EtOH**	**Acn**	**MeOH**	**Water**
7	592.6	598.1	601.7	592.3	595.8	594.1	595.3
8	591.2	597.1	600.3	591.3	594.0	592.5	593.4
15	590.7	594.7	597.3	588.3	590.5	588.6	589.9
17	621.7	628.6	632.3	622.8	626.4	625.1	626.3
19	646.6	639.5	638.7	629.9	632.8	631.3	631.7

Figure S45. Emission spectra of fluorophore **17** in different solvents.

Quantum Yield Calculations

The fluorescence quantum yields of fluorophores were calculated using the Equation 2. In the equation R refers to the reference, which is ICG, S refers to the sample. Φ shows the quantum yield, A is the absorbance at the excitation wavelength, F is the area under the fluorescence intensity curve and n shows the refractive index of the solvent (ethanol). The concentration of dyes used for the calculations was arranged to give absorbance equal or smaller than 0.2. The quantum yields of dyes were found between 0.07-0.19.

$$\Phi_S = \Phi_R * \frac{A_R}{A_S} * \frac{F_S}{F_R} * \left(\frac{n_S^2}{n_R^2}\right) \quad (2)$$

Photostability of Fluorophores

The photostability tests of fluorophores were performed by preparing solutions of fluorophores in methanol to give absorbance 0.6. Two replicates were prepared for each solution and one kept in

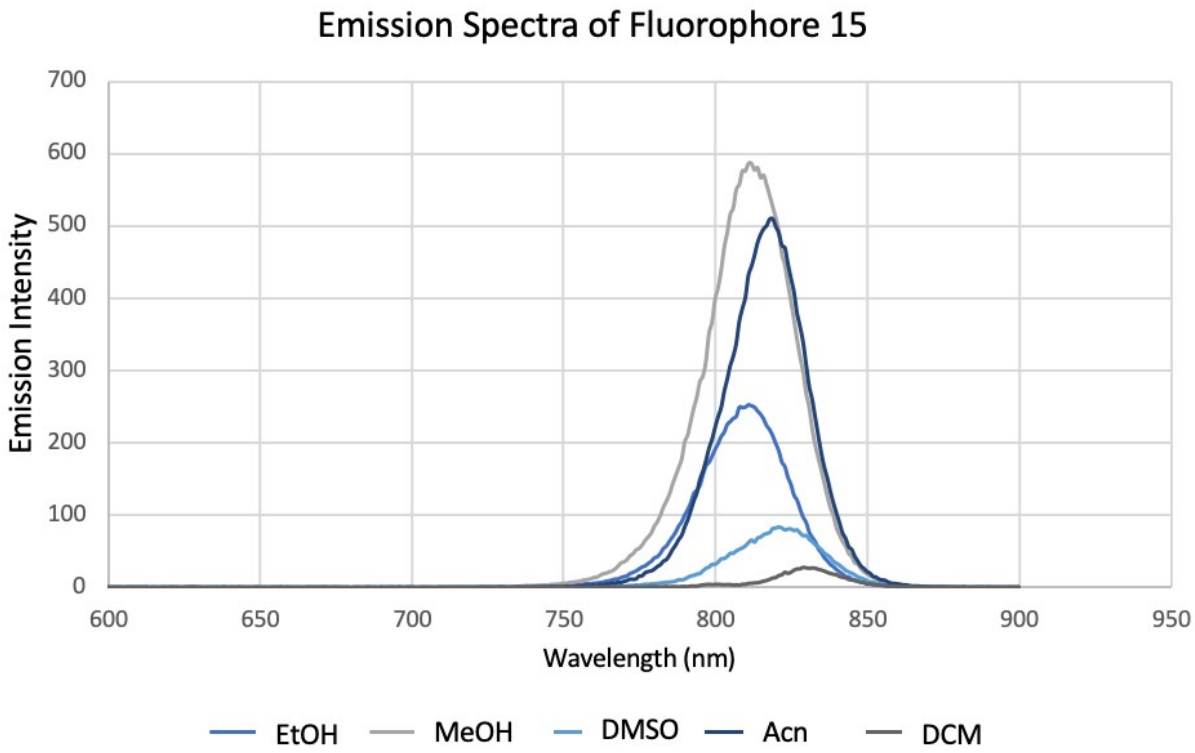

dark while the other kept under irradiation of 15 W UV lamp. The light photostability results are given in Figure 9 and the dark photostability of fluorophores are shown in Figure S46. Indocyanine green (ICG) used as a reference.

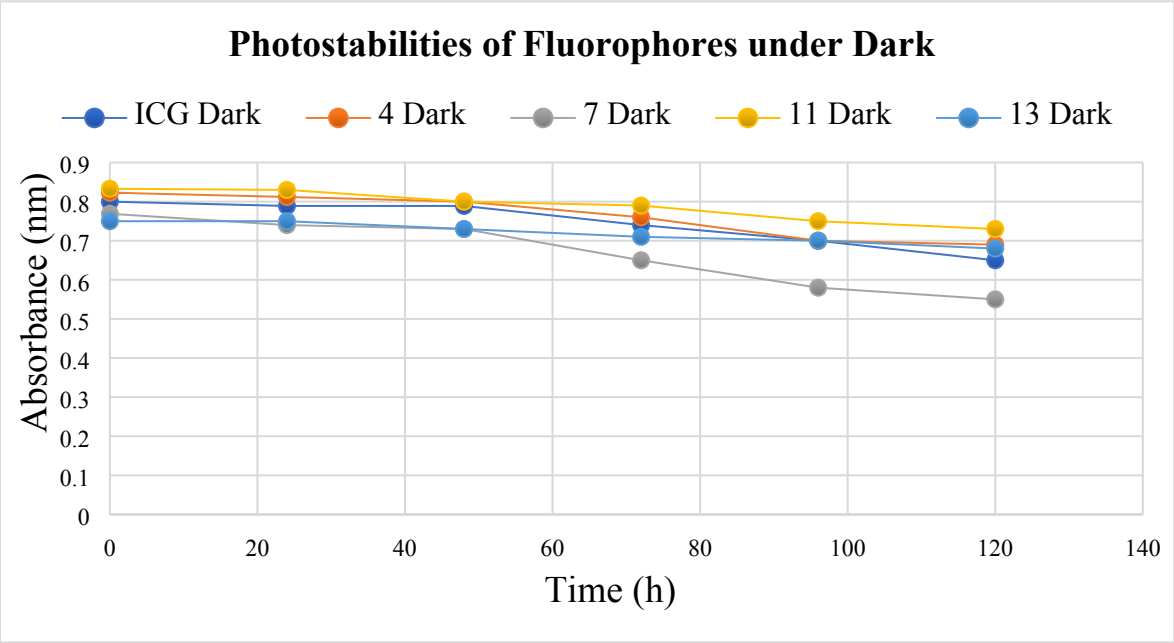

Figure S46. Photostability of fluorophores **4, 7, 11, 13** and ICG both in dark and light.

Cis-Trans Isomerism of Acceptor Unit using TD-DFT Study

According to TD-DFT studies, the cyano acrylic acid acceptor unit of the fluorophores may exist in cis or trans confirmation. Therefore, the absorbance maxima of selected fluorophores **7, 8** (indoles)**, 15** (benzohiazole)**, 17** (benzo[e]indole) and **19** (quinoline) were studied as shown in Table S5. From TD-DFT studies, it is predicted that the cis forms will have their absorption wavelength peaks to be red-shifted between 12-20 nm. These results suggest the excitation energy is lowered by 0.07-0.12 eV. We may hypothesize that the smaller energy gap is either due to

electronic structure stabilization at either ground or excited state, and smaller energy gaps may as well enhance the charge transfer within the fluorophores.

Table S5. TD-DFT predictions of cis and trans isomers of fluorophores **7, 8, 15, 17** and **19**.

Fluorophore	λ_{abs}[trans]	λ_{abs}[cis]	$\Delta\lambda_{abs}$[trans-cis]	ΔE_{exc}[trans-cis]
			(nm)	(eV)
7	592.3	613.2	20.9	-0.120
8	591.3	610.8	19.4	-0.116
15	588.3	607.9	19.6	-0.119
17	622.8	643.3	20.5	-0.105
19	629.9	642.7	12.8	-0.069

Time Dependent Density Functional Theory (TD-DFT) Studies

The TD-DFT studies were performed with three different methods as; BLYP, B3LYP and BH&HLYP. The calculated excitation energies, absorbance wavelengths and oscillator strengths are compared in Table S6. The molecular geometries and natural orbitals of fluorophores were calculated by HF/6-311G (d,p) level of theory in vacuo with TD-DFT studies.

Table S6. Comparison of TD-DFT results between BLYP, B3LYP and BH&HLYP.

Compound	$S_0 \rightarrow S_1$ Excitation Energies (eV)			λmax Abs. Wavelength (nm)			Oscillator Strength		
	BLYP	B3LYP	BH&HLYP	BLYP	B3LYP	BH&HLYP	BLYP	B3LYP	BH&HLYP
4	2.12	2.31	2.51	586	537	493	1.64	1.78	1.96
5	2.11	2.30	2.50	587	540	496	1.67	1.79	1.97
6	2.09	2.31	2.54	592	537	488	1.66	1.83	2.02
7	2.09	2.30	2.53	592	539	491	1.69	1.84	2.03
8	2.10	2.31	2.53	591	538	490	1.67	1.83	2.01
9	2.10	2.32	2.55	591	536	486	1.65	1.82	2.02
10	2.02	2.24	2.46	614	554	504	1.50	1.75	1.98
11	1.99	2.21	2.43	624	561	510	1.48	1.76	1.99
12	2.11	2.27	2.44	588	547	509	1.76	1.85	2.00
13	2.11	2.26	2.43	589	548	510	1.77	1.85	1.99
14	2.10	2.27	2.47	592	545	502	1.79	1.90	2.06
15	2.11	2.26	2.44	588	548	509	1.77	1.85	1.99
16	1.99	2.22	2.46	623	558	505	1.42	1.71	1.95
17	1.99	2.21	2.44	623	561	509	1.46	1.72	1.95
18	1.98	2.16	2.33	627	573	532	2.00	2.16	2.34
19	1.97	2.15	2.29	630	577	541	1.50	1.96	2.20
20	1.94	2.07	2.17	638	599	572	1.83	1.98	2.16

(a)

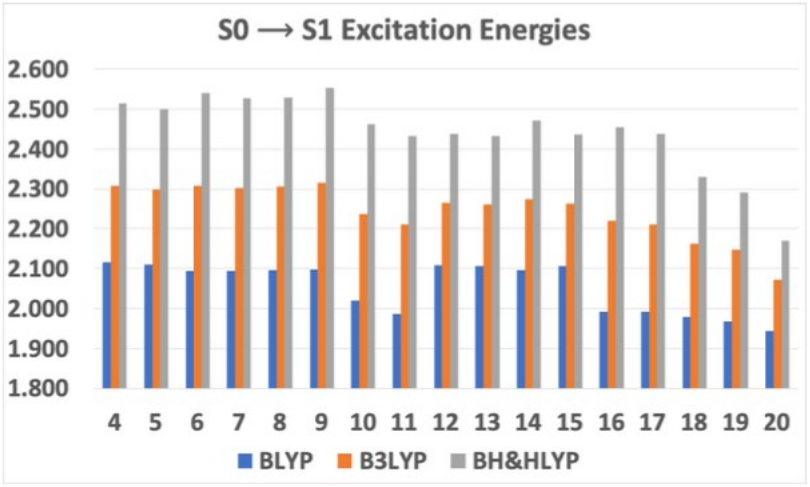

(b)

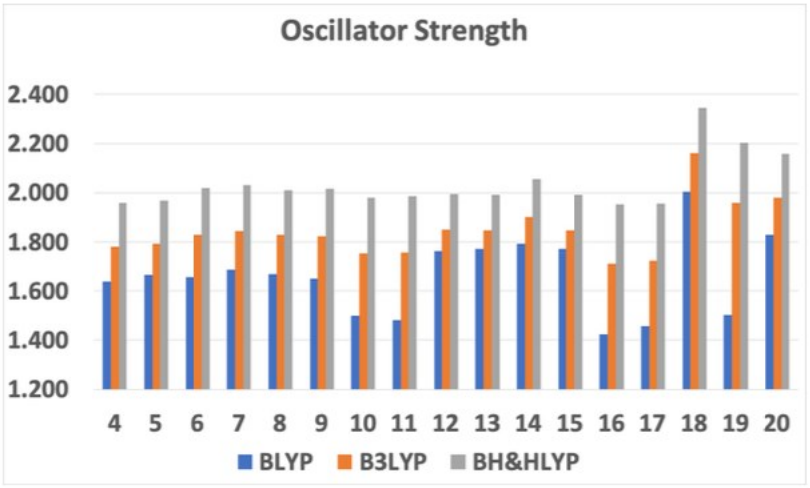

(c)

Figure S47. Comparison of TD-DFT studies between BLYP, B3LYP and BH&HLYP.

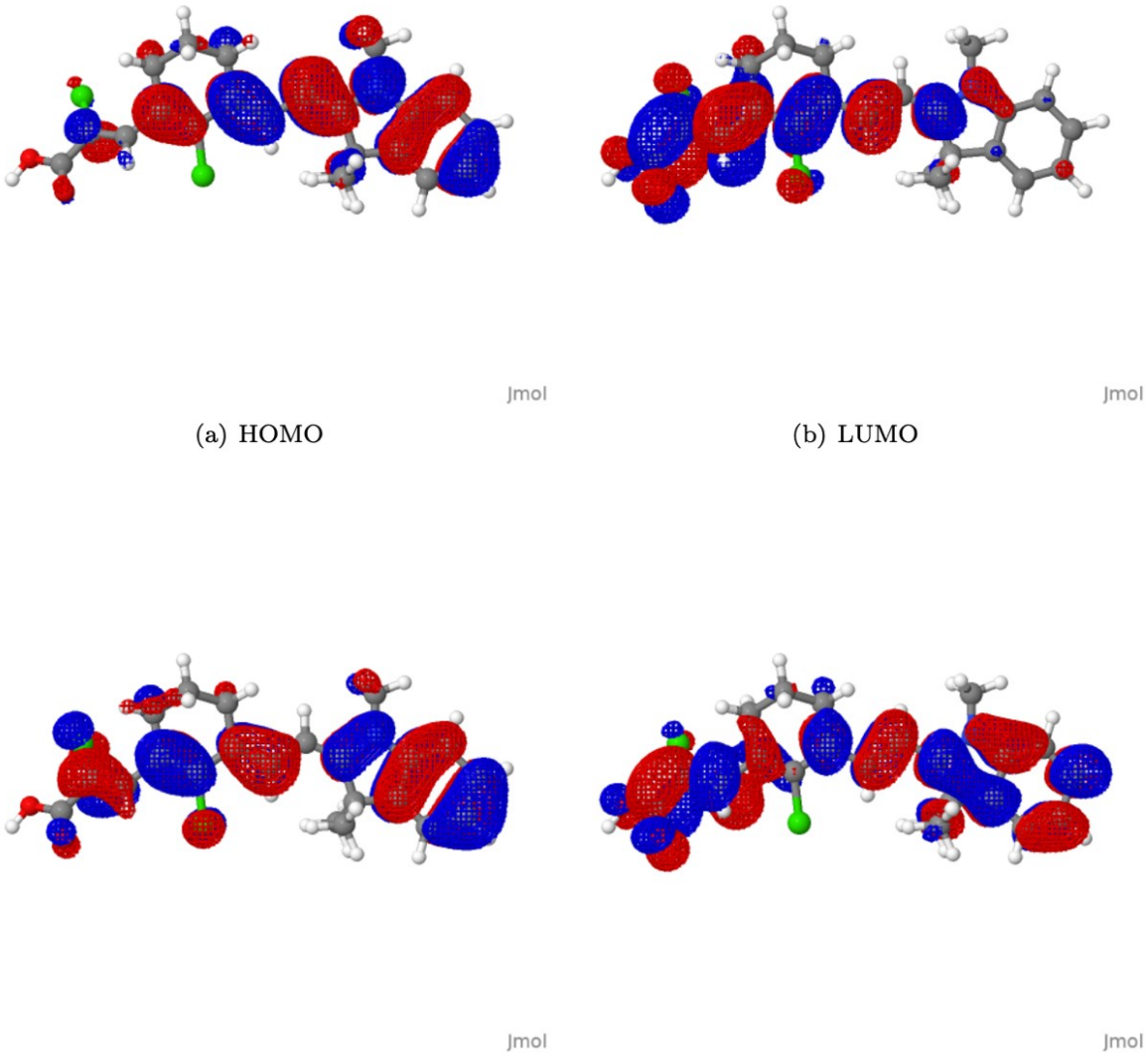

(a) HOMO (b) LUMO

(c) HOMO-1 (d) LUMO+1

Figure S48. Natural orbitals of fluorophore **4**.

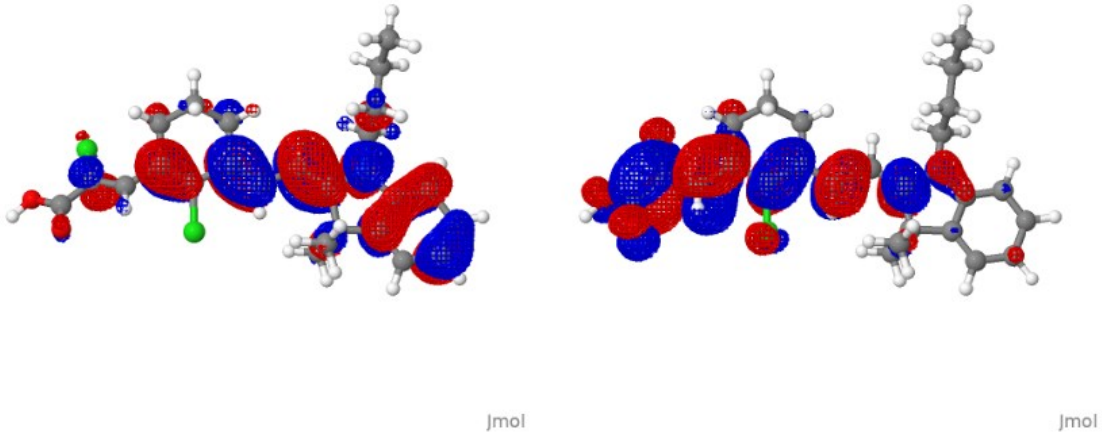

(a) HOMO (b) LUMO

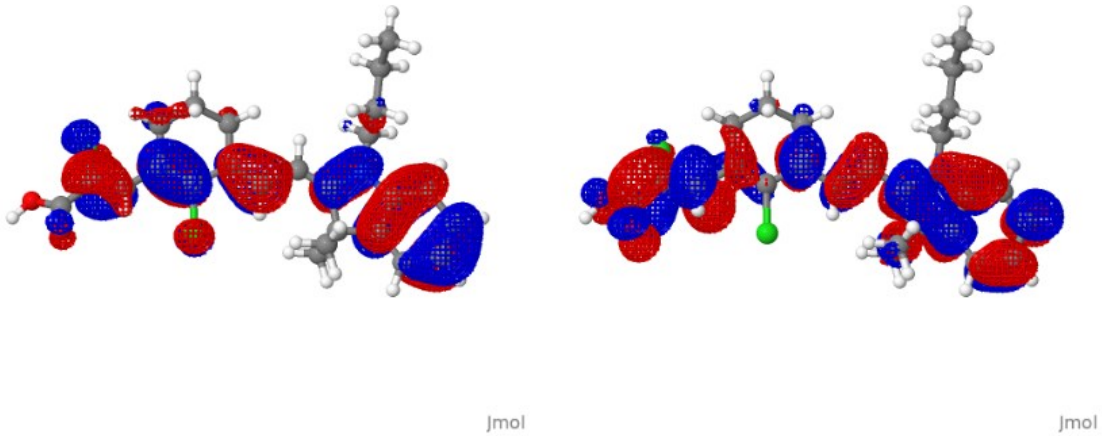

(c) HOMO-1 (d) LUMO+1

Figure S49. Natural orbitals of fluorophore **5**.

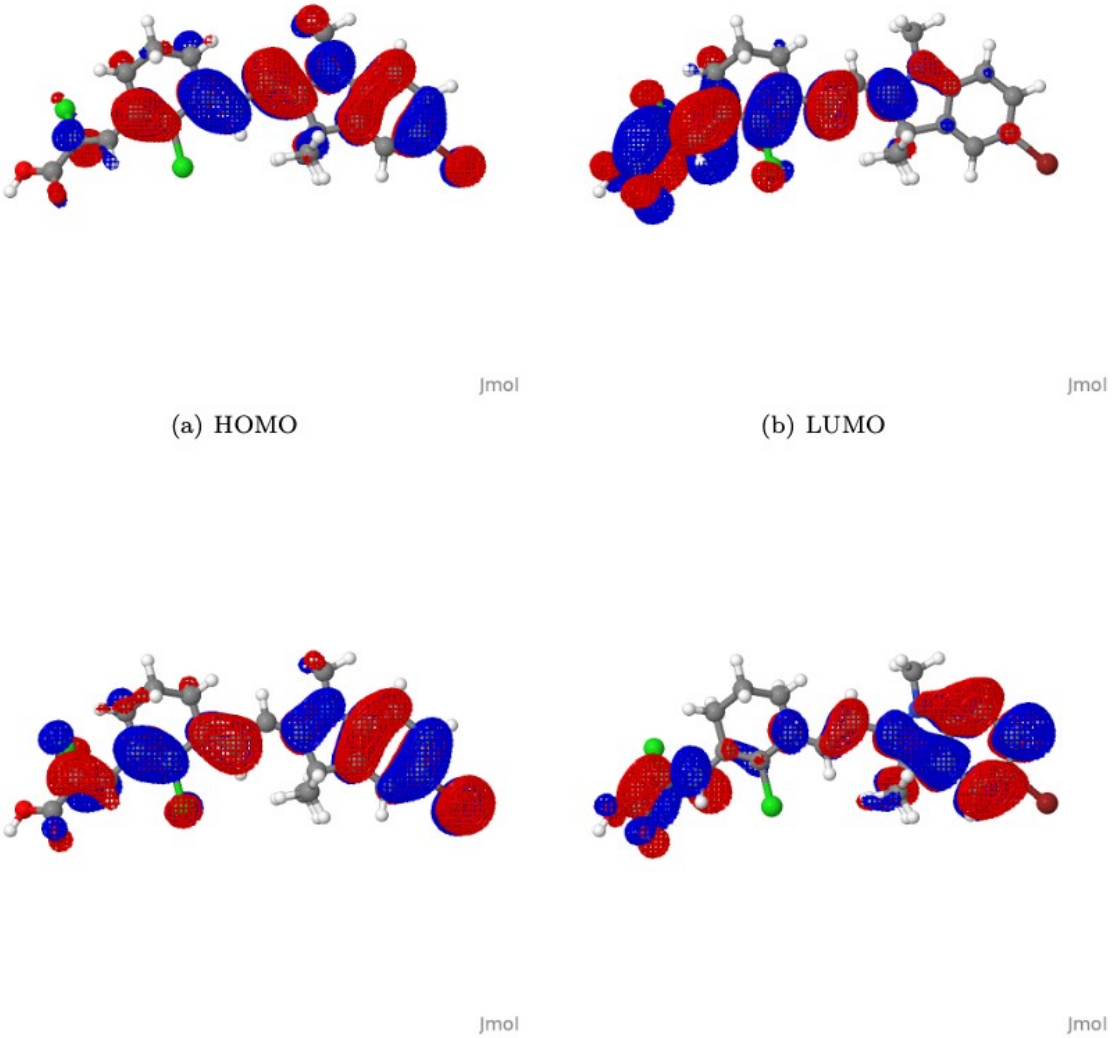

(a) HOMO (b) LUMO

(c) HOMO-1 (d) LUMO+1

Figure S50. Natural orbitals of fluorophore **6**.

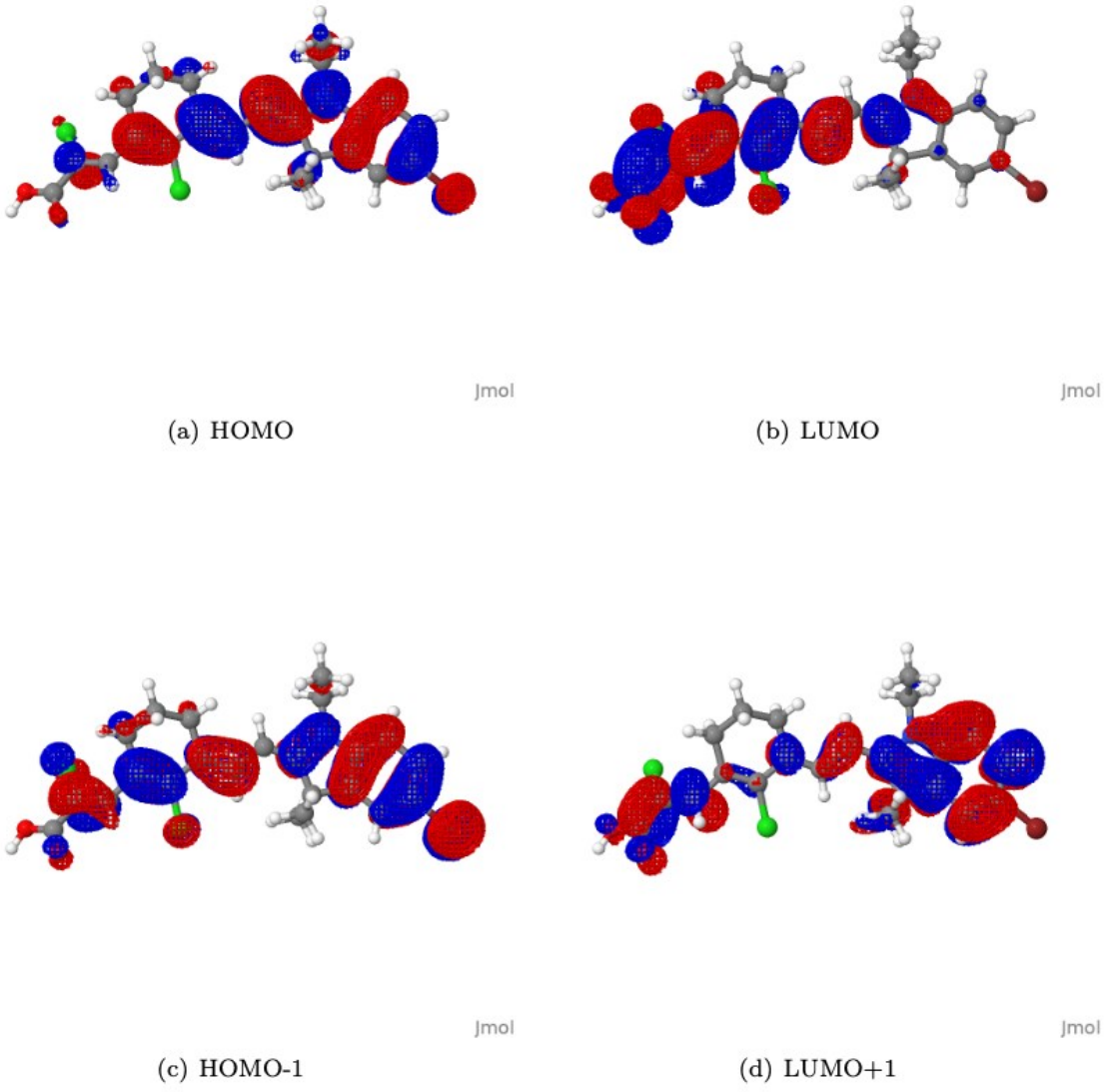

(a) HOMO (b) LUMO

(c) HOMO-1 (d) LUMO+1

Figure S51. Natural orbitals of fluorophore **7**.

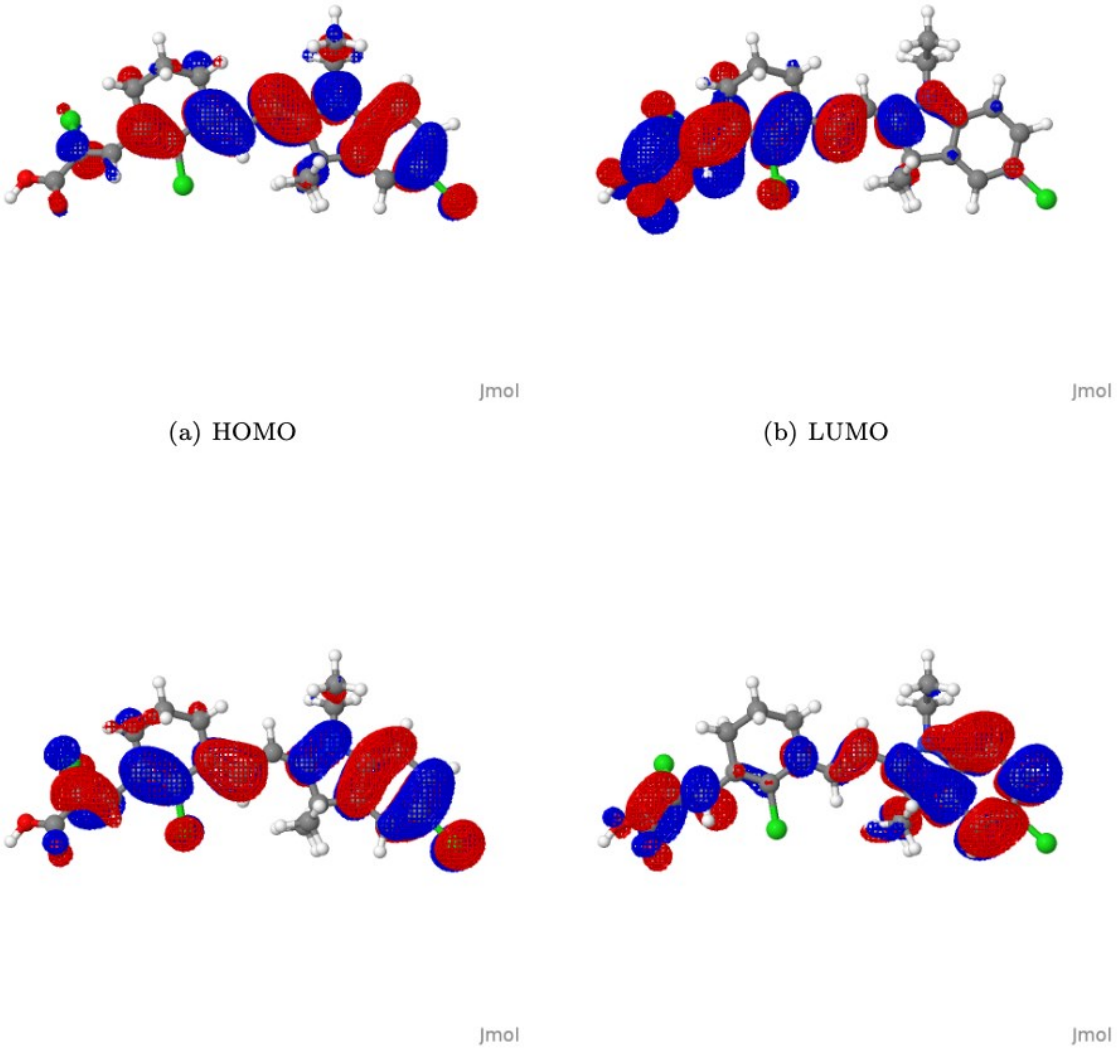

(a) HOMO (b) LUMO

(c) HOMO-1 (d) LUMO+1

Figure S52. Natural orbitals of fluorophore **8**.

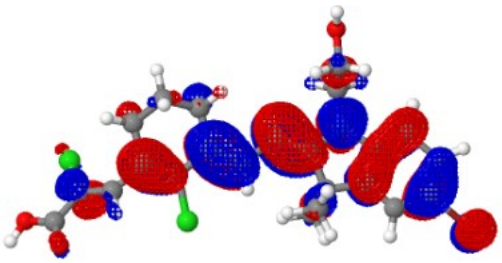

(a) HOMO

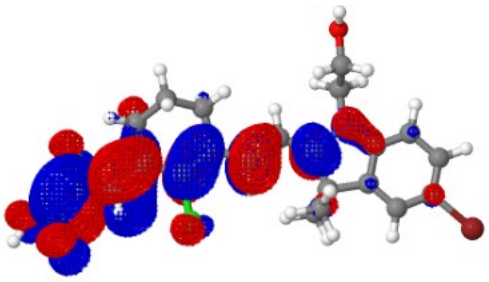

(b) LUMO

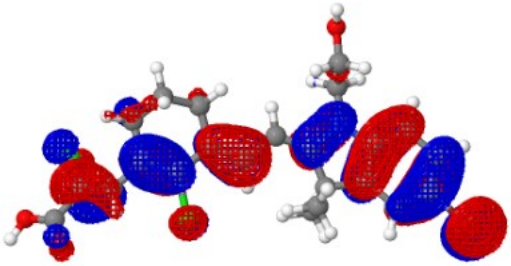

(c) HOMO-1

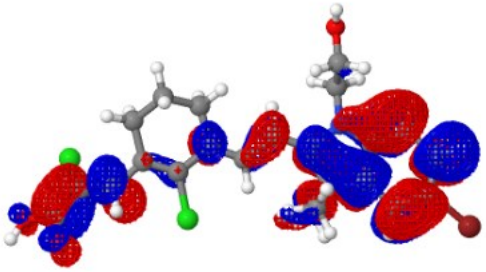

(d) LUMO+1

Figure S53. Natural orbitals of fluorophore **9**.

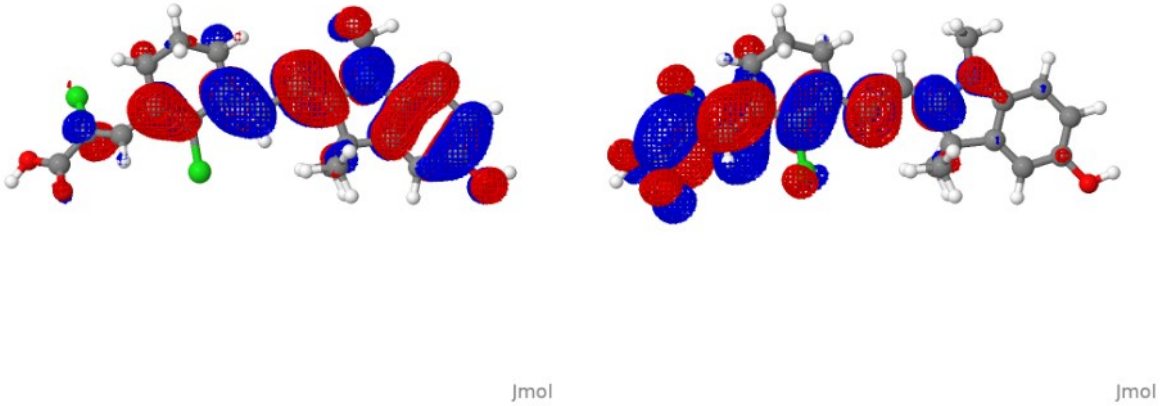

(a) HOMO (b) LUMO

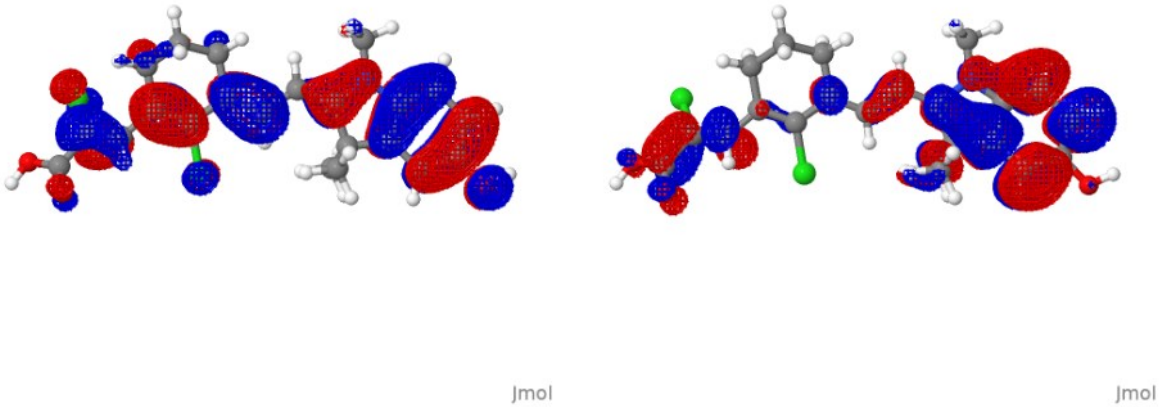

(c) HOMO-1 (d) LUMO+1

Figure S54. Natural orbitals of fluorophore **10**.

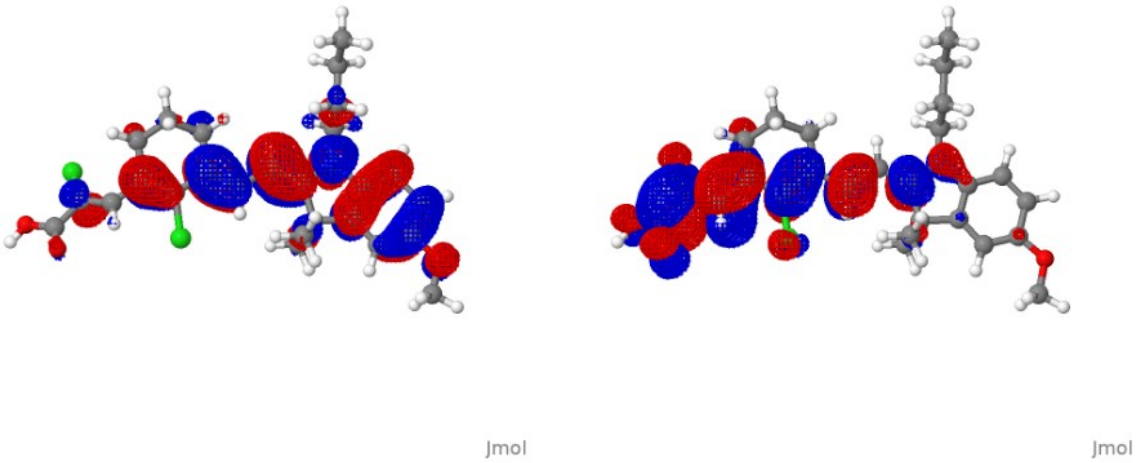

(a) HOMO (b) LUMO

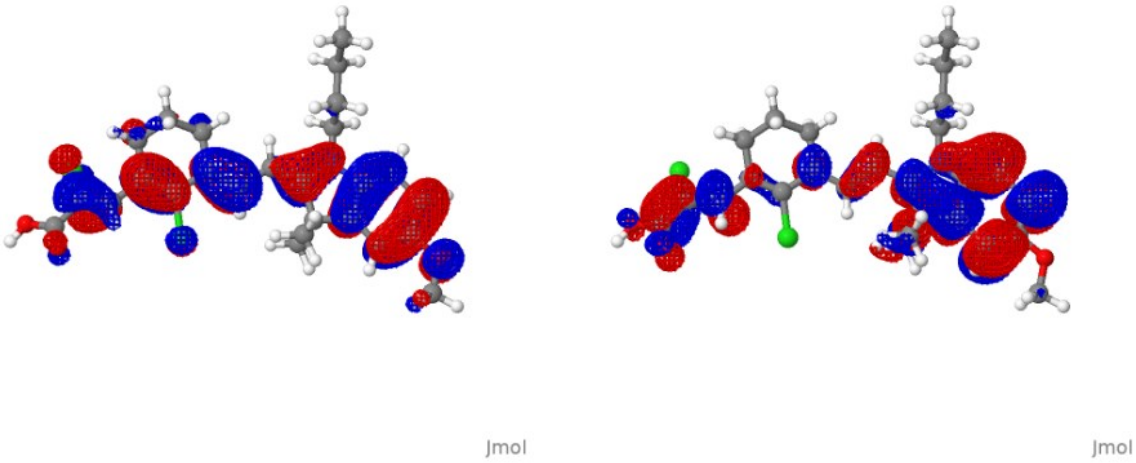

(c) HOMO-1 (d) LUMO+1

Figure S55. Natural orbitals of fluorophore **11**.

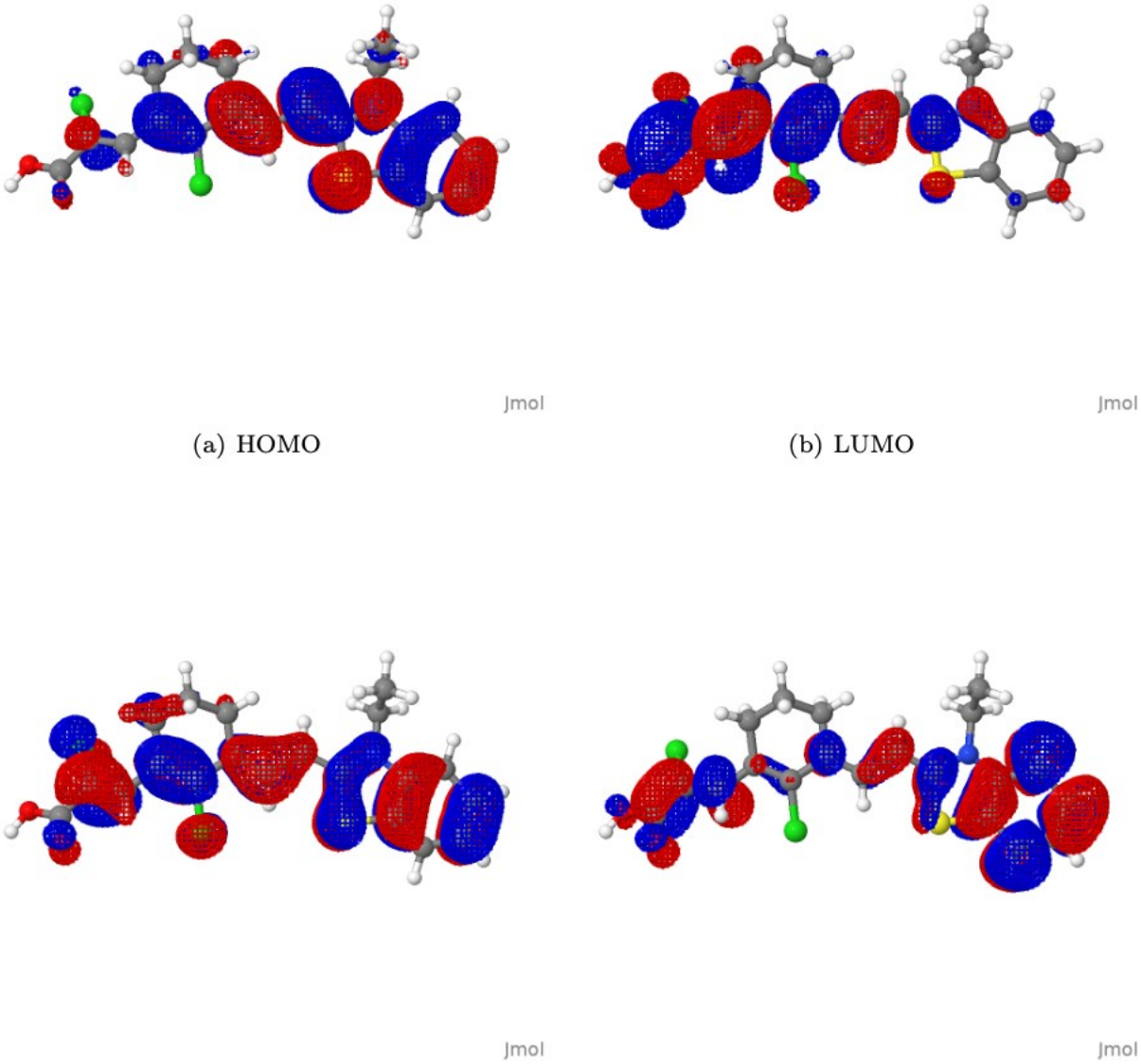

(a) HOMO (b) LUMO

(c) HOMO-1 (d) LUMO+1

Figure S56. Natural orbitals of fluorophore **12**.

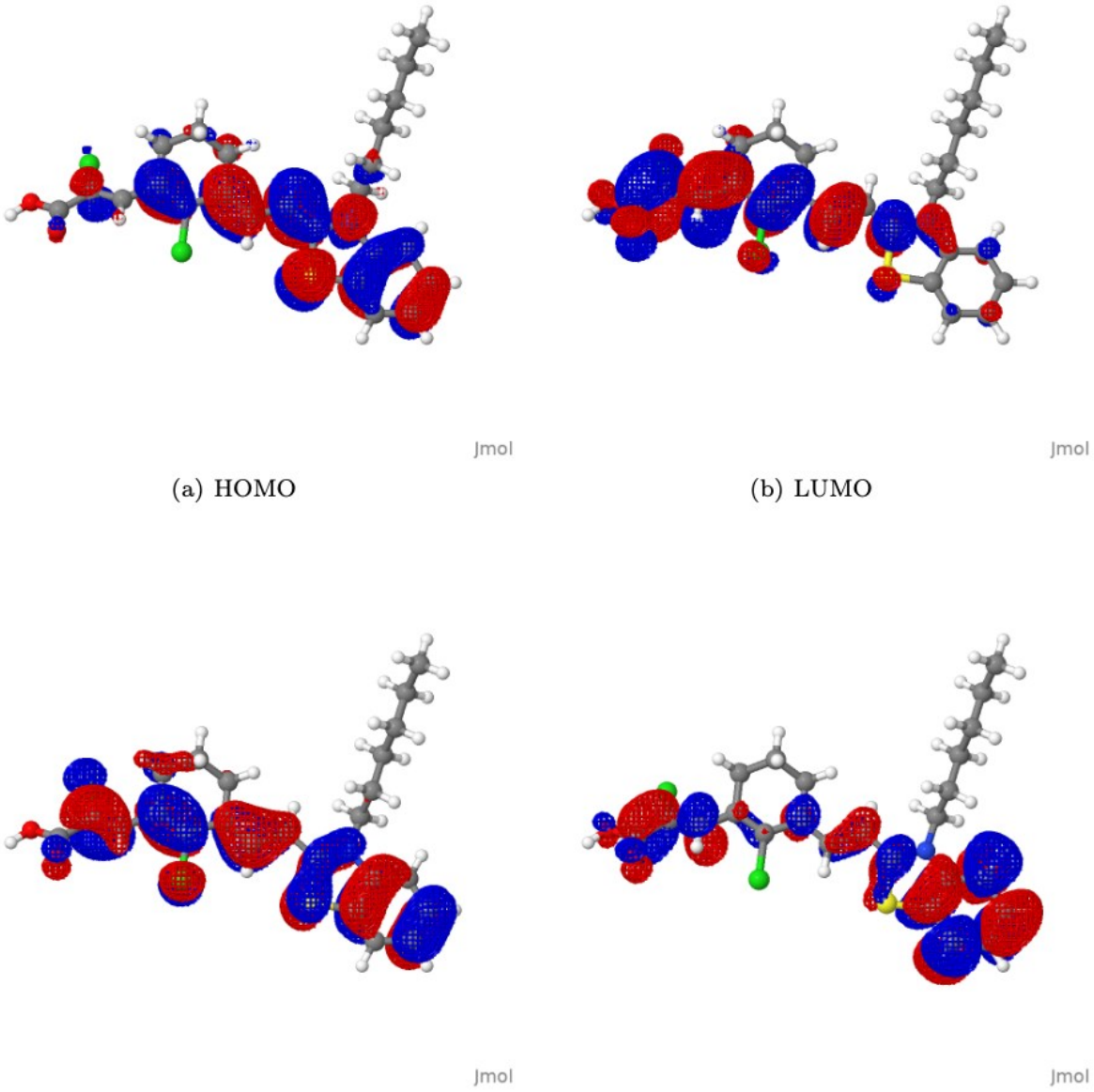

(a) HOMO (b) LUMO

(c) HOMO-1 (d) LUMO+1

Figure S57. Natural orbitals of fluorophore **13**.

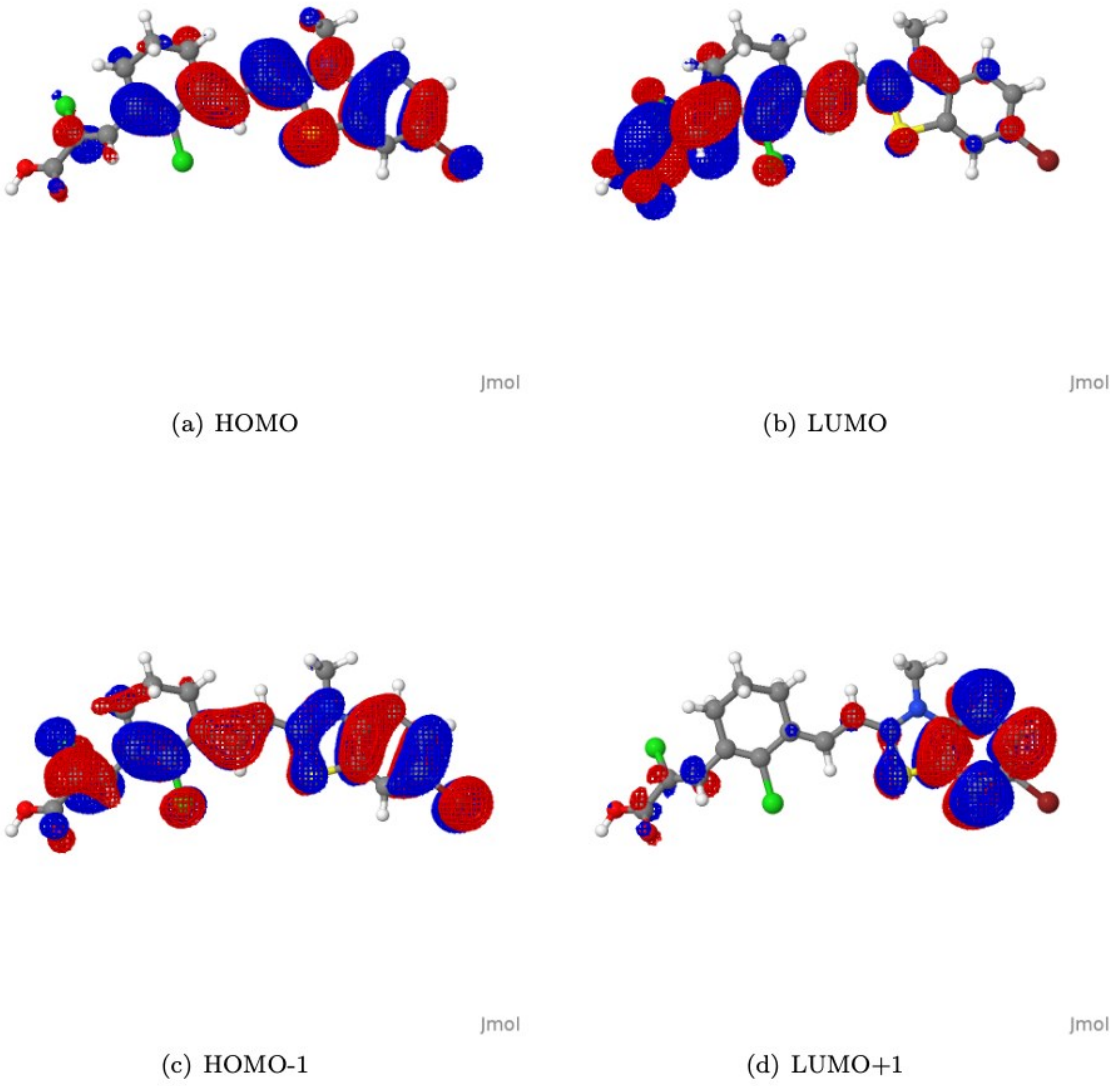

(a) HOMO (b) LUMO

(c) HOMO-1 (d) LUMO+1

Figure S58. Natural orbitals of fluorophore **14**.

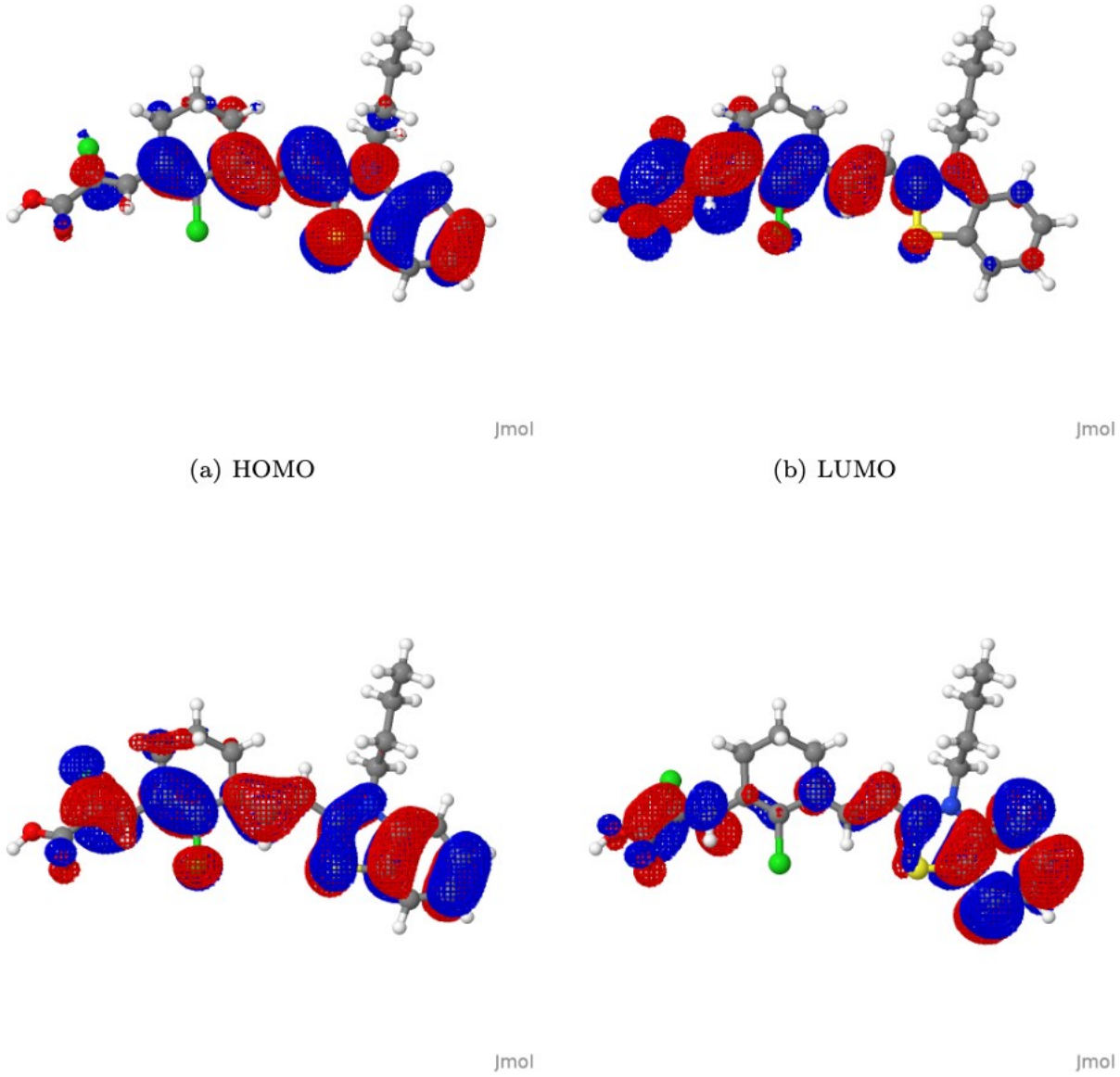

(a) HOMO (b) LUMO

(c) HOMO-1 (d) LUMO+1

Figure S59. Natural orbitals of fluorophore **15**.

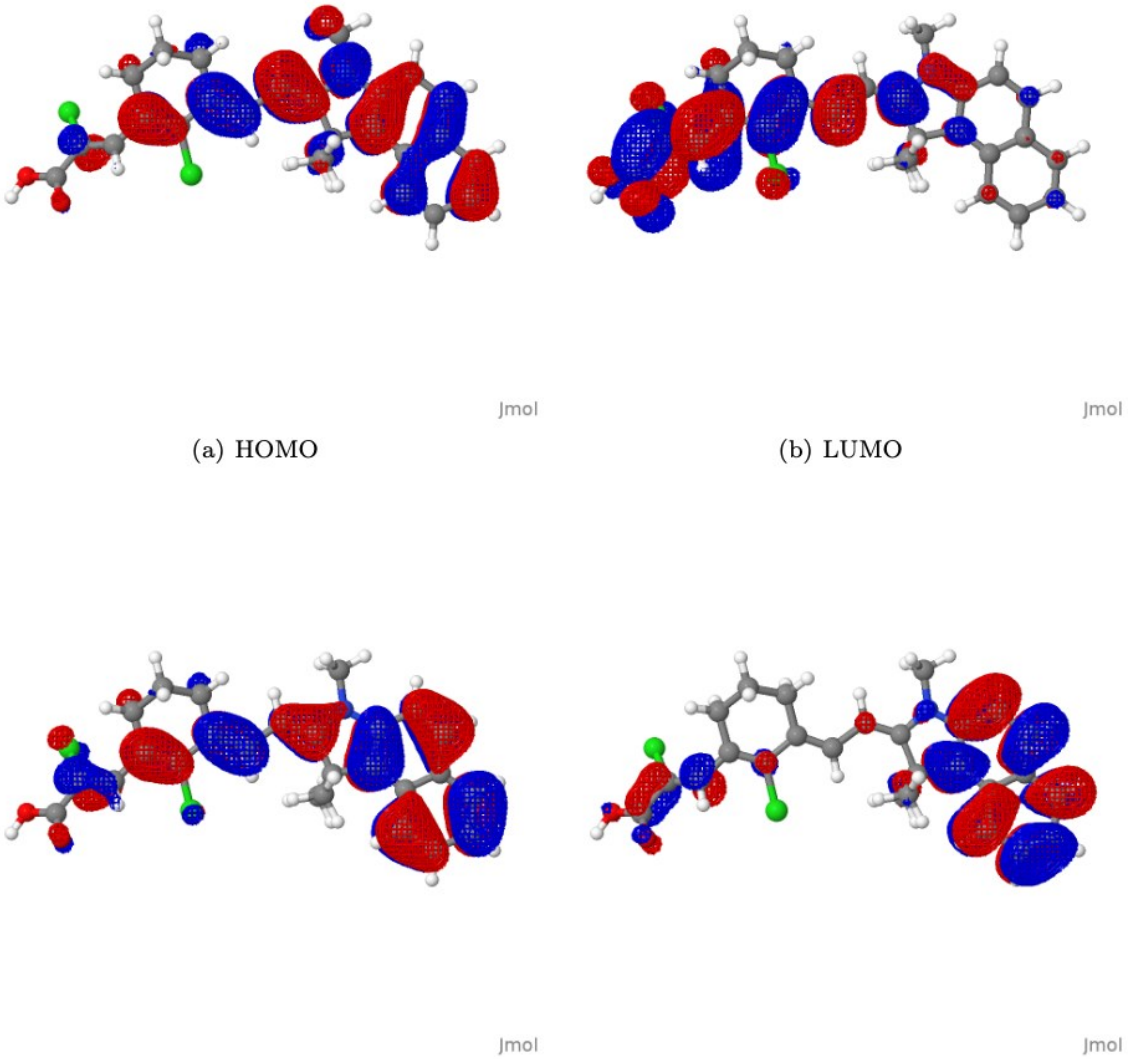

(a) HOMO (b) LUMO

(c) HOMO-1 (d) LUMO+1

Figure S60. Natural orbitals of fluorophore **16**.

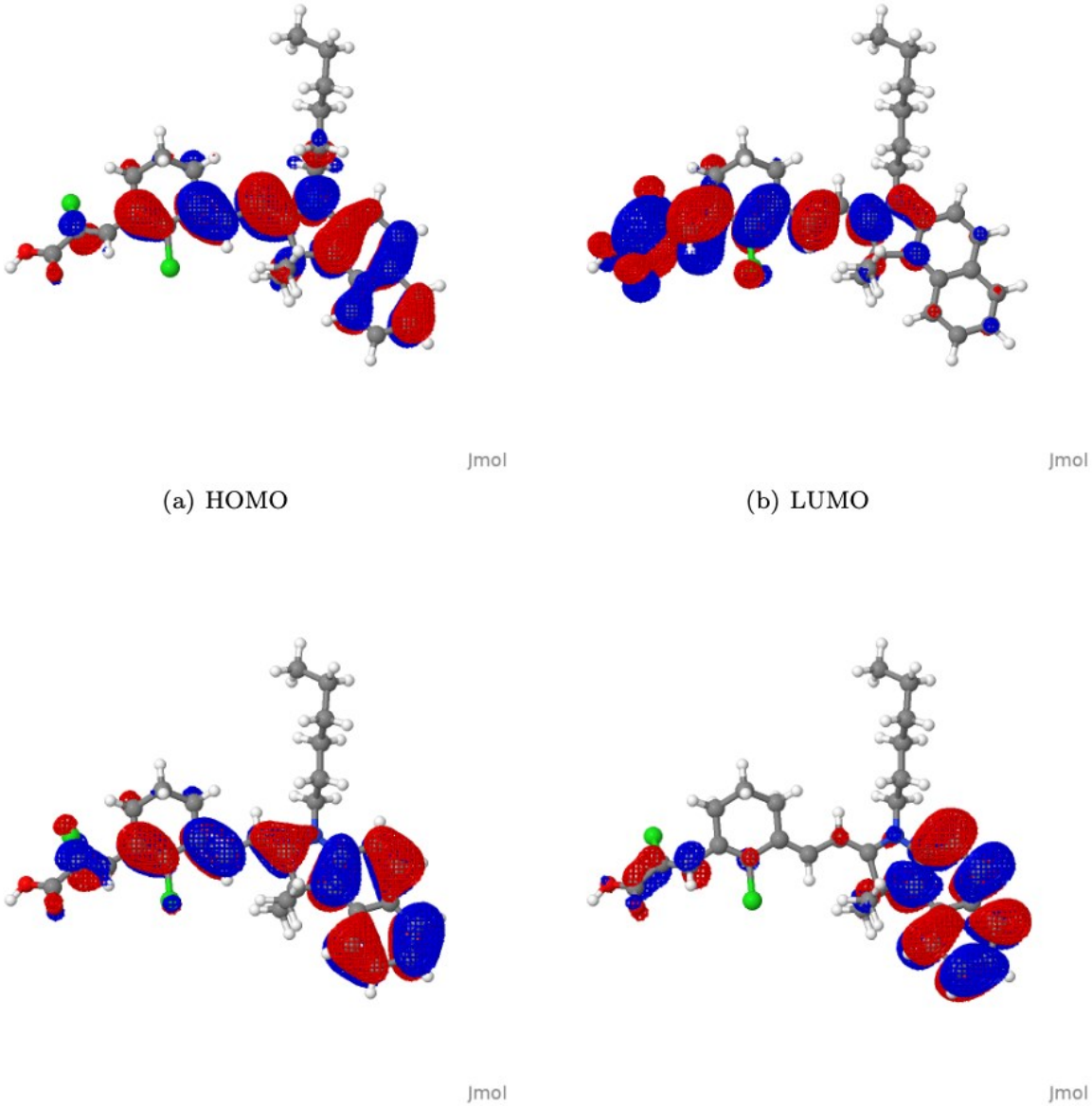

(a) HOMO (b) LUMO

(c) HOMO-1 (d) LUMO+1

Figure S61. Natural orbitals of fluorophore **17**.

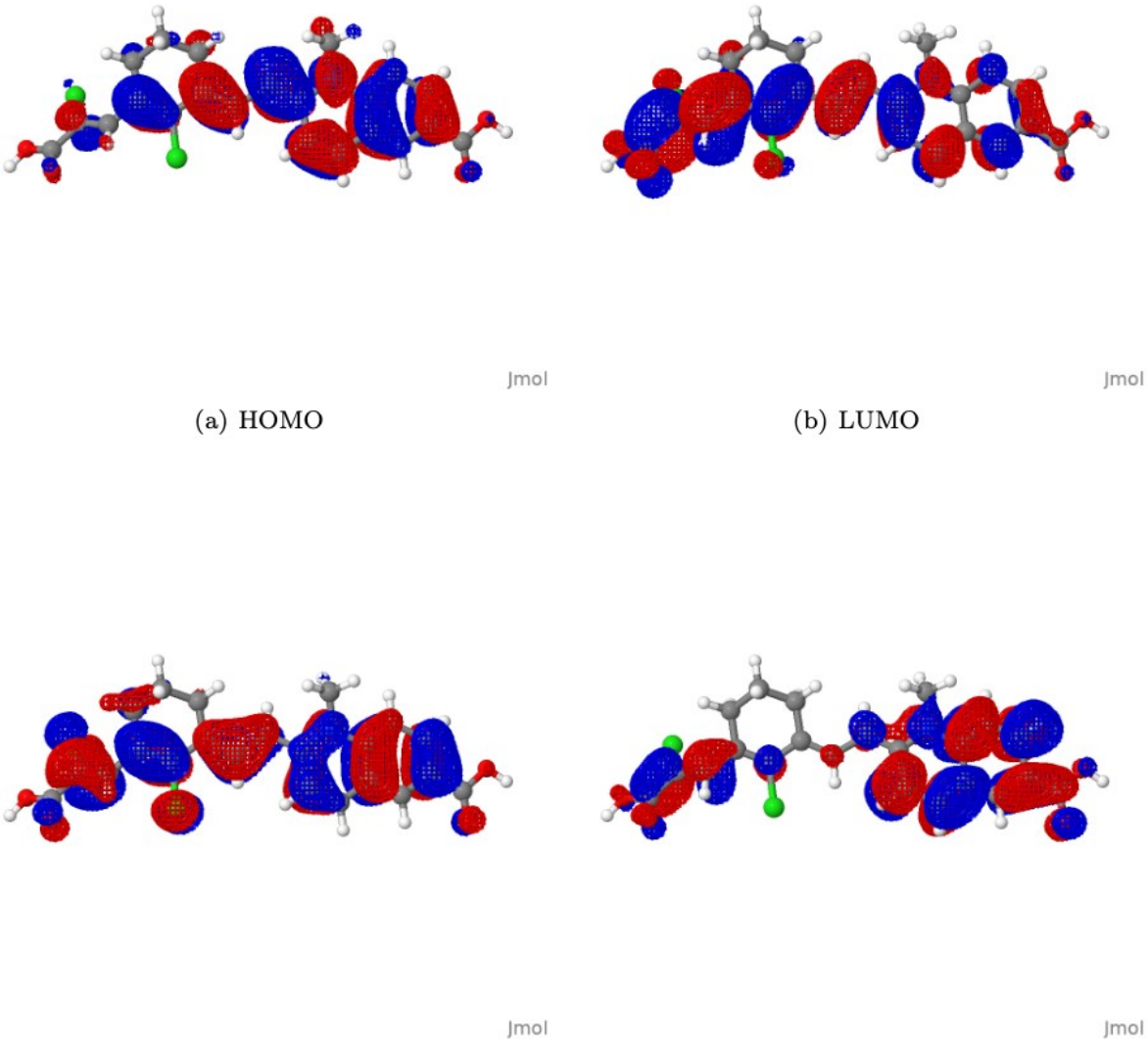

(a) HOMO (b) LUMO

(c) HOMO-1 (d) LUMO+1

Figure S62. Natural orbitals of fluorophore **18**.

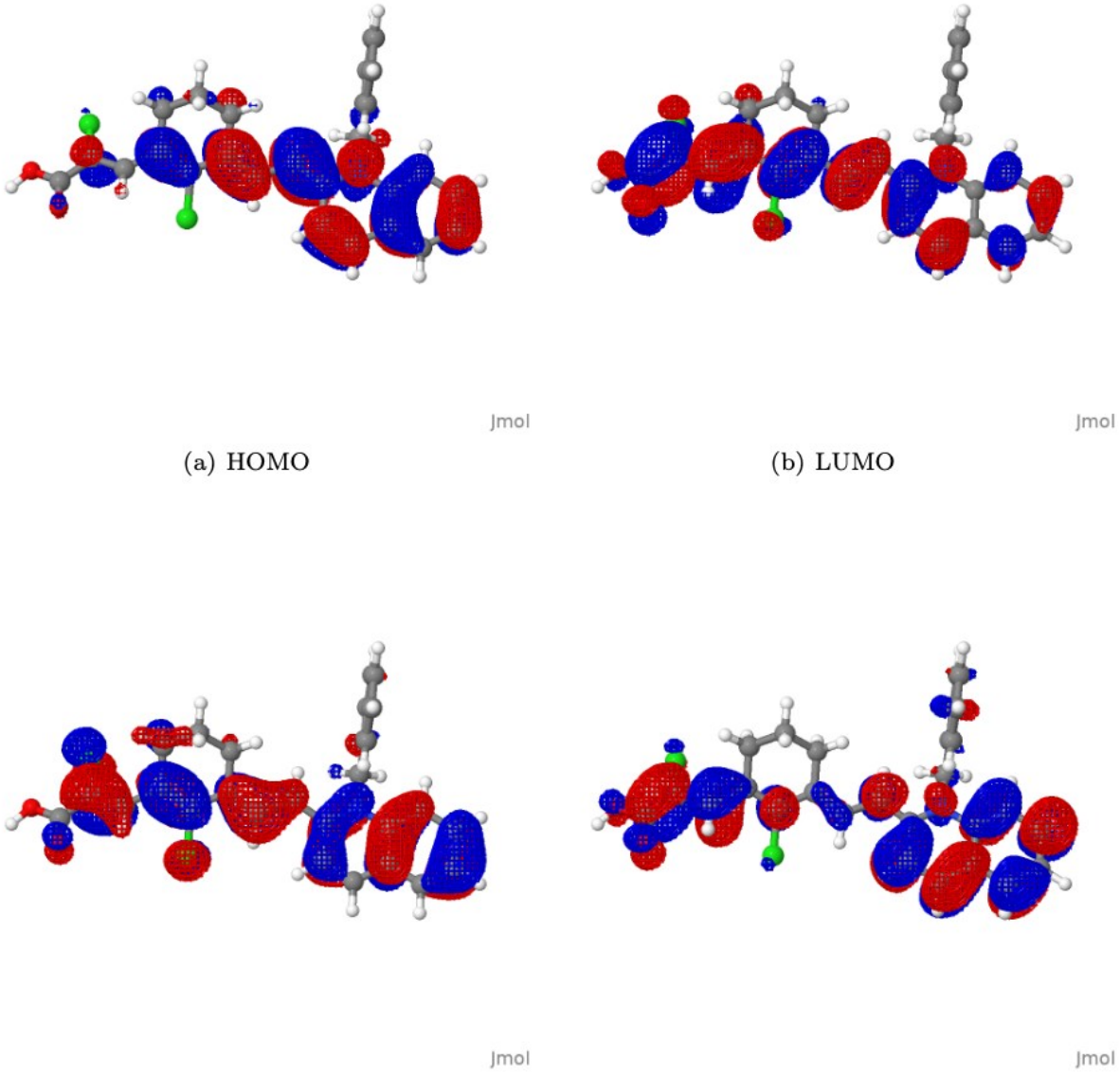

(a) HOMO (b) LUMO

(c) HOMO-1 (d) LUMO+1

Figure S63. Natural orbitals of fluorophore **19**.

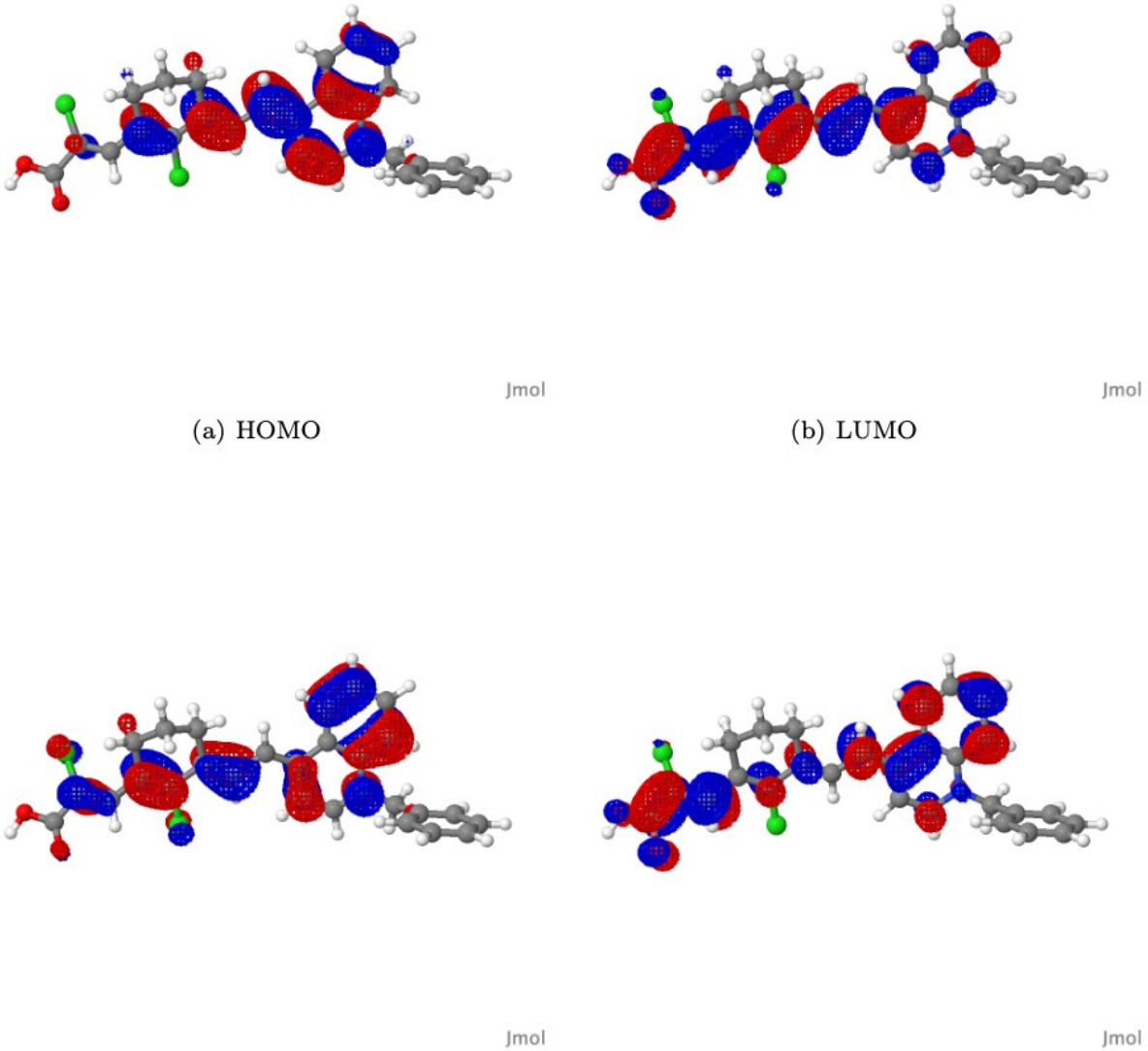

(a) HOMO (b) LUMO

(c) HOMO-1 (d) LUMO+1

Figure S64. Natural orbitals of fluorophore **20**.

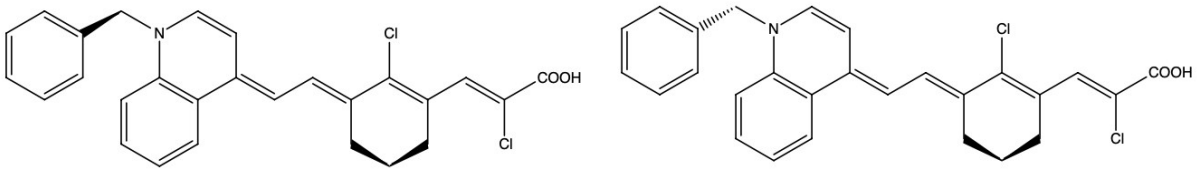

(a) syn (b) anti

Figure S65. Two conformations of fluorophore **20**.

References

1. Ma, X.; Laramie, M.; Henary, M., Synthesis, optical properties and cytotoxicity of meso-heteroatom substituted IR-786 analogs. *Bioorganic & Medicinal Chemistry Letters* **2018,** *28* (3), 509-514.
2. Becke, A. D., Density-functional exchange-energy approximation with correct asymptotic behavior. *Physical Review A* **1988,** *38* (6), 3098-3100.
3. Lee, C.; Yang, W.; Parr, R. G., Development of the Colle-Salvetti correlation-energy formula into a functional of the electron density. *Physical Review B* **1988,** *37* (2), 785-789.
4. Krishnan, R.; Binkley, J. S.; Seeger, R.; Pople, J. A., Self-consistent molecular orbital methods. XX. A basis set for correlated wave functions. *The Journal of Chemical Physics* **1980,** *72* (1), 650-654.
5. Cammi, R.; Mennucci, B.; Tomasi, J., Fast Evaluation of Geometries and Properties of Excited Molecules in Solution: A Tamm-Dancoff Model with Application to 4-Dimethylaminobenzonitrile. *The Journal of Physical Chemistry A* **2000,** *104* (23), 5631-5637.
6. Cossi, M.; Barone, V., Time-dependent density functional theory for molecules in liquid solutions. *The Journal of Chemical Physics* **2001,** *115* (10), 4708-4717.
7. Improta, R.; Barone, V.; Scalmani, G.; Frisch, M. J., A state-specific polarizable continuum model time dependent density functional theory method for excited state calculations in solution. *The Journal of Chemical Physics* **2006,** *125* (5), 054103.
8. Improta, R.; Scalmani, G.; Frisch, M. J.; Barone, V., Toward effective and reliable fluorescence energies in solution by a new state specific polarizable continuum model time dependent density functional theory approach. *The Journal of Chemical Physics* **2007,** *127* (7), 074504.
9. Lebedev, V.; Skorokhodov, A. In *Quadrature formulas of orders 41, 47 and 53 for the sphere*, Russian Acad. Sci. Dokl. Math, 1992; pp 587-592.
10. Furche, F.; Ahlrichs, R., Adiabatic time-dependent density functional methods for excited state properties. *The Journal of Chemical Physics* **2002,** *117* (16), 7433-7447.
11. Martin, R. L., Natural transition orbitals. *The Journal of Chemical Physics* **2003,** *118* (11), 4775-4777.
12. Frisch, M.; Trucks, G.; Schlegel, H.; Scuseria, G.; Robb, M.; Cheeseman, J.; Scalmani, G.; Barone, V.; Petersson, G.; Nakatsuji, H., Gaussian 16 revision a. 03. 2016; gaussian inc. *Wallingford CT* **2016,** *2* (4).
13. M. Howard, E. W., T. Driscoll, N. Vervelle, S. Tyrrell, O. Stuke, R. Kanters, B. Hanson, J. Reichert, F. Dortu, B. Smith, D. Gezelter, C. Steinbeck, T. Grey, C. Fulton, M. Beachy, H. Garcia, M. Meinek, J. Junker, C. Ribeaud, J. Rienstra-Kiracofe, C. Resnikoff, A. S´anchez, C. P. Yang, R. Guha, T. Madalin, F. Livia, I. Sarak, C. Pinto-Neto, P. Vanwing, A. Herraez, and T. White, Jmol: an open-source Java viewer for chemical structures in 3D. **2020**.
14. Berezin, M. Y.; Lee, H.; Akers, W.; Achilefu, S., Near Infrared Dyes as Lifetime Solvatochromic Probes for Micropolarity Measurements of Biological Systems. *Biophysical Journal* **2007,** *93* (8), 2892-2899.